DRAFT

A Pilot Probabilistic Risk Assessment of a Dry Cask Storage System at a Nuclear Power Plant

June 2006

This page intentionally blank.

ABSTRACT

In response to a request from the U.S. Nuclear Regulatory Commission (NRC) Office of Nuclear Material Safety and Safeguards (NMSS), the Office of Nuclear Regulatory Research (RES) and the Office of Spent Fuel Project Office (SFPO) have jointly developed and applied a methodology for performing a pilot probabilistic risk assessment (PRA) of a dry cask storage system at a nuclear power plant site (i.e., an independent spent fuel storage installation). This RES/NMSS joint report documents the pilot PRA which is for a specific dry cask system (Holtec International HI-STORM 100) at a specific boiling-water reactor (BWR) site. The methodology developed can serve as a guide for performing similar PRAs in the future. The pilot study can provide guidance for assessing the risk to the public and identifying the dominant contributors to risk. The cask system consists of a multipurpose canister (MPC) that confines the fuel, a transfer overpack that shields workers from radiation while the cask is being prepared for storage, and a storage overpack that shields people from radiation and mechanically protects the MPC during storage. The study covers various phases of the dry cask storage process, beginning with loading fuel from the spent fuel pool, preparing the cask for storage and transferring it outside the reactor building, moving the cask from the reactor building to the storage pad, and storing the cask for 20 years on the storage pad.

The study develops and assesses a comprehensive list of initiating events. Initiating events considered include dropping the cask during handling and external events during on-site storage, such as earthquakes, floods, high winds, lightning strikes, accidental aircraft crashes and pipeline explosions. Potential cask failures from mechanical and thermal loads are modeled. The study estimates the annual risk for one cask in terms of the individual probability of a prompt fatality within 1.6 Km (1 mile) and a latent cancer fatality within 16 Km (10 miles) of the site.

This page intentionally blank

TABLE OF CONTENTS

This page intentionally blank

LIST OF FIGURES

This page intentionally blank

LIST OF TABLES

This page intentionally blank

EXECUTIVE SUMMARY

The spent fuel pools of commercial nuclear power plants are becoming filled with spent fuel assemblies. To avoid having to cease operations when the pools are full, many utilities have been removing older fuel from the pools and storing it in dry casks on site. In this study, RES and SFPO have jointly developed a methodology for performing a probabilistic risk assessment (PRA) of a dry cask storage system and applied the methodology by performing a pilot PRA of a specific cask system at a specific boiling water reactor (BWR) site. Although the study results do not necessarily apply to other cask systems or sites, the methodology can serve as a guide for performing other such PRAs. The focus of this pilot study is on the methodology and its limited (i.e., case-specific) application. No inferences or conclusions about the regulatory implications of this study should be drawn.

The pilot PRA assesses the risk to the public and identifies the dominant contributors to risk associated with dry cask storage involving a single cask at a specific BWR site. Among the items that were beyond the scope of the study were subsequent versions of the specific cask studied in this report, unloading of the cask, offsite transportation, repository storage, uncertainty analysis, worker risk, human reliability, fabrication errors, mis-loading of spent nuclear fuel, aging effects, and combination of factors that could impact the probability of MPC failure.

The cask system analyzed is the Holtec International HI-STORM 100. This cask system, which is used for on-site storage only, consists of three major components – a multipurpose canister (MPC), a transfer overpack, and a storage overpack. The MPC confines spent fuel assemblies for the duration of the storage period, typically 20 years. When the MPC is removed from the spent fuel pool and prepared for storage, it is placed inside the transfer overpack to shield workers from radiation. During storage on site, the storage overpack shields people from radiation, provides a path to cool the MPC by convection though vents, and protects the MPC during storage. In this study, the transfer overpack containing the MPC is referred to as the transfer cask, and the storage overpack containing the MPC is referred to as the storage cask.

The dry cask storage operation is divided into three phases--handling, transfer, and storage. During the handling phase, spent fuel assemblies are placed into the MPC within a transfer overpack. After the MPC is dried, inerted with helium and sealed, it is removed from the transfer cask and placed in the storage overpack. The transfer phase takes place when the storage cask is moved out of the secondary containment to the storage pad. The storage phase takes place after the storage cask is set down on the storage pad. To analyze the risk of the dry cask storage operation, the phases are divided into 34 stages. A stage is defined as a discrete part of the operation that is convenient for the risk analysis. For example, because the height at which the cask is moved and the composition of the surface over which it is moved determine the mechanical load on the MPC if it were dropped, these aspects of the operation are used to define some of the stages.

A comprehensive list of initiating events is developed, and the risk associated with each initiating event is evaluated. Analyses are performed to determine the response of the cask to the mechanical and thermal loads imposed by the initiating events. For example, the following analyses evaluate the consequences of dropping the transfer cask during the handling phase:

- A mechanical load analysis determines the stresses on the fuel cladding and MPC as a function of drop height.
- Given the stress on the fuel cladding and MPC from dropping the transfer cask, or MPC, failure analyses determine the probability of the fuel cladding and MPC failing.
- Source term analysis is used to determine the releases from the fuel cladding and the MPC.

- An engineering analysis determines the reliability of the secondary containment to isolate if there is an accidental release of radioactivity inside the secondary containment.

To quantify the risk, the study uses best available point estimates. When there is insufficient information or data, conservative bounding assumptions or estimates are used. Because no uncertainty analysis was performed, the identification of the dominant contributors was based on the point estimates developed by the study. The dominant contributors might possibly change if uncertainty is considered. The study measures the risk to the public in terms of the individual probabilities of a prompt fatality within 1.6 km (1 mi) and a latent cancer fatality within 16 km (10 mi) of the site. In calculating the risks, the study also considers weather conditions and the population distribution in the vicinity of the site.

The results of this analysis indicate that the risk is solely from latent cancer fatalities and no prompt fatalities are expected. The risk is dominated by accident sequences occurring in six stages of the handling phase. These involve drops of the transfer cask while it is being lifted out of the cask pit or while it is being moved and lowered to the preparation area, all before the MPC lid is welded shut. The aggregated risk values are quite low. Many of the scenarios have zero risk because either their initiating events cannot occur at the subject plant or no radioactive release will result. The overall risk of dry cask storage was found to be extremely low–the estimated aggregate risk is an individual probability of a latent cancer fatality of $2.0.\times10^{-12}$ during the first year of service and 1.9×10^{-13} per year during subsequent years of storage.

FOREWORD

The spent fuel pools of commercial nuclear power plants are becoming filled with spent fuel assemblies. To avoid having to cease operations when the pools are full, many utilities have been removing older fuel from the pools and storing it in dry casks on site. This activity is regulated by the U.S. Nuclear Regulatory Commission's (NRC) Office of Nuclear Material Safety and Safeguards (NMSS), which is responsible for the public health and safety licensing, inspection and environmental reviews for all activities regulated by the NRC, except for power and all non-power reactors.

In order to further assess the risk to the public from the handling, transfer and storage of the dry casks, NMSS requested NRC's Office of Nuclear Regulatory Research (RES) to develop and apply a methodology for performing a pilot probabilistic risk assessment (PRA) of a dry cask storage system. RES and NMSS have jointly performed the pilot PRA on a specific cask system at a specific boiling-water reactor site.

To analyze the risk, a comprehensive list of initiating events was developed, and the risk associated with each initiating event was evaluated. Initiating events considered include dropping the cask inside the secondary containment building during transfer operations and external events during on-site storage such as earthquakes, floods, high winds, lightning strikes, accidental aircraft crashes and pipeline explosions. Potential cask failures from mechanical and thermal loads, including thermal loads caused by mis-loading events, were modeled. In the event of a cask failure/breach, the fuel inventory available for release was based on 10-year old fuel. Weather conditions and the population distribution in the vicinity of the site were also considered. The risk to the public is measured in terms of the individual probabilities of a prompt fatality within 1.6 km (1 mi) and a latent cancer fatality within 16 km (10 mi) of the site. The resulting calculated risk is extremely small, stemming solely from latent cancer fatalities. No prompt fatalities are expected.

To quantify the risk, the study used best available point estimates. When there was insufficient information or data, conservative bounding assumptions or bounding estimates were used. Among the items that were beyond the scope of the study were subsequent versions of the specific cask studied in this report, unloading of the cask, offsite transportation, repository storage, uncertainty analysis, worker risk, human reliability, fabrication errors, mis-loading of spent nuclear fuel, aging effects, and combination of factors that could impact the probability of MPC failure.

The methodology developed in this study can serve as a guide for performing other such PRAs. Results of this study in conjunction with the methodology can be used to determine the need for other PRAs, improvements in data gathering and analysis, and additional engineering design analysis. The focus of this pilot study was solely on the methodology and its limited (i.e., case-specific) application. No inferences or conclusions about the regulatory implications of this study should be drawn.

This page intentionally blank

ACKNOWLEDGMENTS

Team Members	Area of Contributions
U.S. Nuclear Regulatory Commission	
Ronaldo Jenkins	Overall management
Alan Rubin	Overall management and technical oversight (through March 2006)
Edward Rodrick	Team Leader (through September 2001)
Lee Abramson	Team Leader, data analysis, technical review, report editing (through September 2004)
John Thorp	Team Leader, technical review, report editing (through August 2005)
Asimios Malliakos	Team Leader and final report editing
John Ridgely	Review and compilation of the report
Christopher Ryder	Technical coordination among technical disciplines, report compilation, and review. Flooding analysis, project management of secondary containment analyses at Lawrence Livermore National Laboratory and peer review at Sandia National Laboratories
Christina Antonescu	Effects of lightning. Project management of lightning analysis at Oak Ridge National Laboratory
Gordon Bjorkman	Structural mechanics, stress analysis and buckling, LS-DYNA model modifications and analyses, weld failure methodology, MPC integrity evaluation and failure probability, fuel rod integrity methodology and analyses, aircraft impact analysis
Kim Hardin	SFPO Team Leader, coordination among SFPO technical disciplines, technical review, interface with RES (2004-2005)
Tze-Jer Chuang	SFPO Team Leader, coordination among SFPO technical disciplines, technical review and report editing, interface with RES (2005-2006)
Robert Einziger	Source term methodology and source term estimates
Jason Piotter	Implemented LS-DYNA model modifications, LS-DYNA analyses
Monideep Dey	Fires
Brad Hardin	Frequencies of aircraft crashes and natural events
Douglas Kalinousky	Failure analysis
Jocelyn Mitchell	Consequences
Carlos Navarro	Consequences
Cayatano Santos	Failure analysis
Shah Malik	Failure analysis
Jason Schaperow	Source term and consequences
Syed Shaukat	Structural mechanics. Project management of structural analyses at Brookhaven National Laboratory
Ghani Zigh	Thermal hydraulic analyses of fires and blocked vents
Tony Ulses	Criticality analysis
Brookhaven National Laboratory	
Joseph Braverman	Mechanical load calculations
Charles Hofmayer	Mechanical load calculations
Charles Miller	Mechanical load calculations
Richard Morante	Mechanical load calculations
Jim Xu	Mechanical load calculations

Team Members	Area of Contributions
Jinsuo Nie	Mechanical load calculations
Nikolaos Simos	Mechanical load calculations
Lawrence Livermore National Laboratory	
Peter Prassinos	Reliability of secondary containment isolation
Oak Ridge National Laboratory	
James Yugo	Electromagnetic analysis of lightning effects on dry dask
Sandia National Laboratories	
Douglas Ammerman	Cask and fuel rod response for source term estimates
Robert Kalan	Cask and fuel rod response for source term estimates
Vincent Luk	Seismic load calculations
Jeremy Sprung	Source term estimates

Comment Review Group	Group Leaders
SFPO Thermal Group	Jorge Solis
SFPO Structural Group	Gordon Bjorkman / Henry Lee / Bob Tripathi / Jason Piotter / David Tang
SFPO Materials Group	Robert Einziger / Tze-Jer Chuang / Chuck Interrante
SFPO Criticality Group	Carl Withee / Kim Hardin / Bernie White
SFPO Containment and Radiation Protection	Kim Hardin / Steve Baggett / Mike Waters/ Michel Call
Transportation and Storage Safety & Inspection Section	Rob Temps
Spent Fuel Licensing Section	Steve O'Connor
NMSS Risk Task Group (no longer in existence)	Bret Leslie
Specialists	Dennis Damon / Robert Einziger

ABBREVIATIONS

ASME	American Society of Mechanical Engineers
atm	atmospheric pressure
BNL	Brookhaven National Laboratory
BWR	boiling water reactor
C	Centigrade
CDF	cumulative distribution function
cfm	cubic feet per minute
cm	centimeter
CRUD	Chalk River unidentified deposits
CFR	Code of Federal Regulations
DBE	design basis earthquake
DCF	dose conversion factors
EAB	exclusion area boundary
FAA	Federal Aviation Administration
FAD	failure assessment diagram
FSAR	Final Safety Analysis Report
F	Fahrenheit
ft	feet
g	gravitational constant
GFD	ground flash density
HI-STORM	Holtec International storage and transfer operation reenforced module
HI-TRAC	Holtec International transfer cask
hr	hour
HRA	human reliability analysis
HVAC	heating, ventilation, and air conditioning
IFT	isolation failure types
in	inch
ISFSI	independent spent fuel storage installation
KE	kinetic energy
kg	kilogram
km	kilometer
kPa	kilo-Pascal
kW	kilowatt
lb	pound
LWR	light water reactor
m	meter
MACCS2	MELCOR Accident Consequence Code System
MPa	mega-Pascal
mi	mile
min	minute
MPC	multi-purpose canister
mph	miles per hour
MW	megawatts
MWa/MTU	megawatt-days per metric ton
NG	noble gases
NLDN	National Lightning Detection Network
NMSS	(Office of) Nuclear Material Safety and Safeguards
NRC	U.S. Nuclear Regulatory Commission
NSSS	nuclear steam supply system
ORNL	Oak Ridge National Laboratory
OT	other than noble gases
PE	potential energy

PFM	probabilistic fracture mechanics
PMP	probable maximum precipitation
PRA	probabilistic risk assessment
psi	pound per square inch
PT	dye penetrant (test) examination
PWR	pressurized water reactor
Ref	reference
RES	(Office of) Nuclear Regulatory Research
RNG	Re-normalization Group theory
RT	radiographic (test) examination
RV	reactor vessel
s	second
SA	submerged arc (weld)
SGTS	standby gas treatment system
SIMPLE	Semi Implicit Method for Pressure-Linked Equations
SME	seismic margin earthquake
SNL	Sandia National Laboratories
SRP	Standard Review Plan
SRSS	square-root-of-sum-of-squares
TIG	tungsten-inert-gas (process)
UT	ultrasonic testing (non-destructive test process)
yr	year

GLOSSARY OF SELECTED TERMS

Transfer (HI-TRAC) Overpack: The shielded container designed and fabricated to allow safe loading of fuel assemblies into the MPC, preparation of the MPC for storage, and transfer of the MPC into the storage (HI-STORM) overpack. When the transfer overpack has been loaded with an MPC and associated spent fuel assemblies, it is referred to as the "transfer cask".

Storage (HI-STORM) Overpack: The long term storage container designed and fabricated to allow safe movement of an MPC containing spent fuel assemblies to a storage pad and to provide shielded, safe storage of the MPC in the ISFSI. When the MPC containing fuel assemblies is transferred into the storage overpack, it is then referred to as the "storage cask".

Transfer Cask: A HI-TRAC containing an MPC loaded with fuel assemblies.

Storage Cask: A HI-STORM containing an MPC loaded with fuel assemblies.

PRA: A systematic method for addressing the risk triplet as it relates to the performance of a complex system to understand likely outcomes, sensitivities, areas of importance, system interactions, and areas of uncertainty. The risk triplet is the set of three questions that the NRC uses to define "risk": (1) What can go wrong? (2) How likely is it? and (3) What are the consequences? NRC identifies important scenarios from such an assessment. [From "Staff Requirements - SECY 98-144 - White Paper on Risk-informed and Performance-based Regulation" (Reference 1)]

1. INTRODUCTION

The spent fuel pools of commercial nuclear power plants are becoming filled with spent fuel assemblies. To avoid having to cease operations when the pools are full, many utilities have been removing older fuel from the pools and storing it in dry casks, in an Independent Spent Fuel Storage Installation (ISFSI) on site. In this study, a methodology for performing a probabilistic risk assessment (PRA) of a dry cask storage system is developed and applied by performing a pilot PRA of a specific cask system at a specific boiling water reactor (BWR) site. Although the study results do not necessarily apply to other cask systems or sites, the methodology can serve as a guide for performing other such PRAs. This study does not endorse the use or non-use of a dry cask storage system at any particular site.

The U.S. Nuclear Regulatory Commission (NRC), Office of Nuclear Regulatory Research (RES) jointly with the Spent Fuel Project Office (SFPO), performed this study in response to a request by the NRC Office of Nuclear Material Safety and Safeguards (NMSS), to support their efforts to risk inform NMSS regulated activities. It is expected that NMSS will use the results of this study in conjunction with the methodology to develop a basis to determine the need for other PRAs, improvements in data gathering and analysis, additional engineering design analysis and to identify general program areas which maybe candidates for increased/decreased staff review or inspection focus. Because the focus of this pilot study is solely on the methodology and its limited (i.e., case specific) application, no inferences or conclusions about the regulatory implications of this study should be drawn.

1.1 Purpose

The purpose of this study is to develop and apply a methodology for performing a PRA to assess the risk to the public and to identify the dominant contributors to risk associated with dry cask storage involving a single cask at a specific site. The risk is evaluated using best available estimates, or when there is insufficient information or data, conservative bounding assumptions or estimates are used. The results of this study can help for future studies to determine the extent and depth of any uncertainty analysis that may be needed in the future. Similar to PRAs for nuclear power plants, this PRA includes a list of initiating events, response of system (i.e., cry cask) to initiating events, secondary containment analysis and consequence analysis. Different to PRAs for nuclear power plants this PRA did not include a human reliability analysis.

1.2 Scope

1.2.1 Issues Within the Scope

The cask system analyzed is the Holtec International HI-STORM (Holtec International Storage and Transfer Operation Reinforced Module) 100 (Reference 2). This cask system, which is used for on-site storage only, consists of three major components: a multipurpose canister (MPC), a HI-TRAC (overpack) which in this report is called “transfer overpack,” and a HI-STORM (overpack) called the “storage overpack.” The MPC confines spent fuel assemblies for the duration of the storage period, typically 20 years. When the MPC is removed from the spent fuel pool and prepared for storage it is already inside the transfer overpack to shield workers from radiation. In this study, the transfer overpack containing the MPC is referred to as the “transfer cask,” and the storage overpack containing the MPC is referred to as the “storage cask.” During storage on site, the storage cask shields people from radiation, provides a path to cool the MPC by convection though vents, and mechanically protects the MPC.

The study’s assessment begins when spent nuclear fuel assemblies are loaded into the MPC, within the transfer overpack. The transfer cask is then moved to an area on the refueling floor where the MPC is prepared for storage. The transfer cask is lowered through the equipment hatch to the storage overpack on the ground level where the MPC is moved from the transfer cask into the storage overpack. The loaded storage cask is then moved to the ISFSI where it is set on a concrete pad.

For source term and release fractions, this study considered spent BWR fuel. The fuel considered is high burn-up, having been stored and cooled for ten years, respectively, in the spent fuel pool.

1.2.2 Issues Beyond the Scope

1.2.2.1 Version of the Cask

The version of the cask used in this study is that documented in Reference 2. Any subsequent changes to the design, documented as amendments or performed in accordance with 10 CFR 72.48, are beyond the scope. Changes to the cask would have to be fairly significant to impact the main conclusion of the report, that the overall risk is extremely low.

1.2.2.2 Unloading, Offsite Transportation, and Repository Storage

A storage cask may have to be unloaded. The storage overpack is designed for onsite transfer and storage; it cannot be moved offsite. If spent fuel is moved to a permanent repository, at a minimum, the MPC would have to be removed from the storage overpack and placed in a transport overpack. If, for some reason, the spent fuel needed to be reconfigured, e.g., because incorrect assemblies were mistakenly loaded, then the MPC would need to be opened. Neither circumstance is analyzed in this study. The storage overpack is designed for onsite transportation and storage. Thus offsite transportation and repository storage are not analyzed in this study.

1.2.2.3 Damage to the Plant

The effects of dropping the transfer cask on the floors of the load path from the cask pit (alcove of the spent fuel pool where the transfer cask is loaded) to the equipment hatch was estimated where details of the floors were obtained. Any damage to underlying plant systems, equipment, and components, or capabilities to shut down the reactor were not analyzed and are beyond the scope of this study. Where the floor has supporting beams, girders or concrete walls located underneath, the floor is expected to hold the cask, were it to drop from a distance typical of the height it is lifted while being moved. It is important to note that the crane carrying the transfer cask along the load path between the cask pit and equipment hatch is single-failure-proof.

1.2.2.4 Uncertainty

Although there are inherent uncertainties in the initiating event frequencies, conditional probabilities, and consequences used to calculate the risk, this study does not consider these uncertainties. This is because the purpose of this study was of a limited scope and limited resources for developing and applying a methodology to assess the risk to the public and to identify the dominant contributors to risk associated with dry cask storage involving a single cask at a specific site. An essential element of an uncertainty analysis is a sensitivity analysis whereby the possible ranges of the input variables are determined and their effects on the output measures are systematically evaluated. With a few exceptions, this study did not perform a sensitivity analysis of its input variables. This study uses best available point estimates, when available, or uses conservative or bounding assumptions when best estimates are not available. However, because no uncertainty analysis is performed, the degree of conservatism in the risk estimates cannot be determined.

1.2.2.5 Worker Risk

The PRA methodology developed in this study is patterned after the PRA methodology used for nuclear power plants, which considers public risk. PRAs for reactors, such as those in Reference 3, were performed, in part, to evaluate the extent to which five plants met the NRC's safety goals (Reference 4) for risk to the public. PRAs for reactors and this study do not consider worker risk.

1.2.2.6 Human Reliability

A human reliability analysis (HRA) of loading spent fuel into the MPC, lifting the transfer cask during the handling phase, and welding the MPC when preparing it for storage, was not incorporated into this pilot PRA.

1.2.2.7 Fabrication of the MPC, Transfer Overpack, and Storage Overpack

This study assumes that the cask is fabricated as designed (Reference 2).

- Assumption: The MPC, transfer overpack, and storage overpack are constructed as designed.

Fabrication includes manufacturing and assembly of cask components. While fabrication errors could be modeled and analyzed, this was not done in this study.

Welds made according to accepted standards inherently contain small flaws that depend on the material being welded, the welding materials, and the welding process. Although fabrication errors are not considered in this study, the weld failure evaluation of the MPC does take into account normal flaws that exist in weld-deposited austenitic stainless steel. Statistical distributions describing the densities and sizes of flaws were obtained from results documented in Reference 5.

1.2.2.8 Mis-loading Spent Nuclear Fuel

An HRA to determine the probability of mis-loading spent nuclear fuel into the MPC is beyond the scope of the study for the same reasons discussed in Section 1.2.2.6. Even though the frequency of mis-loading is not estimated, deterministic calculations were performed to investigate the effects of mis-loading on thermal loads, the failure probability of the MPC (Section 8.1), and the possibility for criticality (Section 8.2).

1.2.2.9 Aging Effects

To evaluate possible aging effects, a CASTOR-V/21 dry storage cask was examined for degradation (Reference 6). This cask was produced for testing aging effects on long term dry cask storage. (This cask design was not put into production.) The examination consisted of remote indirect visual examination (cask internal, lid seals, and PWR spent fuel assemblies) and temperature measurements of selected spent fuel assemblies. Interior crud samples were taken and surface gamma and neutron dose rates were measured. Selected fuel rod assemblies were removed from one assembly, visually examined, and subjected to nondestructive, destructive, and mechanical examination. The helium inerting gas was sampled for analysis.

After 14 years of storage, no evidence of degradation that would affect the performance of the cask or integrity of the fuel was evident. The fuel was intact; there was no evidence of creep or rod bow. Crud found on the fuel rods was attributed to oxidized steel while the fuel was in the reactor. None of the oxidation is attributed to dry storage. Fifteen of sixteen stitch welds that attached to borated plates to the basket were cracked. The stitch weld cracking was attributed to the tight fit of the assemblies in the basket, not to storage. Small amounts of air mixed in with the helium were attributed to the process of inerting the cask.

While the results for the CASTOR-V/21 dry cask suggest that there will be no significant aging effects for the subject cask, it is unclear whether the two casks experience similar conditions. Accordingly, except for possible cask and fuel corrosion (see Section 8.3), aging effects are beyond the scope of this study.

1.2.2.10 Combinations of Factors That Could Impact the Probability of MPC Failure

Section 8 discusses several factors that can influence the probability of MPC failure. Individual factors are investigated one at a time with sensitivity studies. It is not expected that combinations of factors will significantly impact the risk estimates.

1.2.2.11 Military Missiles, Sabotage, and Terrorism

Impact of military missiles, sabotage, and terrorism was not incorporated into this pilot PRA.

1.3 Overview of the Risk Calculations

The structure of the risk calculations, as illustrated in Figure 1, closely mirrors the structure of this report. In the figure, boxes indicate analyses, models, and results. The associated section numbers indicate where this report discusses the results needed to estimate risk. Circled numbers are keyed to the discussion below.

The system that is to be modeled consists of the dry cask (MPC, transfer overpack, storage overpack) and the plant layout (load path, floor structure, crane). The structure of the dry cask components is determined from engineering drawings and cask specifications (1). The next step is to describe the secondary containment isolation system (2).

Challenges to the transfer cask and the storage cask are determined from other studies (3), such as Reference 7. The list of initiating events in Reference 7 is a general list that was developed for risk assessments of commercial nuclear power plants. Along with information about the cask system (1) and the subject plant (2), the initiating events are evaluated (4) to derive a list of initiating events (5) that is relevant to the subject cask at the subject site. The frequency of each initiating event in the list is then determined (6) from other reference information (3).

With information about the cask system (1), and information about the plant layout (2), engineering analyses (7) are performed to determine the mechanical loads (8) on the cask that result from initiating events that can occur at the subject site and affect the cask. A mechanical load model (9) is developed with engineering analyses (7). With the mechanical loads for each initiating event, the mechanical load model is used to determine the mechanical stresses (10) in the MPC. The mechanical stresses are then used in a failure model of the MPC (11) to assess the probability of MPC failure (12). The mechanical loads are also used in the fuel failure model (16) to determine the fraction of fuel rods that fail (17).

With information about the cask system (1) and with a list of initiating events (5) that can occur at the subject site and affect the cask, engineering analyses (7) are performed to determine the thermal loads (13). A thermal load model (14) is developed with engineering analyses (7). Given the thermal loads (13), the thermal load model is used to determine the thermal stresses (15) on the MPC and the fuel rods. The thermal stresses are then used in the failure model of the MPC (11) to assess the probability of MPC failure (12) and in the fuel failure model (16) to determine the fraction of fuel rods that fail (17).

From the plant information (2), engineering analyses (7) are performed to assess the reliability of the system to isolate the secondary containment in the event of a release of radioactive material inside the secondary containment. A reliability model (18), is then used to determine the conditional probability that the secondary containment will fail to isolate (19) if the MPC is dropped and fails, releasing radioactive material into the secondary containment.

From other studies (3), source terms (20) are determined. The source terms, adjusted to account for the inventory of radionuclides in the MPC and other information (3) about the plant site (e.g., population

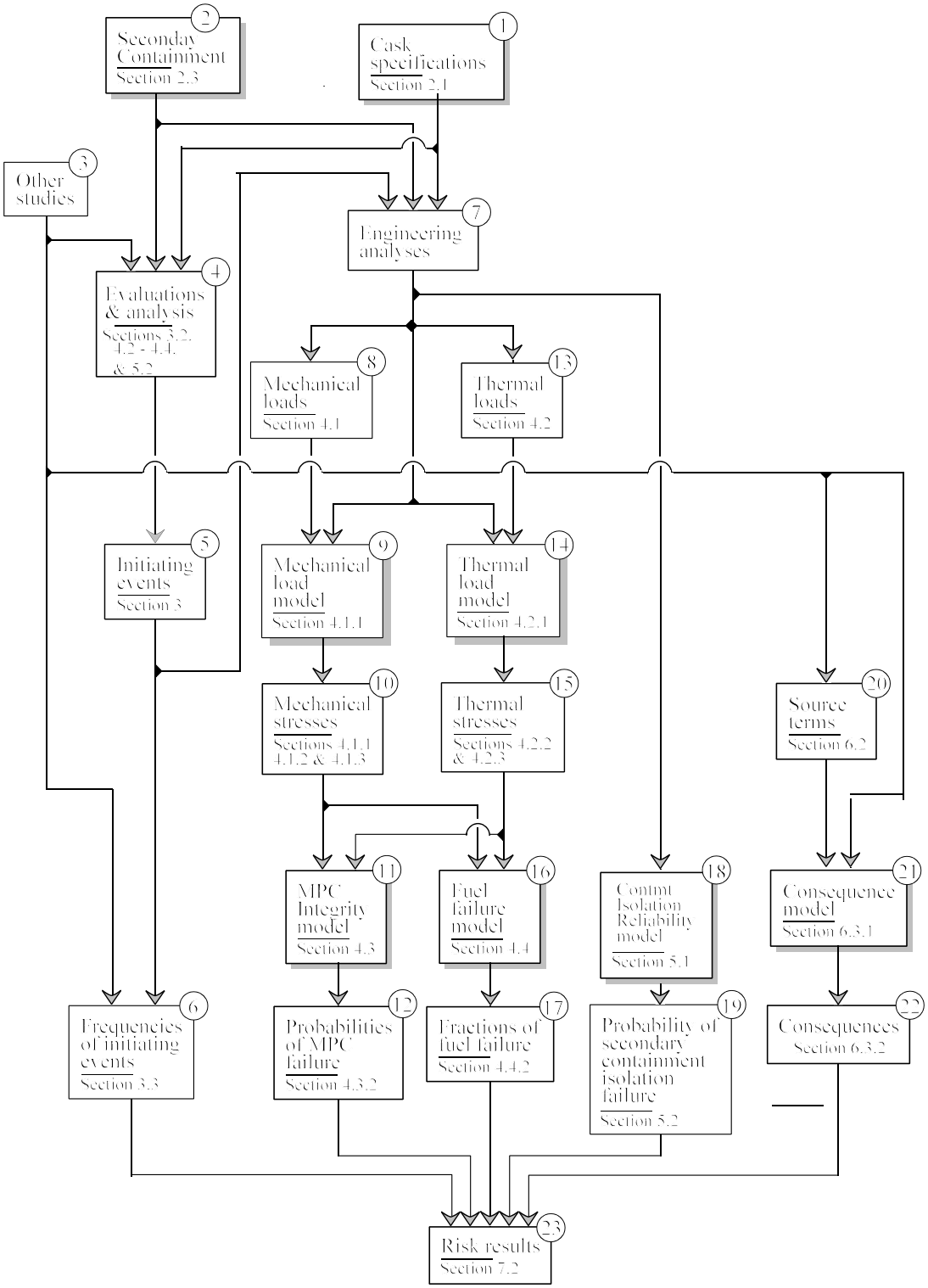

Figure 1. Structure of the Risk Calculations and Organization of the Report

distribution), are then used in a consequence model (21) to estimate the consequences (22) of an accident.

The values needed to assess risk (23) are the frequencies of the initiating events (6), the probabilities of MPC failure (12), the fractions of fuel rods that fail (17), the probability that the secondary containment will fail to isolate (19), and the consequences (22). These five values are combined to calculate the risk to the public.

To quantify the risk, best available point estimates are used. When there is insufficient information or data, conservative bounding assumptions or estimates are used.

1.4 Elements of the PRA

The dry cask storage operation is divided into three phases – handling, transfer, and storage. During the handling phase, spent fuel assemblies are placed into the MPC, within the transfer cask. After the MPC is dried, inerted with helium, and sealed, the transfer cask is lowered through the equipment hatch to the storage overpack on the ground level. The MPC is then moved from the transfer cask into the storage overpack. The transfer phase takes place when the storage cask is moved out of the secondary containment to the storage pad. The storage phase takes place after the storage cask is set down on the storage pad. To analyze the risk of the dry cask storage operation, the phases are divided into 34 stages. A stage is defined as a discrete part of the operation that is convenient for a risk analysis. For example, the height at which the cask is moved and the composition of the surface over which it is moved determine the mechanical load on the MPC if it were dropped, are used to define some of the stages.

A comprehensive list of initiating events is developed, and the risk associated with each initiating event is evaluated. Analyses are performed to determine the response of the cask to the mechanical and thermal loads imposed by the initiating events. For example, the following analyses evaluate the consequences of dropping the transfer cask during the handling phase:

- A mechanical load analysis determines the stresses on the fuel cladding and MPC as a function of drop height.

- Given the stress on the MPC from dropping the transfer cask, failure analyses determine the probability of the fuel cladding and MPC failing.

- Source term analysis is used to determine the releases from the fuel cladding and the MPC.

- An engineering analysis determines the reliability of the secondary containment to isolate if there is an accidental release of radioactivity inside the secondary containment.

The annual risk to the public of handling, transfer, and storage of a single cask is estimated. The risk measures are the individual probabilities of a prompt fatality within 1.6 km (1 mi) and a latent cancer fatality within 16 km (10 mi) of the site. In calculating the annual risks, weather conditions and the population distribution in the vicinity of the site are taken into account. More detailed discussion and basis for emergency planning assumptions are provided in Appendix E. These are the consequence measures that are typically calculated in the risk assessments of nuclear power plants (e.g., Reference 4). Risk to the environment and property are not typically calculated in reactor PRAs and were not done in this study.

2. DRY CASK AND SECONDARY CONTAINMENT SYSTEMS

2.1 Dry Cask System

The Holtec HI-STORM 100 dry cask system consists of a multipurpose canister (MPC) that confines the fuel, a transfer overpack that shields workers from radiation while the cask is being prepared for storage, and a storage overpack that shields people from radiation and protects the MPC during storage. When the transfer overpack contains the MPC, the unit is referred to as the transfer cask. When the storage overpack contains the MPC, the unit is referred to as the storage cask. Details of the cask system are illustrated in Figures 2 and 3. These and other figures are based on drawings in Sections 1 and 8 of Reference 2.

Figure 2 is a composite sketch of the MPC and the transfer overpack. The MPC is 4.8 m (15.8 feet) high and 1.73 meter (5.7 feet) in diameter. When loaded with BWR fuel assemblies, it weighs 36 metric tons (40 tons). The transfer cask is 5.0 meters (16.4 feet) high and 2.3 meters (7.6 feet) in diameter. When loaded with BWR fuel assemblies, the transfer cask weighs 91 metric tons (100 tons). The fuel basket is free standing, but held in position inside the MPC by basket supports. Boral plates along the walls of each cell prevent the spent fuel from becoming critical. Upper and lower fuel spacers keep the fuel assemblies vertically positioned in the basket. Except for the boral plates and the heat conduction elements, all components of the MPC are made of stainless steel. The transfer overpack consists of an inner steel shell, lead shield, and outer steel shell. A water jacket provides additional shielding. The pool lid at the bottom of the transfer overpack seals the inner cavity, thereby retaining clean demineralized water that prevents the exterior of the MPC from being contaminated. A lift yoke (not shown) attaches to lift trunnions on the transfer overpack.

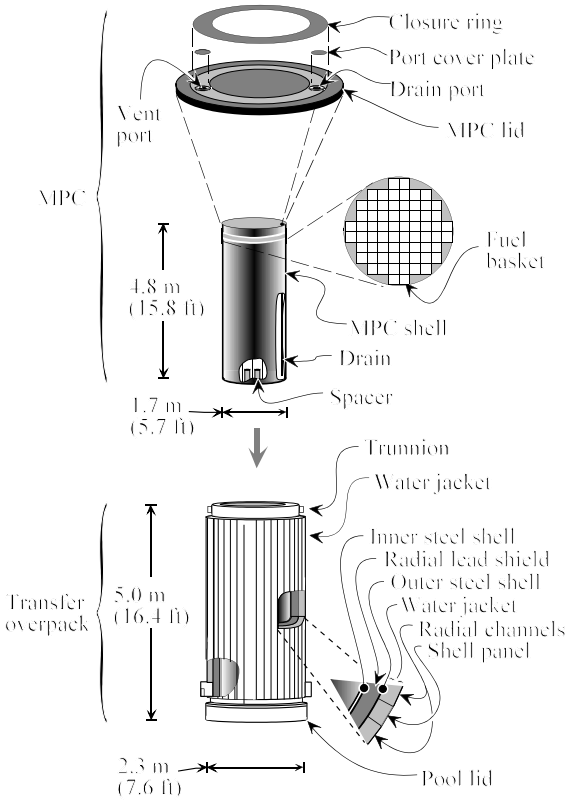

Figure 2. MPC and Transfer Overpack

Figure 3 is a composite sketch of the storage cask with the MPC partially inserted. The overpack consists of inner and outer steel shells connected by full-length steel radial plates that extend from the bottom to the top. The volume between the shells is filled with unreinforced concrete. The shells and the radial plates form the structural member. The concrete is for radiation shielding. The lid is bolted to the overpack at the anchor blocks that are attached to the radial plates. Channels between the overpack and the MPC allow air to circulate, entering the inlet vent at the bottom of the overpack and exiting the outlet vent at the top of the overpack. The channels are designed to progressively collapse during a severe impact, absorbing some of the impact that could be transmitted to the MPC. Shield cross-plates reduce radiation streaming through the vents. Screen covers prevent insects, birds, and animals from entering the vents to build nests that might block the vents.

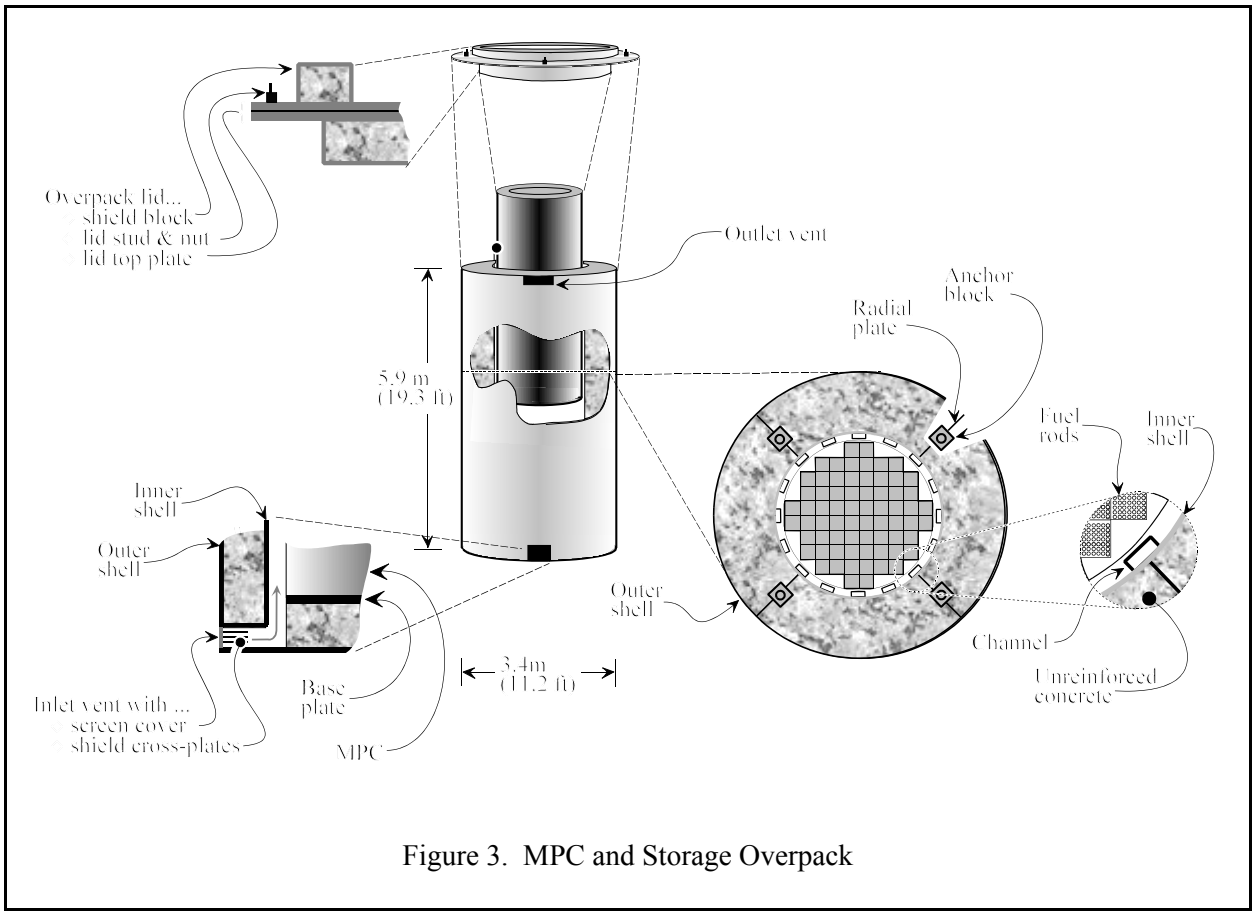

Figure 3. MPC and Storage Overpack

2.2 Stages of the Dry Cask Storage Operation

The dry cask storage operation is divided into three phases – handling, transfer, and storage.

During the handling phase, activities take place on the refueling floor and ground level. From the refueling floor, about 29.9 meters (98.1 feet) above ground level, the transfer cask is lowered about 13 meters (42.7 feet) to the bottom of the cask pit next to the spent fuel pool. There, the dry cask storage operation begins when spent fuel assemblies are loaded into the MPC. After the basket of the MPC is full and the lid is installed, the transfer cask is lifted out of the spent fuel pool and moved to a preparation area on the refueling floor. The MPC is drained, dried, inerted, and sealed. After other preparations, the transfer cask is lowered to the storage cask, still inside the secondary containment. The MPC is then lowered from the transfer cask to the storage cask.

After the Kevlar stays and the alignment device are removed, the storage cask, with the MPC inside, is moved through an airlock to outside the secondary containment. Here the transfer phase begins. The storage cask is moved away from the secondary containment where final preparations are made before it is moved to the storage pad with a specially designed tractor called an overpack (cask) transporter. There, the storage cask is set down in a predetermined location that is indicated by paint marks on the storage pad. The predetermined storage footprint ensures that the storage casks are adequately spaced and their weight is properly distributed over the storage pad.

During the storage phase, storage casks remain on the storage pad for 20 years. The storage cask does not have, nor does it require, instruments or other mechanisms to detect heat loads or leaks in the MPC. Routine surveillance is done to ensure the vents remain unblocked.

The handling, transfer, and storage phases of the dry cask storage operation are divided into 34 stages, as listed in Table 1. Figure 4 is a schematic diagram illustrating the movement of the transfer cask and the storage cask through the stages in Table 1 as the MPC is moved from the spent fuel pool to the independent spent fuel storage installation (ISFSI), where the storage pads are located. The numbers along the paths in Figure 4 correspond to the stages in Table 1. A stage is defined as a discrete part of the operation that is convenient for risk analysis. Examples of factors used to define different stages include the following:

- the height at which the cask is carried
- the direction in which the cask is moved
- the rigging of the cask
- the surface (e.g., concrete, asphalt, gravel) over which the cask is moved

These phases described above reflect the process used at the particular plant site which served as the basis for this study. Terminology may vary to some extent from plant to plant, so in such cases the reader is advised to compare their terminology with the way in which the terms are used in this report.

Table 1. Stages of the Dry Cask Storage Operation

Stages		Height [A] m	Height [A] ft
1	Loading fuel assemblies into the MPC [B]	4.8	16
2	Placing MPC lid onto MPC and engaging lift yoke on transfer cask [©]	0	0
3	Lifting the transfer cask out of the cask pit	13	42.5
4	Moving the transfer cask over a railing of the spent fuel pool	0.9	3
5	Moving the transfer cask to the preparation area (1st segment).	0.3	1
6	Moving the transfer cask to the preparation area (2nd segment)	0.3	1
7	Moving the transfer cask to the preparation area (3rd segment)	0.3	1
8	Lowering the transfer cask onto the preparation area [D]	0.3	1
9	Preparing (drain, dry, inert, seal) the MPC for storage	0	0
10	Installing the short stays and attaching the lift yoke [D]	0	0
11	Lifting the transfer cask	0.6	2
12	Moving transfer cask to exchange bottom lids of transfer cask (1st segment)	0.6	2
13	Moving transfer cask to exchange bottom lids of transfer cask (2nd segment)	0.6	2
14	Replacing the pool lid with the transfer lid	0.1	1/4
15	Moving the transfer cask near the equipment hatch	0.6	2
16	Holding the transfer cask	0.6	2
17	Moving the transfer cask to the equipment hatch	0.6	2
18	Lowering the transfer cask to the overpack through the equipment hatch	24.4	80
19	Preparing (remove short stays, disengage lift yoke, attach long stays) to lower MPC	0	0
20	Lifting MPC and opening doors of transfer lid	5.8	19
21	Lowering MPC through the transfer cask into the storage cask	5.8	19
22	Moving the storage cask into the airlock on Helman rollers	0	0
23	Moving the storage cask out of the airlock on Helman rollers	0	0
24	Moving storage cask away from secondary containment on Helman rollers	0	0
25	Preparing (install lid, vent shield cross-plates, vent screens) storage cask for storage	0	0
26	Lifting the storage cask above the Helman rollers with the overpack transporter	0.1	1/4
27	Moving the storage cask above a cushion on the preparation area	< 0.1	<1/4
28	Holding the storage cask above the cushion while attaching a Kevlar belt	< 0.1	<1/4
29	Moving the storage cask above the concrete surface of the preparation area	0.3	1
30	Moving the storage cask above the asphalt road	0.3	1
31	Moving the storage cask above the gravel surface around the storage pads	0.3	1
32	Moving the storage cask above the concrete storage pad	0.3	1
33	Lowering the storage cask onto the storage pad	0.3	1
34	Storing the storage cask on the storage pad for 20 years	0	0

[A] Height is the distance the cask would fall if support system failed.

[B] Prior to Stage 1, MPC is inserted into the transfer cask, and after other preparations, lowered into the cask pit. The storage overpack is placed on Helman rollers and moved under the equipment hatch.

[©] Lift yoke attaches to the trunnions of the transfer cask.

[D] Stays attach to the lift yoke on one end and cleats of the MPC on the other end.

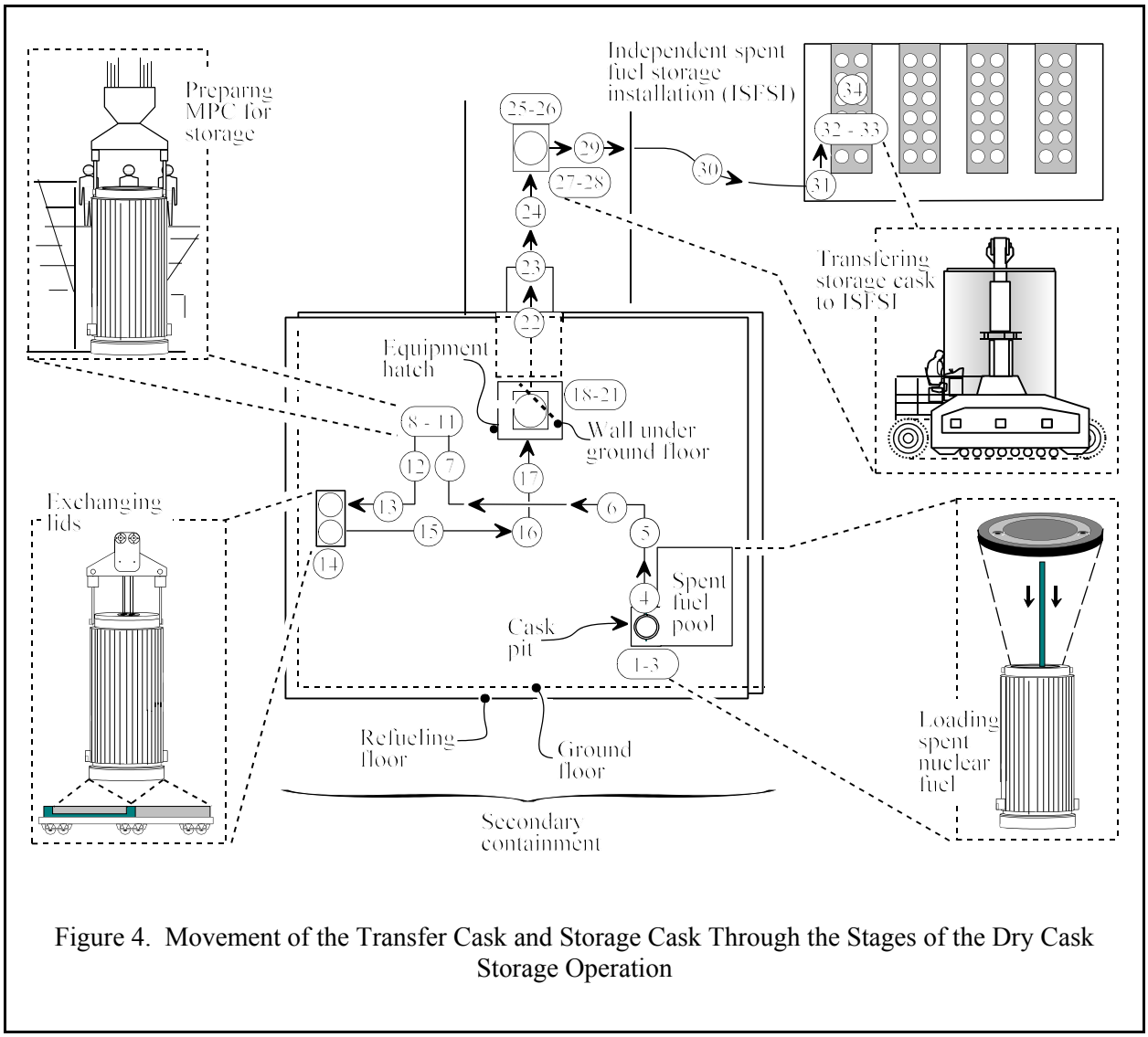

Figure 4. Movement of the Transfer Cask and Storage Cask Through the Stages of the Dry Cask Storage Operation

Figure 5 shows a vertical view of the stages where the transfer cask is in the equipment hatch. Except for the floor thicknesses, the vertical axis is drawn to scale; the inset shows the wall supporting the overpack at ground level. The steel beams and concrete walls supporting the refueling floor along the path where the transfer cask is carried are not shown. The lift height is kept to the minimum necessary to clear obstacles on the floor, such as railings, pipes, and raised edges of floors.

Variations in the lift height and path that the transfer cask or storage cask are normally carried are considered uncertainties. Uncertainty is beyond the scope of this study (see Section 1.2.2.4).

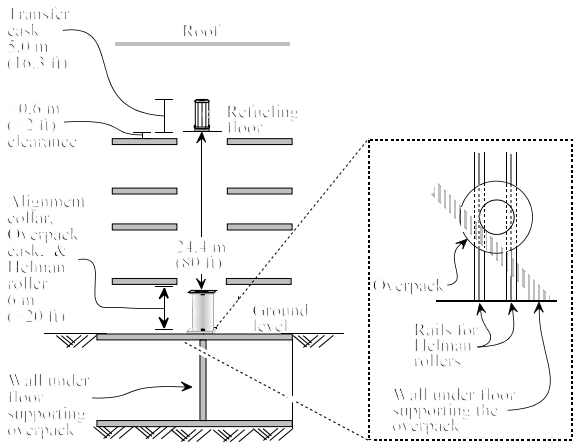

Figure 5. Vertical View of the Equipment Hatch and Detail of the Ground Floor

<u>Pre-stage conditions and preparations prior to Stage 1</u>

The secondary containment is closed because the reactor is at full power. The normal slightly negative pressure inside the secondary containment is established.

The storage overpack is on Helman rollers on the ground floor underneath the equipment hatch.

The MPC is inserted into the transfer overpack (transfer cask). After the MPC is filled with water, the transfer cask is lowered into the cask pit, an alcove of the spent fuel pool.

Gates between the spent fuel pool and the cask pit, above the level of the fuel, have been removed to allow movement of spent fuel assemblies from the spent fuel pool into the MPC inside the empty transfer cask in the cask pit. After the MPC is filled with 68 spent fuel assemblies, the gates are replaced and the MPC lid is placed on the MPC.

The analysis has used the following assumptions:

- The secondary containment remains closed during the handling phase.
- The transfer cask and storage cask are carried at the heights specified in the formal procedures (see Table 1).
- The transfer cask is carried along the load path over the refueling floor of the secondary containment.
- The storage cask is carried along the designated route to its placement on the storage pad in the ISFSI.

<u>Stages 1 - 3</u>

In Stage 1, fuel assemblies are placed inside the basket of the MPC. Specific assemblies are loaded into specific spaces of the basket to take advantage of the shielding, criticality control, and heat rejection capabilities of the cask system. After the MPC is loaded with spent fuel assemblies, the MPC lid is installed to shield workers from radiation emanating from the top (the transfer cask shields workers from radiation emanating from the sides and bottom). The lift yoke is engaged on the trunnions of the transfer cask (Stage 2). The transfer cask is lifted out of the cask pit to about 13 meters (43 feet) above the bottom of the cask pit where it is rinsed with clean water (Stage 3).

Stages 4 - 7

The transfer cask is moved over the cask pit to clear a railing and a pipe (Stage 4), then lowered to about 0.3 meters (1 feet) as it is moved along a predetermined path to the preparation area. The load path of the refueling floor is supported by steel beams and walls such that it can hold a static load of 125 tons. The load path to the preparation area consists of three perpendicular segments.

Stages 8 -13

At the preparation area, the transfer cask is lowered to the refueling floor (Stage 8) where the MPC is prepared for storage (Stage 9). The MPC is partially drained. After the lid is welded to the shell of the MPC, the MPC is filled with water to hydrostatically test the weld. The water is drained and the MPC is dried. The MPC is purged and filled with helium. A port cover and drain cover are welded to the lid. The closure ring is welded to the lid and the shell for redundant sealing. The top lid of the transfer cask is installed and bolted to the transfer overpack.

After the MPC is prepared, the transfer cask is rigged to move (Stage 10). While the yoke is over the cask with the holes of the arms below the trunnions, rigging personnel, on scaffolds, install the short Kevlar stays. Kevlar support stays are attached from the lift yoke through an access hole in the top lid of the transfer cask to cleats on the MPC. In Figure 6, the body of the yoke is close to the transfer cask so the stays are slack while being attached to the cleats. As the yoke is raised, the stays become taut, lifting the MPC off of the pool lid. When the holes of the arms are next to the trunnions, the yoke arms are placed over the trunnions. The lift yoke is attached to the trunnions. The transfer cask is lifted about 0.6 meters (2 feet) above the refueling floor (Stage 11). The transfer cask is moved along a load path to another area of the refueling floor (Stages 12 and 13).

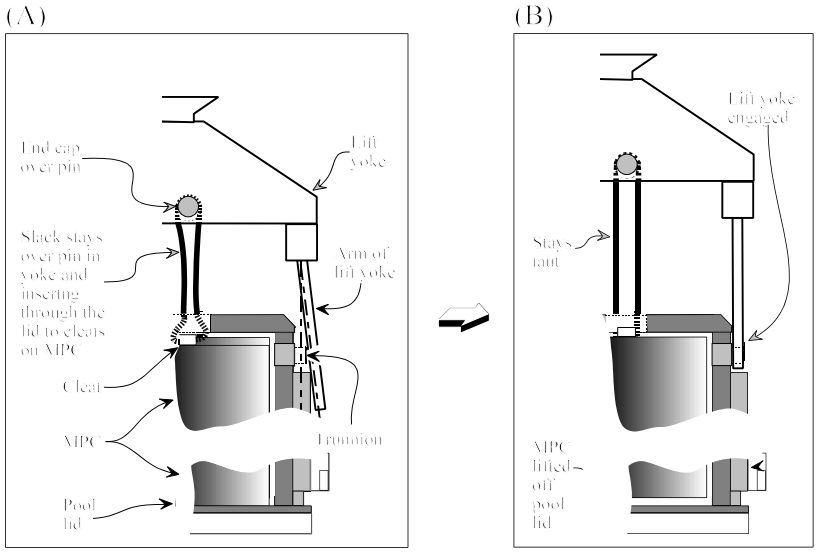

Figure 6. Lift Yoke with Stays Attached (A) Prior to and (B) after Engaging the Yoke Arms on the Trunnions

Stages 14 - 22

The pool lid at the bottom of the transfer cask is replaced by a transfer lid (Stage 14) for use in Stage 20. The transfer lid is on a carriage. Short stays hold the MPC above the pool lid inside the transfer cask. The transfer cask is set down in the empty side of the carriage. The pool lid is unbolted. The transfer cask is then raised slightly. The carriage is moved to bring the transfer lid underneath the transfer cask. The transfer cask is lowered and the transfer lid is bolted to the transfer cask shell. The bottom lid exchange is illustrated in Figure 7. With the transfer lid attached, the transfer cask is lifted to a height of about 0.6 meters (2 feet) above the refueling floor and moved (Stage 15) to a holding area near the equipment hatch (Stage 16).

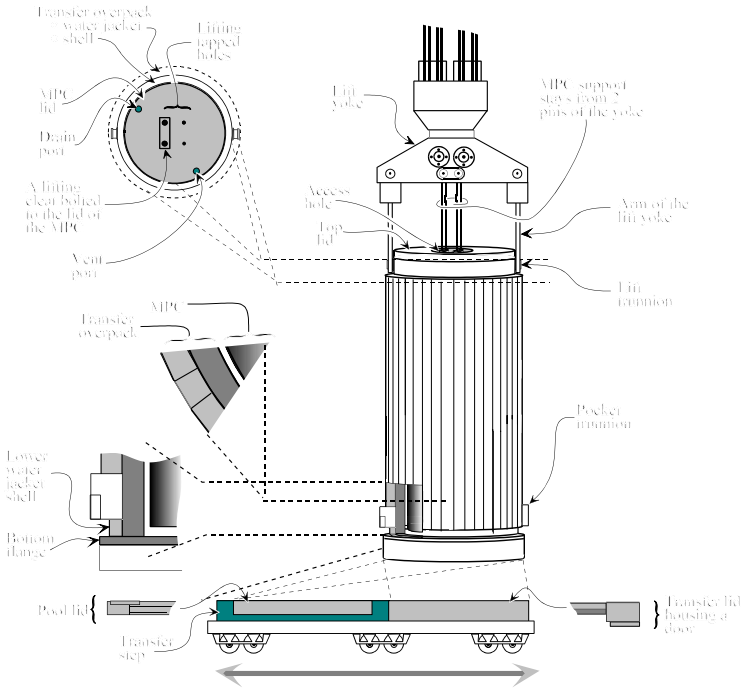

Figure 7. Replacing the Pool Lid with the Transfer Lid

The transfer cask is held while preparations are made on the ground floor to receive the transfer cask. The transfer cask is then moved to the equipment hatch (Stage 17). The height is sufficient to clear a raised lip around the hatch on the refueling floor. The transfer cask is then lowered through the equipment hatch of the refueling floor, 80 feet to the top of the storage overpack (storage cask) at ground level (Stage 18). Two workers assist in guiding the transfer cask onto the storage cask. An alignment device (i.e., collar on the storage cask) has receptacles that determine the correct position of the transfer cask on the storage cask. The lift yoke is removed and the short stays are replaced with long stays, which are used to lift the MPC off the transfer lid (Stage 19). After the MPC is lifted several inches off the transfer door by the Kevlar stays (Stage 20), the transfer doors are opened, and the MPC is lowered into the storage cask (Stage 21). As it is lowered, the MPC is guided by the transfer cask and, when in the storage cask, by channels in the storage cask. Once lowered, the MPC comes to rest on the pedestal inside the storage cask. The storage cask is moved along tracks on Helman rollers into the airlock of the secondary containment (Stage 22). The movement is accomplished by pulling the storage cask with a diesel-powered rail vehicle called the trackmobile. The airlock is needed to maintain the negative pressure inside the secondary containment that is developed by the ventilation system.

Stages 23 - 28

The trackmobile continues to pull the storage cask from the airlock, outside the secondary containment (Stage 23). The storage cask is moved a short distance outside the secondary containment, still on the Helman rollers (Stage 24), to an area where the storage cask is prepared for storage (Stage 25). The storage cask lid is installed. Shield cross-plates are inserted into the vents on the top and bottom of the storage cask, and screens are installed over the vents. Cleats are bolted to the top of the storage cask. A transporter is moved up to the storage cask, and the lift yoke is attached to the cleats. The lift yoke is engaged and the storage cask is lifted about 0.3 meters (1 feet) above the ground (Stage 26). Four pins are inserted into the hydraulic lifting mechanism of the storage cask transporter to lock them. The hydraulic mechanism is deactivated, bringing the weight of the storage cask onto the four pins. The storage cask is moved over a cushion (Stage 27). While it is held over the cushion (Stage 28), a Kevlar belt is wrapped around the midline of the storage cask keep the storage cask from swaying while being moved to the ISFSI.

Stages 29 - 33

The storage cask is moved by the transporter about 0.6 km (about 0.4 mi) from the reactor building at a speed of about 0.64 km/hr (0.4 mi/hr). This travel begins on concrete (Stage 29). The road from the preparation area to the ISFSI is asphalt (Stage 30). Inside the ISFSI, the road between the storage pads is gravel (Stage 31). The transporter travels along the gravel road and pivots next to the place on the storage pad where the storage cask will be placed. The storage cask is then moved onto the concrete storage pad (Stage 32). The storage cask is set down on the concrete storage pad in a predetermined location (Stage 33).

Stage 34

Storage casks are kept in the ISFSI. The ISFSI of the subject plant has four concrete pads. Each pad holds 12 storage casks. Storage casks are placed on the pads in a pattern that distributes their weight. Paint marks on the concrete indicate where each storage cask is to be placed.

2.3 Secondary Containment Isolation System

Stages 1 through 22 (Table 1) occur inside the secondary containment. The secondary containment is a large concrete structure that encloses the refueling and spent fuel pool areas, both reactor units, and associated equipment rooms and areas. The secondary containment has a total free volume of approximately 84,951 m^3 (3×10^6 ft^3). The atmosphere inside is cooled by four heating, ventilation, and air conditioning (HVAC) systems.

If a release of radioactive material were to occur inside the secondary containment following a drop of the transfer cask, three distinct functions would occur: detect radioactive material, isolate the secondary containment, and operate the standby gas treatment system (SGTS). Each of these functions is accomplished by redundant and independent trains of systems. The release of radioactive material is detected by one or more of six detector systems that signal the containment to isolate. Each of these detector systems consists of two trains, each train having two detectors. Both detectors in a train must detect radiation to isolate the containment. Only one of the 12 trains is needed to isolate the secondary containment.

The radiological monitoring system for the secondary containment is part of the process radiation monitoring system. Table 2 shows the process and effluent radiological monitors of the secondary containment. This table provides a brief description of each radiological monitor in these systems.

Table 2. Detectors in the Secondary Containment System

Location	Purpose	Principal Radionuclides Detected
Reactor building ventilation stack	Monitor discharge to environment	Kr-85m, Kr-87, Kr-88, Xe-135
Main stack	Monitor discharge to environment	Ar-41, Xe-133
Reactor building ventilation exhaust	Isolate building and initiate SGTS	Kr-85m, Kr-87, Kr-88, Xe-135
Reactor building ventilation filter discharge	Monitor filter exhaust	Kr-85m, Kr-87, Kr-88, Xe-135
Refueling floor zone ventilation exhaust	Isolate building and initiate SGTS	Kr-85m, Kr-87, Kr-88, Xe-135
Refueling floor ventilation filter	Monitor filter exhaust	Kr-85m, Kr-87, Kr-88, Xe-135
Standby gas treatment system	Monitor process duct	Ar-41, Xe-133

Table 3. Volumetric Flow Rates of Secondary Containment Ventilation

		HVAC					
		Supply		Exhaust		SGTS	
		m^3/min	ft^3/min	m^3/min	ft^3/min	m^3/min	ft^3/min
Unit 1	Refueling Area	850	30000	905	31970		
	Rx Bldg Accessible	1699	60000	850	30000	85	3000
	Rx Bldg Inaccessible			950	31970		
Unit 2	Refueling Area	850	30000	905	31970		
	Rx Building	170	6000	170	6000	113	4000
	Total:	3568	126000	3735	131910	198	7000

Normally, the HVAC systems ventilate the secondary containment, maintaining a slight negative pressure inside with respect to the outside environment. If the containment is opened to atmosphere, fans will trip on overload as they throttle to maintain the negative pressure, and indicators will alarm in the control room. Table 3 shows that total exhaust flow rates are greater than total supply flow rates, to maintain a negative pressure in the secondary containment. The difference in the flow rates is due to leakage through cracks and joints into the secondary containment. The SGTS is normally in a stand-by mode. If a small amount of radioactive material is released into the accessible area (where people are working), then the exhaust of this area isolates, and flow is redirected to the inaccessible area where it is filtered before being exhausted. This arrangement utilizes the more effective filters on the exhausts of the inaccessible area ventilation system and avoids isolating the entire secondary containment when small amounts of radioactive material are released in the secondary containment, as would be expected during normal plant operations. If a larger amount of radioactive material passes through the filter, radiation monitors signal the HVAC systems to isolate the entire secondary containment.

In the event of a breach of the MPC and release of radioactive material into the secondary containment building after a transfer cask drop, the HVAC system is designed to isolate the secondary containment to prevent the release of radioactive material to the environment. The containment is isolated by stopping the HVAC fans and closing one of two serial isolation valves located on each HVAC supply and exhaust duct. One isolation valve is located inside and the other is located outside the secondary containment. While all HVAC fans receive an isolation signal, six of the twelve detector trains will generate an isolation signal for the inside isolation valves while the other six detector trains will generate an isolation signal for the outside isolation valves. This arrangement allows for independence between the two serial isolation valves and their isolation trains.

Each SGTS consists of two trains of filters and exhaust fans. Both trains of both SGTSs receive a start signal from any one of the 12 detector trains. While the capacity of both SGTSs is not enough to overcome the flow generated by a single operating HVAC fan (supply or exhaust), only one SGTS is needed to mitigate an uncontrolled and unfiltered release with all HVAC fans off. Even if the isolation valves fail to close, the containment effectively isolates if all fans are off and either SGTS operates.

3. INITIATING EVENTS

3.1 List of Initiating Events

An initiating event is a disturbance in the normal operation of the dry cask storage system which could potentially lead to a release of radioactive material to the environment. For this study, a comprehensive list of initiating events was developed. Those initiating events that could not affect the subject plant, the transfer/storage cask or the MPC were eliminated from further consideration. For the remaining initiating events, estimates of their frequencies, probability of MPC failure, and consequences were developed.

Tables 4, 5, and 6 are lists of initiating events during the handling, transfer, and storage phases, respectively, at the subject plant. The initiating events were identified from Reference 7, and from design and operational data for the specific cask and plant being studied. Information on the design of the cask system was obtained from licensing documents (e.g., Reference 2). Analysts visited the subject plant to observe the operation and equipment used during the handling, transfer, and storage phases. Written descriptions of the procedures were obtained and studied, and additional details were obtained through discussions with plant personnel.

The lists of initiating events were reviewed by NRC staff who had reviewed and licensed the dry cask storage system. This review drew upon extensive knowledge and diverse perspectives on the cask system. Based on these reviews and the process used to construct the list, Tables 4, 5, and 6 are believed to be a complete list of all initiating events that could conceivably affect the cask system.

The initiating events represent potential challenges to the confinement function of the cask. They are grouped by operational phase (i.e., handling, transfer, storage) and by type of load placed on the cask (i.e., mechanical and thermal).

In Tables 4, 5, and 6, initiating events that are marked with an × under the status column have a risk of zero, either because the frequency is zero for the subject site, or the probability of the MPC failing is zero, or the fraction of the fuel failing is zero. If any one of these parameters is zero, the risk is zero.

Table 4. Initiating Events During the Handling Phase and Section Where Frequency, MPC Failure, and Fuel Failure Are Discussed

Mechanical Events	**Status**	**Frequency**	**MPC failure**	**Fuel failure**
Drop of the Transfer Cask				
Into the cask pit		3.3.2	4.1.2.1	4.4
Cask tip-over		3.3.2	4.1.2.2	4.4
Onto storage overpack		3.3.2	4.1.2.3	4.4
Onto concrete floor		3.3.2	4.1.2.4	4.4
Onto refueling floor		3.3.2	4.1.2.5	4.4
Drop of the MPC into the storage overpack		3.3.2	4.1.2.6	4.4
Thermal Events				
Fire from diesel fuel in the trackmobile	X		4.2.1.2	

LEGEND: X indicates that the initiator does not affect the subject plant or does not breach the MPC.

Initiating events that are not predicted to occur due to physical limitations are not included in the list of initiating events. For example, water level from the hypothetically largest possible storm, along with

three dams failing, and 35 mph winds causing waves, is not predicted to reach the ISFSI. Because this is the largest conceivable flood height, flooding is excluded as an initiating event.

A zero probability of the MPC failing means that based on the weld failure data and methodology discussed in Appendix B, and the MPC maximum stress (strain) levels calculated in Appendix A, the probability of weld failure is less than $1x10^{-6}$ for the mechanical load event.

Table 5. Initiating Events During the Transfer Phase and Section Where Frequency, MPC Failure, and Fuel Failure Are Discussed

Mechanical Events	Status	Frequency	MPC failure	Fuel failure
Drop of the Storage Cask				
On concrete	X		4.1.3.1	4.4
On asphalt	X		4.1.3.1	4.4
On gravel	X		4.1.3.1	4.4
Tip-over of the Storage Cask				
While the cask is being moved	X	4.1.3.1	4.1.3.2	4.4
Cask impacted by a vehicle	X	4.1.3.1	4.1.3.2	4.4
Thermal Events				
Fire from diesel fuel in trackmobile	X		4.2.1.2	
Fire from diesel fuel in cask transporter	X		4.2.1.2	

LEGEND: × indicates that the initiator does not affect the subject plant or does not breach the MPC.

Reference 8 describes the modeling of the individual risk of prompt fatality, using a two parameter Weibull function. In the model, zero probability of a prompt fatality is typically assumed at doses below a threshold of 150 Rem to the red bone marrow and 500 Rem to the lungs. A "prompt" fatality can be described as any death which occurs as a result of a large acute total body exposure sufficient to cause one or more of three major classes of fatal syndromes (Reference 9): cerebrovascular syndrome – death within 30 to 50 hours from exposures of about 100 Gy (10,000 Rads), gastro-intestinal syndrome – death within about 9 days from exposures of about 10 Gy (1000 Rads) and hematopoietic (bone marrow death) – death in several weeks from exposures of 2.5 to 8 Gy (250 to 800 Rads). While a single threshold value is not easily cited as that exposure below which there is zero probability of prompt fatality, the assumption discussed above is consistent with the findings discussed in Reference 9. The levels of exposure that could result from the events considered in this study do not approach those which would be of concern for "prompt" fatality.

Two general models were considered relative to the probability of latent cancer fatalities. The linear threshold model predicts that doses below a threshold do not cause latent cancer fatality. The linear no-threshold model predicts a probability of a latent cancer fatality that is proportional to dose. In the current study, the no threshold model is used.

Table 6. Initiating Events During the Storage Phase and Section Where Frequency, MPC Failure, and Fuel Failure Are Discussed

Mechanical Events	Status	Frequency	MPC failure	Fuel failure
Water currents during a flood	X	3.2.1		
Tsunamis	X	3.2.2		
Seismic events		3.3.3	4.1.3.2	
Volcanic activity	X	3.2.3		
High winds	X	3.3.4	4.1.3.2	
Soil erosion from intense precipitation	X	3.2.4		
Strikes from heavy objects				
Aircraft		3.3.7	4.1.3.3	
Wind-driven objects	X		4.1.3.3	
Heavy objects in flood waters	X	3.2.1		
Vehicle	X		4.1.3.3	
Meteorite		3.3.5	3.3.5	
Shockwaves from explosions				
Pipelines	X		4.1.3.4	
Nearby trucks and railcars	X		4.1.3.4	
Transformers	X	3.2.5		
Nearby barge	X	3.2.5		
Storage tanks	X	3.2.5		
Military missile	X	3.2.5		
Other facilities	X	3.2.5		
Thermal Events				
Vent Blockage				
Flood water over vents but below MPC	X	3.2.1		
Flood water over vents contacting MPC	X	3.2.1		
Flood water over vents submerging MPC	X	3.2.1		
Snow	X		4.2.1.2	
Ice	X		4.2.1.2	
Hail	X		4.2.1.2	
Intense precipitation	X		4.2.1.2	
Dirt & debris from winds	X		4.2.1.2	
Dirt from landslide due to heavy rains	X		4.2.1.2	
Dirt from landslide due to volcanic activity	X		4.2.1.2	
Volcanic ash deposits	X		4.2.1.2	
Accumulations or biological intrusions	X		4.2.1.2	
Lightning	X	3.3.6	4.2.2.2	
Fire causes pressurization or differential heating				
Fire from aircraft fuel	X	3.3.7	4.2.1.2	
Fire from burning barge contents	X		4.2.1.2	
Fire from site specific materials	X		4.2.1.2	
Fire from a gas main	X		4.2.1.2	
Forest Fire	X		4.2.1.2	

LEGEND: X indicates that the initiator does not affect the plant or does not breach the MPC.

If an uncertainty analysis were performed, then some of the risks shown in Tables 4, 5, and 6, which are zero, might become positive, but would still be extremely small. However, such an analysis is beyond the scope of this study.

The initiating events that can occur during the handling phase are shown in Table 4. When the cask is lifted out of the cask pit (Stage 3) and moved (Stages 4 through 8) to the preparation area, the lid of the MPC is on, but not welded. MPC failure is not an issue because the MPC is unsealed. Since the MPC is filled with water, for any fuel cladding failure that may occur during these stages, the fuel particulate would be scrubbed since the gap release passes through the water in the MPC. In a case of a tip-over there is no cladding failure. In Stage 8, the transfer cask is lowered to the preparation area where the MPC is prepared for storage (Stage 9). In Stages 11 through 18, the transfer cask is prepared and lowered to the storage overpack on the ground floor. In Stage 18, the height of a drop from the equipment hatch to the top of the storage cask is about 80 feet. The probability of the MPC failing when the transfer cask is dropped 80 feet onto the storage overpack is 0.0002, based on a weld failure probability distribution and stain values produced by LS-DYNA analyses of drops from various heights. (See Appendix A for details.) In Stage 19, the transfer cask is resting on the storage cask where the rigging is changed to lower the MPC into the storage cask. While the transfer cask is on the storage cask, it cannot be dropped. Momentum calculations show that it cannot be tipped over.

After rigging the MPC, the MPC is lifted off of the transfer lid doors (Stage 20) and lowered into the storage cask (Stage 21). The drop height is as high as 5.8m (19 ft). The probability of the MPC failing when dropped 5.8m (19 ft) into the storage cask is 0.28, based on a weld failure probability distribution and strain values produced by LS-DYNA analyses of drops from various heights. This drop of the MPC by itself into the storage overpack produces a much higher calculated probability of MPC failure compared to the 80 foot drop of the transfer cask containing the MPC, an indicator of the protection afforded to the MPC by the transfer cask during an accidental load drop. The mass and ruggedness of the transfer cask locally crushes any target it impacts. This crushing acts as an impact limiter to absorb large amounts of kinetic energy, which, in turn, significantly limits the strain levels in the MPC. On-the-other-hand, the drop of the MPC into the storage overpack is a very hard impact where virtually all of the MPC kinetic energy is absorbed by the MPC shell. This results in the higher strains in the MPC and a higher probability of failure.

The storage cask is on rollers when it receives the MPC. The rollers allow the storage cask to be moved inside an airlock of the secondary containment (Stage 22). The storage cask cannot be dropped during this process. Stage 22 is the last stage in the handling phase.

In the assessment of the risk from the dry cask storage operation, only a single initiating event is postulated to occur at a time during an otherwise normal operation. For example, the assessment does not account for multiple initiating events, such as:

- aircraft crashes that might damage the secondary containment during an initiating event in the handling phase
- seismic event during the handling phase

Neither does the analysis take into account certain other circumstances, such as the following:

- The containment is normally closed (Section 5.1). The effect of the containment inadvertently being opened is not addressed.

Even though such simultaneous occurrences could increase the consequences, the incremental risk is negligible because the incremental frequency of such events occurring simultaneously is minuscule.

The initiating events during the transfer phase are shown in Table 5. Stage 23 begins the transfer phase when the storage cask is moved out of the secondary containment airlock and away from the secondary containment. As in Stage 22, the storage cask is on rollers, and cannot be dropped. In Stage 25, the storage cask is being prepared for storage before it is moved to the ISFSI. During Stages 26 though 32, the storage cask is lifted above the rollers, over a cushion, and then transferred over concrete, asphalt, and

gravel surfaces before being set down on the concrete storage pad (Stage 33). The transfer phase ends in Stage 33 with the storage cask being set down on the storage pad. During the transfer phase, the cask is lifted no more than 0.3 meters (1 foot) above the surface level. At this height, the failure probability of the MPC is zero.

The initiating events that can occur during the storage phase are shown in Table 6. There is only one stage, Stage 34, but many postulated initiating events.

3.2 Initiating Events that Cannot Affect the Subject Plant

3.2.1 Floods

The flooding analysis at the subject plant is based on the probable maximum precipitation (PMP), which is defined as the "theoretically greatest depth of precipitation for a given duration that is physically possible over a particular drainage area at a certain time of the year." The National Weather Service determines the maximum precipitation by maximizing the parameters of a hypothetical storm over a drainage area. The maximum is called "probable" because there is a chance, albeit unknown, that a storm could be more severe. However, to the extent that the maximum can be determined, the PMP is the most severe case.

To obtain the PMP for the subject site, the rainfall from a hurricane that occurred in Florida during 1916 was considered to occur at the drainage basin at the subject site. The storm was analytically positioned within meteorological limits over the drainage basin so as to result in the maximum volume of precipitation at the subject site. The 19 inches of rain produced an estimated volumetric flow rate of 17,330 m^3/s (612,000 ft^3/s). A stage-discharge model was developed from the limited amount of data. From the models, a peak discharge of 17,330 m^3/s (612,000 ft^3/s) is expected to result in a flood stage of 32 meters (105 feet).

Hydrologists also determined the effects of winds to create waves. The maximum sustained wind was taken to be 72 km/hr (45 mph). From these winds, a maximum wave height of 2.0 m (6.5 ft) (crest to trough) was predicted. The wave crests would add 1.0 m (3.3 feet) to the maximum flood stage of 32 m (105 ft).

In the drainage basin, two dams are in series. A third dam is in parallel with the other dams. A break of the lower serial dam would add about 2,832 m^3/s (100,000 ft^3/s) to the flood waters at the subject site. This would increase the water level by about 1.2 m (4 ft). If both serial dams failed, the predicted wave would be 1.5 meters (5 feet). If the parallel dam failed instead, a wave of 1 ft is predicted. Combining all of these effects results in a maximum flood height of 35 m (114 feet).

Reference 10 requires that the flood analysis at plants be updated using revised maximum precipitation estimates from Reference 11. The largest hypothetical storm in the drainage area for the subject site has a duration of 72 hours and produces 63.0 cm (24.8 inches) of rain. Given that a storm of 19 inches produced a volumetric flow rate of 17,330 m^3/s (612,000 ft^3/s), 63.0 cm (24.8 inches) of precipitation would produce a volumetric flow rate of 22,625 m^3/s (799,000 ft^3/s). According to the previously determined relation of flood stage to flow rate, a flood stage of 33 meters (110 feet) would result. Sustained winds of 28 km/hr (45 mph) would raise the flood stage by about 1 meter (3.3 feet). Dam failure would result in waves at the subject site of 0.3 to 1.5 meters (1 to 5 feet). Therefore, the maximum flood height is 36 meters (119 feet).

The ISFSI is at an elevation of 38 meters (126 feet). The flood waters from a combined maximum storm, sustained winds, and dam failures would be insufficient to reach storage casks on the storage pad.

3.2.2 Tsunamis

Tsunamis, the large ocean waves resulting from earthquakes originating near or in the ocean, occur mainly in the Pacific Ocean where they can threaten shoreline areas such as the west coast of Washington, Oregon, and California in the United States. Historically, there have been some tsunamis in the Carribean but none on the East Coast that could conceivably affect the subject storage site. The U.S. National Oceanic and Atmospheric Administration states that tsunamis typically lose their energy within 8.5 km (5 mi) due to frictional losses and impact with trees, vertical land masses and other structures. The subject plant is far enough inland and will not be affected by a tsunami.

3.2.3 Volcanic Activity

According to the U.S. Geological Survey, volcanic regions are located in California, Oregon, Washington, Alaska, and Hawaii. The hazards from volcanoes are as follows:

- Lava flows are streams of molten rock from an erupting vent during either nonexplosive or explosive activity.

- Pyroclastic flows are high-density mixtures of hot, dry rock fragments and hot gases that move away from the erupting vent at high speeds. Most pyroclastic flows consist of a basal flow of coarse fragments that moves along the ground, and a turbulent cloud of ash that rises above the basal flow. Ash may fall from the cloud over a wide area downwind from the pyroclastic flow.

- Tephra are fragments of volcanic rock and lava that are blasted into the air by explosions or carried upward by hot gases in eruption columns or lava fountains. The fragments can be in the form of ash or large rocks. Large-sized tephra typically falls back to the ground close to the volcano. Ash can travel hundreds to thousands of kilometers downwind from a volcano.

- Lahar is a hot or cold mixture of water and rock fragments flowing down the slopes of a volcano or river valleys.

- Landslides are large masses of rock and soil that fall, slide, or flow rapidly under the force of gravity.

- Eruption-induced atmospheric shock waves are strong compressive waves driven by rapidly moving volcanic ejecta. Although most volcanic eruptions are not associated with such waves, examples are known. Air-shock waves can be sufficiently energetic to damage structures far from their source. Air shocks can couple to the ground strongly enough to cause damage to buildings at 100 km away from an eruption.

- Floods can be produced by melting of snow and ice during eruptions of ice-clad volcanoes, by heavy rains that may accompany eruptions, and by transformation of lahars to stream flow. Floods caused by an eruption can occur suddenly and have a large volume if other flood conditions preexist.

The subject plant is far from these regions, well out of the influence of volcanic activity.

3.2.4 Intense Precipitation

Intense precipitation can erode soil. However, the ISFSI is designed so that graded land and drains conduct water away from storage pads. Accordingly, intense precipitation will not affect the storage cask.

3.2.5 Storage Tanks, Transformers, Barges, Trucks, Railcars, and Nearby Industrial Facilities

- There are no storage tanks near the route of the storage cask to the storage pad.

- There are no transformers near the route of the storage cask to the storage pad.

- There is no commercial traffic on the nearby river in the vicinity of the site. The only barge traffic on the river in the vicinity of the storage pad is a snagging barge operated by the Army Corps of Engineers. This barge passes the site about two times per year, once going upstream and the other time going downstream. The barge does not carry explosive or flammable materials.

- Other than a spur track from a railroad line, there are no railway lines near the route of the storage cask from the reactor building to the storage pad or at the storage pad.

- Within a 5 mile radius of the subject plant, there are no manufacturing plants, chemical plants, refineries, storage facilities, mining operations, military bases, military bombing ranges, aircraft low-level flight patterns, missile sites, transportation facilities, oil wells, gas wells, or underground storage facilities. The area within 5 miles of the subject plant is mostly rural; the land is either residential or agricultural. The area is not expected to change significantly in the foreseeable future.

3.3 Frequencies of Initiating Events

3.3.1 Dropped Fuel Assembly

Data from the time period 1968 through 2002 show that there have been 11 events where reactor fuel assemblies have been dropped during movement of the assemblies either prior to loading into a reactor, during loading, or after removal as spent fuel (Reference 12). None of the 11 dropped fuel assemblies failed.

Data from the Department of Energy (Reference 13) show for the same time period, that the projected number of permanently discharged spent fuel assemblies is approximately 159,600 (including both BWR and PWR fuel assemblies). Each permanently discharged fuel assembly has been moved at least twice during fuel loading and for storage in the spent fuel pool. Given the number of assemblies typically found in the core of reactors (Reference 14) and the number of reactors in operation (Reference 15), the number of fuel assemblies in the reactor cores is at least 24,800; it may be as large as 40,800, depending on how many assemblies are assumed in the reactors of Reference 14. The assemblies in the cores have been lifted at least once. Thus, the total number of lifts is at least 344,000 from 1968 through 2002. Therefore, an estimate of the probability of a fuel assembly being dropped is $11/344{,}000 = 3.2\times10^{-5}$.

3.3.2 Dropped Transfer Cask

The frequency of dropping the transfer cask depends on the number of lifts and the probability of dropping the transfer cask given a lift. There are two approaches to estimating the drop probability. The first approach is to perform a reliability analysis of the crane used to lift the transfer cask and a human reliability analysis of the actions of workers to rig the cask and operate the crane. The second approach is to obtain an empirical estimate based on experience with lifting heavy loads. The second approach is used in this study.

The first approach, while providing more insight and possibly being more accurate, is much more complex than the second approach. It must account for both the reliability of the lifting equipment (e.g., crane, yoke) and the reliability of workers to rig the transfer cask and operate the crane. A fault tree analysis of the crane equipment must be based on detailed design and operational information (e.g., lift heights, lift speeds, lift times, movements of the bridge, movements of the trolley). While the fault tree analysis can be performed with standard methods, the human reliability analysis requires further evaluation of human performance issues relevant to dry cask storage operations and, possibly, further development of HRA methods. For example, the kinds of actions that could result in dropping the

transfer cask, such as the potential for human error in attaching the lift yoke to the trunnions at the subject plant, are not well understood, and not every erroneous action would necessarily cause the transfer cask to fall.

The probability of dropping the transfer cask can be estimated from data on lifts of very heavy loads at U.S. nuclear power plants. A very heavy load is defined as weighing 27 metric tons (30 tons) or more. The data used in Reference 16 was evaluated for use in this study. The data base of very heavy loads in Reference 16 is considered relevant to the transfer cask.

Industry-wide experience on moving very heavy loads can be used to make inferences about the risk at a given nuclear power plant. The application of industry-wide data is not a matter of having identical plants, but of having relevant aspects of lifting a cask similar enough to analytically treat them the same. Reference 12 describes the results of a survey of crane operating experience at U.S. nuclear power plants from 1968 through 2002, and includes the responses of the industry to NRC Bulletin 96-02. Of 74 respondents to NRC Bulletin 96-02, 18 reported they have a single failure proof crane, 7 reported they do not have such a crane, 39 did not specify which type of crane they have, and another 10 indicated their cranes meet the heavy load requirements of NUREG-0612. All crews are qualified according to accepted standards. At some plants, professional riggers are used. At other plants, trained plant staff are used, but all follow the guidance discussed in Reference 16.

In contrast to some plants in the industry data base, the subject plant has a single failure proof crane, and professional rigging personnel are contracted to move the cask. Therefore, the estimated drop frequency for the industry is a conservative estimate of the drop frequency at the subject plant.

The drop height probability used in this study is determined from empirical data that reflects lifts of different heights. In some cases, the probability of dropping the transfer cask may depend on the height of the lift. Two drop scenario examples are a drop that results when the block of the lift yoke is forced against the block of the crane boom ("two-blocking") or a drop due to a failure of a flawed cable. In this study, the drop probability is over all possible lift heights.

As reported in Reference 12, nine sites were visited to collect operational data on very heavy load lifts. Each site was chosen to represent one type of plant (i.e., nuclear steam supply system (NSSS). The type of NSSS reflects the type of loads that have to be lifted. Although some sites were selected for convenience, the nine sites are broadly representative of all nuclear power plant sites in the United States. There are a total of 19 plants at the nine sites.

At each of the 19 plants, the number of very heavy load lifts was determined from maintenance logs. Table 7 lists the number of lifts, from both refueling and power operation, at the representative sites from 1968 to 2002. Most, but not all of the lifts were done during refueling outages. Thus, the number of refueling outages is used to determine the total number of lifts throughout the population of plants in the United States.

Table 7. Very Heavy Load Lifts at Representative Sites from 1968 to 2002

Group	Type of Plant	Representative Site and Units	Number of Very Heavy Load Lifts
1	BWR, Mark I, G4	Brown's Ferry 1, 2, 3	980
2	PWR, Westinghouse, 4-loop	Comanche Peak 1, 2	230
3	PWR, Westinghouse, 4-loop	Diablo Canyon 1, 2	344
4	BWR, Mark-I, G3	Dresden 2, 3	554
5	BWR, Mark-III, G6	Grand Gulf	118
6	BWR, Mark-II, G4	Limerick 1, 2	950
7	PWR, B&W	Oconee 1, 2, 3	1656
8	BWR, Mark-I, G2	Oyster Creek	504
9	PWR, CE80	Palo Verde 1, 2, 3	2277

The estimated total number of heavy lifts for all operating plants in United States of 54,000 was obtained from Reference 12 and is used as a reasonable surrogate value in the determination of a load drop frequency.

The number of times that drops occurred were obtained from docketed information and licensee event reports of all plants in the United States, not just the representative plants. In the period of 1968 through 2002, there were three related drop events. Based on these events, a conservative estimate of the drop probability in the period 1968 through 2002 is obtained by taking the number of drops of very heavy loads as three.

The probability of a drop given a lift is estimated by Equation 1.

$$\Pr\{drop\} = \frac{N_{drops}}{L_{total}} \qquad (1)$$

where: N_{drops} = number of drops of a very heavy load
L_{total} = number of lifts of a very heavy load

Solving Equation 1 with $N_{drops} = 3$ and $L_{total} = 54{,}000$, the probability of dropping a cask given a lift is 5.6×10^{-5}.

The estimated drop probability is considered to be a conservative estimate for two reasons.

- The subject plant has a single failure proof crane to move its transfer cask. Most plants use non-single failure proof cranes, which are not as reliable as single failure proof cranes. The collective experience during the 1968 through 2002 period should therefore reflect more unreliability than would be expected from a single failure proof crane.

- The initiating events of dropping a cask in Table 4 are drops of very heavy loads. During the study period of Reference 12, only one free fall drop occurred. Two of the three events used in the numerator of Equation 1 were not drops but were uncontrolled descents of loads. Because these events had the potential of damaging the transfer cask if it were being lifted, they were included in the numerator of Equation 1.

3.3.3 Seismic Events

The storage cask will not see significant stresses due to a seismic event unless it tips over. For any given ground acceleration, the likelihood of a tip-over can only increase as the coefficient of friction between the storage cask and the storage pad increases. From Section 4.1.3.2, the maximum coefficient of friction is 0.53. With this maximum coefficient of friction and at an acceleration of 1.35 g (nine times the design basis earthquake (DBE) of the subject plant), the storage cask will slide but not tip-over. Therefore, only seismic events with ground accelerations exceeding 1.35g have the potential to tip-over the storage cask.

Figure 8 shows the annual probability of exceedance as a function of ground acceleration due to a seismic event at the subject site in terms of the mean, 15th, and 85th percentiles, of the uncertainty distribution. The curves in Figure 8 are based on information in Reference 17, which provides frequency estimates for ground accelerations up to 1.0g at nuclear power plant sites in the Eastern United States. These estimates are linearly extrapolated on a semi-log scale as the dotted portion of the curves in Figure 8. From the extrapolation of the curve for the mean of the uncertainty distribution, the annual probability of an earthquake with ground acceleration exceeding 1.35g is 7×10^{-7}/year. Since even this ground acceleration will not cause a tip-over, a conservative estimate of the frequency of an earthquake that will cause the storage cask to tip-over is 7×10^{-7}/year.

The potential for soil liquefaction at the site was evaluated. The portion of soil susceptible to liquefaction at the subject site is within the range of 45 feet to 90 feet below grade. The region of potential liquefaction at the site is too far below the surface to expect appreciable dispersal of soil into the cask vents.

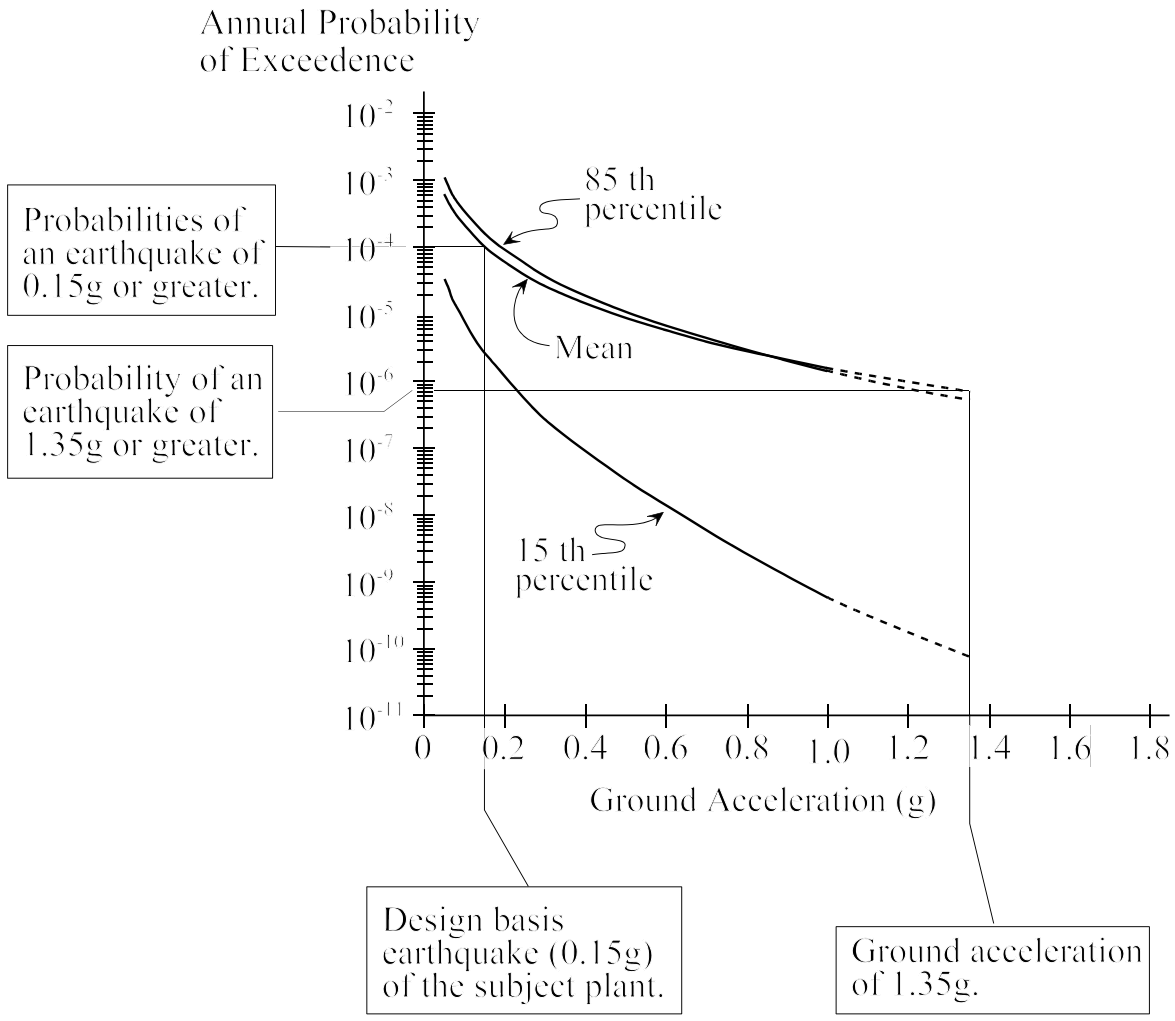

Figure 8. Annual Probability of Exceedance as a Function of Ground Acceleration Due to a Seismic Event at the Subject Plant

3.3.4 High Winds

The effect of a tornado on the storage cask could be to slide the storage cask on the storage pad, tip it over, or propel a heavy object into it. The weight of the storage cask that is loaded with BWR fuel assemblies is about 163,293 kg (360,000 lb). Analysis (Section 4.1.3.2) indicates that a wind speed of approximately 644 km/hr (400 mph) would be required to cause sliding of a storage cask on the storage pad. A speed of 966 km/hr (600 mph) is needed to cause the storage cask to tip-over. Winds in excess of 1448 km/hr (900 mph) would be needed to propel a heavy object into a storage cask with enough force to cause significant damage.

Table 8. Probability of Exceeding Selected Tornado Wind Speeds (Reference 18)

Wind Speed (mph)	Exceedance Probability
73	0.746
113	0.336
158	0.0766
207	0.0138
261	0.00118

The probability of a tornado affecting a storage cask is determined as follows. Reference 18 gives the probabilities that any given tornado occurring in the United States will equal or exceed a specific wind speed (exceedance probability). The exceedance probabilities for selected wind speeds were deduced from the tornado data for the period from 1954 to 1983 (Reference 18). The reported speeds were derived from inspection of damage caused by tornados and the assignment of intensity ratings using the Fujita system of classification (Reference 19). In Figure 9, the data in Table 8 is plotted on a lognormal scale. On the ordinate, the wind speeds needed to affect the storage cask are also indicated.

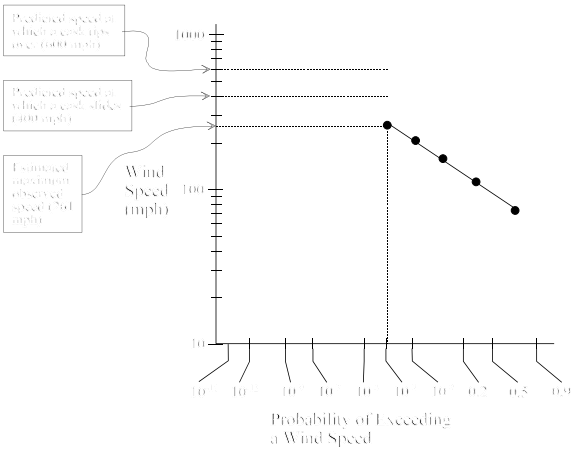

Figure 9. Probability of Tornado Winds Exceeding Speeds

There is no recorded evidence of tornado wind speeds beyond 300 mph from 1955 to the present, the period for which reliable records have been kept. The highest recorded wind speed reported in Reference 18 is 261 mph. There is no experimental or empirical information supporting a physical limit of tornado wind speeds, however, some scientists believe there may be a limit. Accordingly, for this study, the maximum wind speed is taken to be 300 mph. The wind speeds required to affect the cask are significantly larger than 300 mph. Thus, high winds are treated as having no effect on the storage cask.

3.3.5 Meteorites

Meteorites continually enter the earth's atmosphere with initial speeds of tens of thousands of miles per hour. However, most disintegrate to a large extent as they are slowed by friction with the Earth's atmosphere. Over 90% of the meteorites are of a stony composition that tend to break apart upon entering the atmosphere. A smaller number, approximately 6%, are of an iron-like composition that are more likely to reach the ground with less break up than the stony meteorites (Reference 20, Reference 21, Reference 22).

A dynamic structural analysis was performed to determine the size, weight and velocity of a meteorite that would have just enough energy to fail the storage cask. It was assumed that a meteorite striking the cask vertically with sufficient kinetic energy to cause the concrete to reach an ultimate strain of 0.003 would result in failure of the cask (Section 10.3 of Reference 23). Meteorites weighing less than 10 tons are slowed by the earth's atmosphere such that they strike the earth with terminal velocities varying between 200 and 400 miles per hour (mph) depending on the meteorite's mass and cross-sectional area. By iteratively solving the equations used to predict terminal velocity and the kinetic energy (various combinations of mass and velocity) predicted to cause failure, it was determined that a stony meteorite with a mass less than 3400 lb would not be expected to cause cask failure. It was similarly predicted that

an iron-like meteorite with a mass less than 2400 lb would not result in failure. Knowing the meteorite diameters associated with the failure masses, the frequency of meteorites striking the earth that could fail the cask can be estimated. For stony meteorites, for which there is the most data, meteorites having a diameter corresponding to a mass of about 3400 lb would strike the earth intact approximately once per year. Considering the differences in density and in frequency of occurrence for stony and iron-like meteorites, iron meteorites weighing 2400 pounds would strike the earth intact about once each 1½ years. Given the sparseness of data for iron-like meteorites, it is believed that this latter prediction is less robust than that for stony meteorites. Based on the above estimates, it is conservatively assumed that the total frequency of strikes from meteorites that could fail the storage cask is about twice per year. Thus the following assumption was used in this assessment:

- A meteorite capable of breaching the storage cask strikes the earth about twice per year.

The surface area of the earth is 5.08×10^{8} km^2 (1.96×10^{8} mi^2). Thus, a meteorite with sufficient energy to fail the cask is predicted to strike the earth with a frequency per unit of surface area of 4.0×10^{-9} events/yr-km^2 (1.0×10^{-8} events/yr-mi^2).

The storage cask is 3.35 m (11 ft) in diameter, giving a surface area on the top of the storage cask of 8.8 m^2 (95 ft^2) or 8.8×10^{-6} km^2 (3.41×10^{-6} mi^2). Considering the meteorite to approach the storage cask from directly above, the additional surface area from the sides of the storage cask can be ignored. Using this as the target area, A_T, the impact frequency estimated above as f_M, and assuming that a meteorite that strikes the storage cask breaches it, the annual frequency of a breach of a single storage cask by a meteorite is estimated by Equation 2.

$$F_C = f_M \, A_T \qquad (2)$$

where: F_C = annual frequency of meteorites breaching a storage cask
f_M = annual frequency of meteorite strike which could breach the cask (events/km^2)
A_T = target area of a storage cask (km^2)

Substituting $f_M < 4.0\times10^{-9}$/yr-km^2 and $A_T = 8.8\times10^{-6}$ km^2 into Equation 2 results in a frequency of meteorites breaching the storage cask of $F_C < 3.5\times10^{-14}$events/yr.

3.3.6 Lightning Strikes

Lightning activity in the United States is monitored by the National Lightning Detection Network (NLDN). Data from the monitoring system is collected and disseminated by Global Atmospherics, Inc. The geographical region of the subject plant has a moderately high occurrence of lightning strikes in comparison with other areas of the United States (Reference 24). Data from the NLDN taken over the past 10 years indicate that there has been an average lightning strike density of about 4.3 strikes/yr-km^2 (11 strikes/yr-mi^2). This parameter is often referred to in the literature (Reference 25) as the ground flash density (GFD). Knowing the GFD and an effective target area for the lightning to strike, the annual number of strikes on the target may be estimated from Equation 3 (Reference 25).

$$F_L = \rho_{GF} \, A_{ET} \qquad (3)$$

where: F_L = frequency of lightning strikes in a target area per year
ρ_{GF} = ground flash density, frequency of strikes per year per km^2 in the target area
A_{ET} = equivalent target area (km^2)

There are no structures in the vicinity of the storage pad that are close enough to affect either the strike location or the frequency of strikes on the casks. The storage casks are the tallest objects in the area of the storage pad, and their height is accounted for in the calculation of the equivalent area.

The equivalent target area must include an adjustment to account for the height of the target structure. Higher structures present a larger attractive target area than those of less height. A_{ET} is defined as an area of ground surface that has the same annual frequency of direct lightning strikes as the target structure. For an isolated single structure with a height less than 55 meters (180 feet), the equivalent area can be determined using the standard approach in Reference 25. This area was estimated as a circular area surrounding the target, with a radius determined by extending a line with 1:3 slope (3 units of horizontal distance for each vertical unit) from the top of the structure to the ground. The storage cask height is 5.7 m (18.7 ft); the extended radius of the equivalent target area is then 17.1 m (56.1 ft) and, therefore, the equivalent target area is $A_{ET} = \pi\ (17.1)^2 = 918.6\ m^2 = 9.2\times10^{-4}\ km^2$.

As indicated by NLDN data, the average lightning strike density for the past 10 years in the vicinity of the subject plant is $\rho_{GF} = 4.3$ strikes/yr-km^2 (11 strikes/yr-mi^2). From Equation 3, the lightning strike frequency is 4.0×10^{-3} strikes/year.

3.3.7 Aircraft

Two categories of aircraft flights that pose a crash threat to the storage cask are (1) crashes of planes landing or taking off from airfields in the vicinity of the subject plant, and (2) crashes of planes flying en route in the vicinity of the subject plant (i.e., overflights).

There are four airfields in the vicinity of the subject plant. These airfields are listed in Table 9, along with other information needed to determine the frequency of crashes due to landing and taking off into the storage cask.

Table 9. Airfields near the Subject Plant Site

Airfield	Distance from Subject Plant (mi)	Annual Number of Flights	Crash Frequency (Crashes/mi^2)
I	16	10,500	10^{-9}
II	18	6,100	10^{-9}
III	18	6,000	10^{-9}
IV	29	6,000	10^{-9}

Reference 26 describes a standard approach for estimating the frequency of an aircraft crashing into a target during takeoff or landing by the use of Equation 4.

$$F_{tl} = A_{tl} \sum_{j=1}^{n} C_j\ N_j \qquad (4)$$

where: F_{tl} = frequency of crashes during takeoffs or landings
A_{tl} = effective target area for a plane to strike the target on takeoff or landing
C_j = probability per square kilometer of a crash per aircraft movement at airfield j
N_j = number of movements per year at airfield j
n = number of airfields near the subject plant

The summation is over all airfields in the vicinity of the storage cask. The crash parameter, C_j, is a decreasing function of the distance from the end of the runway of each airfield to the storage cask. From Reference 26 (Section 3.5.1.6), values of C_j for different values of distance from the runway are given for distances of 10 miles and less. Since the closest airfield to the subject plant is approximately 25.7 km (16

mi), the values in Reference 26 were extrapolated using a logarithmic plot and regression analysis to determine values of C_j for the subject plant. The extrapolated value of C_j for the nearest airfield is estimated to be 3.9×10^{-10} crashes / km^2-movement. This value of C_j is conservatively used for all four airfields.

The effective target area, A_{tl}, depends on the dimensions of the storage cask and the plane and the length of the skid path. The diameter of the storage cask is 3.35 m (11 ft). The largest aircraft which is able to land at any of the four local airfields is the Gulfstream IV. The Gulfstream IV has two engines on either side of the fuselage, spaced about 4.2 m (13.8 ft) from centerline to centerline, and each engine is about 1.6 m (5.2 ft) in diameter. In order for the crash to possibly cause cask failure, one of the plane's two engines must strike the cask. The engines are spaced such that both engines shafts cannot fully strike the cask together. Evaluating aircraft trajectories that would result in impact by either engine, the lateral dimension (width) of the target area (perpendicular to the plane's trajectory) is the sum of the spacing between the engines, twice the diameter of an engine, and the diameter of the storage cask. This dimension is 9.2 m (30.3 ft). A conservative value for the skid length is 30.5 meters (100 feet), which takes into account the terrain surrounding the storage cask and the angular window through which a plane must pass to strike the storage cask. The impact area is considered to be a rectangle with length equal to the skid length, 30.4 meters (100 feet), and width equal to 9.2 m (30.3 ft). Using these values, $A_{tl} = 2.8\times10^{-4}$ km^2 for the Gulfstream IV.

The frequency, F_{tl}, is conservatively estimated using the values of parameters from Table 9 and the value of A_{tl} for the Gulfstream IV. Because C_j is the same for every airfield, F_{tl} depends only on the total number of flights, which is 28,600/yr. Substituting into Equation 4 values of $A_{tl} = 2.8\times10^{-4}$, $C_j = 3.9\times10^{-10}$, and $N_j = 28{,}600$ yields a conservative value for frequency of crashes during takeoffs or landings at airfields in the vicinity of the site of $F_{tl} = 3.1\times10^{-9}$ crashes/yr which could impact the cask.

A large aircraft could potentially crash into the storage cask during overflights. To analyze the crash frequency for overflights, F_{of}, a method given in Reference 27 is used. In this approach, the frequency of crashes during overflights is estimated using Equation 5.

$$F_{of} = C_{of}\ A_{of} \qquad (5)$$

where: F_{of} = frequency of overflight crashes
C_{of} = overflight crash rate per square kilometer per year
A_{of} = equivalent target area for overflight crashes (km^2)

The value of C_{of} to be used in Equation 5 for air carriers is 1.0×10^{-6} crashes/km^2-yr (4×10^{-7} crashes/mi^2-yr). From Reference 26, the overflight crash rate for commercial aviation is 1.6×10^{-7} crashes/km^2-year.

Similar to the analysis for takeoffs and landings, the impact area is conservatively taken to be a rectangle with length equal to the skid length, 30.4 meters (100 feet), and width equal to the sum of the distance between the outermost parts of the two outer engines (102.9 m + 3.4 m) plus the diameter of the storage cask. The value of A_{of} is 3.2×10^{-3} km^2 (1.2×10^{-3} mi^2).

Substituting in Equation 5 values of $C_{of} = 1.6\times10^{-7}$ crashes/km^2-yr, $A_{of} = 3.2\times10^{-3}$ km^2, yields a conservative value for the frequency of overflight crashes from air carriers that could impact the storage cask of 5.1×10^{-10} crashes/year.

The total frequency of aircraft crashes which could impact the cask is the sum of the crash frequency for take-offs and landings and the crash frequency for overflight related crashes, or 3.6×10^{-9} crashes/year. As noted in Section 4.1.3.3, Strikes on the Storage Cask from Heavy Objects, and Section 7.0, Risk Assessment, the probability of MPC failure is assumed to be directly related to the overflight crash rate

for commercial aviation, since only commercial aircraft, larger than a Gulfstream IV, which cannot takeoff or land at any of the nearby airfields, and traveling at high velocity, could possibly cause a breach of the MPC on impact. For convenience, it is assumed that all overflights consist of large commercial aircraft and impact the cask at high velocity. Therefore, the probability of MPC failure and release, if struck by an aircraft, is, for the purpose of the PRA, equal to the frequency of overflight crashes (5.1×10^{-10}) divided by the total frequency of aircraft crashes (3.71×10^{-9}) which is 0.14.

An alternative approach for estimating the overflight crash rate is given in Reference 26. The approach allows for a more location-specific analysis in that it utilizes flight information on traffic in flight corridors that are approved by the Federal Aviation Administration (FAA). Four such corridors are in the vicinity of the subject plant, but information on the cumulative number of flights in these corridors is unavailable because it is not collected by the FAA.

4. MULTIPURPOSE CANISTER AND FUEL

4.1 Mechanical Loads

4.1.1 Mechanical Load Models

To evaluate the structural behavior of the transfer cask and storage cask for the postulated initiating events, simplified and conservative analyses were used in many cases. Key parameters of the storage cask and ISFSI are presented in Table 10. The methods of analysis used included hand calculations based on first principles, common analytical methods and industry recognized approaches, and solution of the differential equations of motion for which closed form solutions were obtained. When an analysis required sophisticated computer codes and large amounts of resources, existing calculations performed by Holtec and reviewed by the staff were used in addition to independent analyses described in this report. In some cases the LS-DYNA computer code was utilized to perform non-linear dynamic impact analyses (Reference 28). The loads and stresses calculated for all of the examined initiating events were used in subsequent analyses to determine the probability of failure of the MPC and fuel cladding.

The following assumptions were made in this assessment:

- The transfer cask falls in a nearly vertical orientation.
- In most simplified analyses, the transfer cask and the storage cask are considered rigid.
- A drop of the transfer cask in the fuel-handling building occurs on a reinforced concrete floor supported by a 76 cm (30 in) thick concrete shear wall beneath the floor. The worst case impact occurs if the cask falls on the area of the floor that is supported by the wall because the stiffness provided by the wall maximizes the impact acceleration and forces in the MPC.
- During the transfer phase, the storage cask is carried by the cask transporter at a height of 0.3 meters (1 foot) above the ground surface.
- If the storage cask were dropped from the cask transporter during the transfer phase, the cask transporter is traveling in the direction of the open end of the cask transporter.

An analysis was done to evaluate the response of the MPC in the cask to the design basis earthquake (DBE) at the ISFSI of the subject plant; this was set equal to one-half of the subject plant's seismic margin earthquake (½ SME) ground response spectrum. Seismic events were evaluated for different levels of seismic forces with different coefficients of friction between the bottom steel plate of the cask and the concrete pad using three-dimensional coupled finite element models of the cylindrical cask, a flexible concrete pad, and an underlying soil foundation. Two coefficients of friction are considered at the interface between the cask bottom steel plate and the concrete pad. A lower-bound friction coefficient of 0.25 is used for investigating the sliding of the storage cask, and an upper-bound friction coefficient of 0.53 is used for examining the possibility of storage cask tip-over.

Table 10. Storage Cask and ISFSI Parameters for Load and Stress Calculations

Storage Cask	
Parameter	**Value**
Diameter of the storage cask	3.4 meters (11 feet)
Height of the storage cask	5.9 meters (19 feet)
Height of the center of gravity	3.0 meters (10 feet)
Weight of storage cask, MPC, BWR fuel assemblies	163,293 kg (360,000 lb)
ISFSI	
Parameter	**Value**
Thickness of concrete	0.61 m (2.0 ft)
Concrete compression strength	20.7 MPa (3,000 psi)
Yield strength of reinforcement top and bottom	413,685 kPa (60,000 psi)
Soil effective modulus of elasticity	193,058 kPa (28,000 psi)

For missiles caused by tornado or flood, the Spectrum II missiles identified in the Standard Review Plan (SRP, Reference 29) are considered. Based on the SRP, the most severe missile which has the potential to cause sliding or tip-over of the storage cask is an automobile weighing 1,810 kg (3,990 lb) at a velocity of 59 m/s (132 mi/hr). An automobile of this weight is comparable to one of today's common sport utility vehicles. Based on studies of the behavior of heavy objects in high winds such as tornadoes, it has been determined that the maximum velocity of an automobile propelled by a tornado may be approximated by taking 0.2 times the maximum velocity of the tornado wind speed (SRP Section 3.5.1.4). An automobile velocity of 59 m/s (132 mi/hr) would then correspond to a maximum tornado wind speed of about 295 m/s (660 mi/hr) indicating that the analysis based on the SRP model is quite conservative. The frequency of tornado winds in excess of 600 mi/hr at the storage site is estimated to be 4×10^{-11} events/yr (See Section 4.4 of this report).

4.1.2 Response of the Transfer Cask to Loads

Analyses were performed for the initiating events to determine the stresses in the MPC while being moved in the transfer cask. Though the transfer cask can be carried on its side or in the upright position when the MPC is sealed, at the subject plant it is always carried in the upright position. All transfer cask drop analyses are conducted assuming an upright cask position. Thus the following assumption was used in this assessment:

- The transfer cask is always carried in the upright position.

4.1.2.1 Drop of the Transfer Cask into the Cask Pit

In Stage 3, the transfer cask, which is filled with spent nuclear fuel assemblies, is lifted from the cask pit. The depth of the cask pit is 37.5 feet. When the transfer cask is out of the water, it is lifted an additional 1.5 m (5 ft) to a height of 42.5 feet. It takes 0.5 m (1.5 ft) to get to the level of the refueling floor and an additional 1.1 m (3.5 ft) to get high enough above the refueling floor to clear a railing on its way to the preparation area (Stage 4).

If the transfer cask were accidentally dropped while being lifted in Stage 3, the cask would fall a total of 5 feet through the air, drops through 37.5 feet of water, and impacts the concrete floor of the pit. The analysis included buoyancy and drag effects, which slightly reduce the velocity and the energy at impact.

Because the subject plant has a single-failure-proof crane and professional rigging personnel are contracted to move the cask, the consequences of a drop of the transfer cask on the structural integrity of the cask pit do not have to be evaluated. However, should the cask be accidently dropped, based on information available for design of the reinforced concrete spent fuel cask pit, the results of the impact analysis show that the shear stresses developed in the concrete exceed the ultimate capacity of the concrete floor. Therefore, cracking and possibly more severe damage or failure of the spent fuel cask pit floor may occur if the cask is dropped from the maximum height of 42.5 feet above the floor of the cask pit. It is assumed that the consequences to the integrity of the MPC and fuel from such a drop are the same as for a free drop in air of 40 feet. For a 40 foot drop onto concrete, Table 13 shows that 100% of the fuel cladding is breached. Since the MPC is not sealed during this stage, the probability of a release from the MPC is 1.0.

4.1.2.2 Tip-over of the Transfer Cask

In Stages 4 through 17, the crane is moving the transfer cask over the refueling floor. Analyses were performed to determine the effects of this movement at the maximum speeds; the bridge moves at 15 meters/min (50 feet/min); the trolley moves at 3 meters/min (10 feet/min); the hoist moves at 1.3 meters/min (4.2 feet/min). These velocities are very small and will have negligible effect on the conditions required for the cask to tip-over.

If the crane were not moving, the transfer cask would tip-over only if it is dropped at an angle such that the center of gravity of the cask is over the point of first contact with the floor. This angle requires that the cask axis be oriented at less than 67° with the horizontal. This angle cannot be reached unless the drop height is more than 40 cm (16 in) measured at the center of the transfer cask base. From Table 1, the transfer cask is lifted more than 40 cm (16 in) in Stages 4, 11, 12, 13, 15, 16, and 17. Accordingly, the transfer cask may tip-over if it is dropped in any of those stages at an angle such that the center of gravity is over the point of first impact. It will not tip-over if it is dropped in Stages 5 through 10 or Stage 14. A discussion of the consequences associated with cask tip-over is found in Section 4.1.3.2

4.1.2.3 Drop of the Transfer Cask onto Storage Cask

The accidental vertical drop of the transfer cask is analyzed during Stage 18 if the cask were dropped while being lowered from the operating floor, striking the storage cask. The maximum vertical drop in this case is 24.4 meters (80 feet). For this analysis, a detailed finite element model is used that includes the transfer cask, MPC, fuel assemblies, fuel basket, fuel basket support, and storage cask. Drop heights of 1.5, 12.2, and 24.4 meters (5, 40, and 80 feet) were selected for analysis. Analysis of this model using the LS-DYNA computer code calculated the maximum effective plastic strain in the MPC which was used in the weld failure analysis to calculate the probability of MPC failure. In Section 4.3.2, Table 12 summarizes the MPC failure probabilities for all of the drop scenarios evaluated. For the drop of the transfer cask onto the storage overpack, the probability of MPC failure is very small and, as expected, varies with drop height. For an 80 foot drop the probability of MPC failure is 0.0002. This low probability of failure is due to the fact that the drop of the rugged transfer cask onto the storage overpack results is a relatively soft impact with most of the impact energy being absorbed by the storage overpack.

For the purpose of the PRA, fuel cladding failure is linked to a 1.0% failure strain, which is a typical lower bound value for high burnup fuel with circumferential hydrides. Table 13 summarizes fuel cladding failure for various drop heights and scenarios. For the 80 foot drop of the transfer cask onto the storage overpack, 100% of the fuel cladding is assumed to fail. Therefore, the probability of release of radionuclides from the MPC is set equal to the probability of MPC failure.

4.1.2.4 Drop of the Transfer Cask onto Concrete Floor

The accidental vertical drop of the transfer cask while it is being lowered from the operating floor to the ground floor were analyzed. If the transfer cask were to drop from the operating floor and strike the concrete floor at ground level, the maximum drop would be 30.5 meters (100 feet). To perform the analysis a detailed finite element model was developed that included the transfer cask, MPC, fuel assemblies, fuel basket, fuel basket support, concrete floor, and the wall beneath the floor. Drop heights of 1.5, 12.2, 21.3, and 30.5 meters (5, 40, 70, and 100 feet) were selected for analysis. Analysis of this model using the LS-DYNA computer code calculated the maximum effective plastic strain in the MPC which were used in the weld failure analysis to calculate the probability of MPC failure. In Section 4.3.2, Table 12 summarizes the MPC failure probabilities for all of the drop scenarios evaluated. For the drop of the transfer cask onto the concrete floor, the probability of MPC failure is small and, as expected, varies with drop height. For an 100 foot drop the probability of MPC failure is 0.020 (0.0196). The probability of failure is relatively low because the drop of the rugged transfer cask onto the concrete floor results in a soft impact with most of the impact energy being absorbed by the concrete floor and wall beneath the floor.

For the purpose of the PRA, fuel cladding failure is linked to a 1.0% failure strain, which is a typical lower bound value for high burnup fuel with circumferential hydrides. Table 13 summarizes fuel cladding failure for various drop heights and scenarios. For the 100 foot drop of the transfer cask onto the concrete floor, 100% of the fuel cladding is assumed to fail. Therefore, the probability of release of radionuclides from the MPC is set equal to the probability of MPC failure.

The relative deformation between the transfer cask top lid and the top of the MPC was reviewed to ensure that there is no contact/impact between the transfer cask and the MPC. A review of the relative displacement, throughout the time history for the maximum drop (worst case), demonstrated that a gap is maintained, and therefore, the transfer cask top lid does not impact the top of the MPC.

4.1.2.5 Drop of the Transfer Cask onto Refueling Floor

When the transfer cask is moved from the fuel pool to the handling area, the transfer cask may fall from a height of 0.3 meters (1 foot). For this drop, the refueling floor is expected to hold the transfer cask when the floor has beams, girders, or concrete walls underneath. For a one (1) foot drop, Tables 12 and 13 show that the probability of MPC failure is $1x10^{-6}$ and that there is no fuel cladding failure.

4.1.2.6 Drop of the MPC While Lowered into the Storage Cask

When the MPC is lowered from the transfer cask into the storage cask (Stages 20 and 21), it could possibly fall a maximum of 5.8 m (19 ft). This fall is analyzed using a finite element model that includes the MPC, storage cask inner shell, storage cask vertical channel sections, and the storage cask bottom lid (which serves as the target plate). The MPC model, its material properties model, fuel assemblies, and fuel basket and fuel basket support model are the same as those utilized in the drop of the transfer cask onto the concrete floor. The top plate of the storage cask bottom lid is modeled as a rigid target plate for the vertical impact of the MPC and its internal components. The storage cask vertical wall is modeled using a rigid shell to represent the storage cask inner shell, which surrounds the MPC shell wall.

A dynamic analysis using LS-DYNA was performed to calculate the maximum effective plastic strain in the MPC for input into the weld failure analysis to calculate the probability of MPC failure. From Table 12 in Section 4.3.2, the probability of the MPC failing when it is dropped during Stages 20 and 21 is 0.28. For the purpose of the PRA, fuel cladding failure is linked to a 1.0% failure strain, which is a typical lower bound value for high burnup fuel. Table 13 summarizes fuel cladding failure for various drop heights and scenarios. For the 19 foot drop of the MPC into the storage overpack, 100% of the fuel cladding is assumed to fail. In contrast, for the 20 foot drop of the transfer cask onto concrete, fuel cladding failure is not expected to occur. These different outcomes for essentially the same drop height

are due to the fact that the 19 foot drop is a much harder impact and results in a very different mode of fuel rod buckling, as explained in Appendix C. Because fuel failure occurs for the 19 ft drop, the probability of release of radionuclides from the MPC is equal to the probability of MPC failure, which is 0.28.

4.1.3 Response of the Storage Cask to Mechanical Loads

4.1.3.1 Drop of the Storage Cask onto Concrete, Asphalt, or Gravel Surfaces

During Stages 29 through 33, the storage cask is moved by the cask transporter to the ISFSI at a height of 0.3 m (1 ft). A 0.3 meter drop of the storage cask onto concrete, asphalt, and gravel, was also evaluated. The two bounding cases considered were a drop without any rotation (i.e., end drop) and a drop causing the maximum rotation.

- During an end drop, calculations show that the frictional resisting force of the storage cask sliding against the concrete was much less than the overturning force; thus, the storage cask would slide and not tip-over regardless of the velocity of the cask transporter.

- Calculations demonstrate that it is geometrically impossible for the rotation of a dropped storage cask to be large enough to cause a tip-over. The maximum amount of rotation possible is 5.14° (with respect to the ground), which occurs when one of the two vertical supports holding the storage cask at the top breaks and the storage cask makes contact with the ground at one edge. Since this angle is less than 29.5°, the storage cask will not tip-over. Furthermore, the force required to tip-over the storage cask from the rotated orientation was calculated to be greater than the frictional resisting force. Therefore, the storage cask would slide but not tip-over.

In both the end drop and the rotation drop, the cask transporter can cause the storage cask to slide, not tip-over. The maximum stress in the MPC shell for a 0.3 m (1 ft) drop on a concrete pad is calculated to be 53.3 MPa (7,732 psi). This stress produces extremely small strains in the MPC and in Section 4.3.2, Table 12 shows that the probability of failure is less that $1x10^{-6}$.

If the cask transporter is traveling at the maximum operating speed of 0.64 km/hr (0.4 mi/hr) and the storage cask that it is carrying strikes another storage cask on the storage pad, the storage cask on the storage pad will slide but not tip-over. If the cask transporter does not stop and continues pushing the struck storage cask, the storage cask on the storage pad could slide into another storage cask or be pushed off the storage pad onto the surrounding gravel area. In any case, for the struck storage cask, the maximum stresses in the base plate, lid, and the MPC shell will be much less than the stresses of a 0.3 meter (1 ft) drop.

The stresses resulting from a drop onto the asphalt or gravel surface are bounded by a drop onto the ISFSI concrete pad. This is because asphalt and gravel are more flexible and have a lower strength and modulus than concrete, and neither of these surfaces have steel reinforcing bars. When the storage cask is dropped from a height of 0.3 m (1 ft) onto concrete, asphalt, or gravel, the failure probability of the MPC is less than 1.0×10^{-6}.

4.1.3.2 Tip-over of the Storage Cask

Hypothetically, if the storage cask were to tip-over because the center of gravity of the cask passes over the point of rotation without an initial force or velocity, the maximum circumferential stress in the MPC shell is approximately 421 MPa (61,044 psi) at 4.53 m (178.5 in) above the bottom of the MPC. This is based on Reference 2 where the stress in the MPC shell was calculated using a finite element model of a slice of the MPC and fuel baskets subjected to an acceleration of 45g. Under this loading, the MPC and fuel baskets deform outward until portions of the MPC shell reach the rigid boundary of the storage cask inner steel shell. This analysis is consistent with the methodology of the ASME Code and is based on a

linear elastic approach. The maximum calculated stress in the MPC shell is less than the allowable stress intensity of 450 MPa (65,200 psi) based on the Level D Service Condition of the ASME Code (Reference 30). ASME Code Division 1 - Subsection NG, Paragraph NG-3225 and Appendix F, Paragraph F-1331, limit the primary membrane (general or local) plus primary bending stress intensity to 150% of the general primary membrane stress intensity. For the purpose of evaluating MPC weld failure, the allowable stress limit of 65,200 psi was used.

Since the weld failure criterion is based on plastic strain, the elastically calculated maximum stress must be converted to a plastic strain that could have reasonable resulted from a non-linear analysis of the same event. Also, since the "damage" that can be inflicted on the MPC during a tip-over event is energy limited, an energy balance approach can be used to estimate the maximum plastic strain. In this approach the strain energy per unit volume absorbed at the point of the elastically calculated maximum stress is equated to the strain energy per unit volume absorbed through elastic-plastic deformation of the material using the idealized engineering stress-strain curve in the LS-DYNA program that was used for the drop analyses.

Using this approach, and the data in Appendix A, Table A.2, the calculated maximum plastic strain is 0.0031 in/in. Since the maximum membrane plus bending stress must have occurred on the boundary, the maximum value that the triaxiality factor can be is 2.0 (see Appendix B, Section B.1.4). The maximum adjusted plastic strain is therefore 0.0062 in/in. Assuming that the maximum plastic strain occurs at one of the axial or circumferential welds, the probability of weld crack initiation from Appendix B, Table B.2 is less that $1x10^{-6}$.

Two initiating events could potentially tip-over the storage cask – seismic events and high winds.

- Seismic events. A seismic event is evaluated for different levels of seismic forces with different coefficients of friction between the bottom steel plate of the cask and the concrete pad using three-dimensional coupled finite element models of the cylindrical cask, a flexible concrete pad, and an underlying soil foundation. When higher levels of seismic excitations are used in the analyses, the coefficient of friction at the cask/pad interface plays an increasingly important role in the sliding and rotational behavior of the storage cask. For a minimum friction coefficient, the storage cask exhibits a translational motion without much rotation. If the friction coefficient is 0.25 and an earthquake occurs equal to eleven times the design-basis earthquake of the ISFSI (i.e., 11 DBE), the seismic excitations will cause the storage cask to slide 0.93 m (36.6 inches). Even though the sliding storage cask may hit a neighboring storage cask, neither storage cask will tip-over. Assuming a maximum friction coefficient, the storage cask experiences more rotational movement, but does not tip-over. When the friction coefficient is 0.53 and an earthquake occurs equal to nine times the design-basis earthquake of the ISFSI (i.e., 9 DBE), the storage cask top will move 1.19 m (47 inches) and the storage cask base will slide 0.84 m (33 inches). Even though the sliding storage cask may hit a neighboring storage cask, neither storage cask will tip-over.

- High winds. The wind speed required to slide the storage cask is at least 644 km/hr (400 mi/hr), and the wind speed required to tip-over the storage cask is at least 966 km/hr (600 mi/hr). The design wind speed for the plant is 580 km/hr (360 mph). Detailed calculations are discussed in Section A.5.9.6.

4.1.3.3 Strikes on the Storage Cask from Heavy Objects

Vehicle impact. A car or a truck crashing into the cask while stored on the ISFSI pad is not analyzed directly. However, by extrapolation from the analyses done for sliding and tip-over due to missile impact, it can be concluded that a 4,536 kg (10,000 lb) vehicle traveling at a speed of 241 km/hr (150 mi/hr) speed will slide the cask less than 66 cm (26 in), and will not cause tip-over. This conservatively considers that the impact for a tip-over occurs at the top of the cask for tip-over and the lowest coefficient of sliding friction applies for sliding. The MPC remains intact.

Accidental crash by an aircraft. Based on the results of the aircraft impact analysis (Section A.4.9.3), the probability of breaching the MPC, if struck by Gulfstream IV aircraft during landing or takeoff. is extremely small and is assumed to be zero. However, many commercial aircraft overflying the site would be larger than a Gulfstream IV and could impact the cask at high velocity. Since the makeup and characteristics of commercial aircraft overflying the site are not known and have not been evaluated, it is conservatively assumed for the purpose of the PRA that all commercial aircraft overflying the site are larger than a Gulfstream IV and that the probability of MPC breach due to the impact of an overflying commercial aircraft is, for the purpose of the PRA, 1.0. Therefore, the probability of MPC failure and release, if struck by an aircraft, is, for the purpose of the PRA, equal to the frequency of overflight crashes (5.1×10^{-10}, see Section 3.3.7) divided by the total frequency of aircraft crashes (3.71×10^{-9}, see Section 3.3.7), which is 0.14.

Wind-driven missiles. Missiles generated by a tornado have been analyzed. Two different cases of wind-driven missiles are discussed in Section 4.1.1 of this report. The first case analyzed is based on the Standard Review Plan (SRP) section addressing missiles generated by natural phenomena (Reference 26). This involves an impact from an automobile weighing 1,810 kg (3,990 lb), traveling with a velocity of 59 m/s (132 mpr). Such missiles will not penetrate the storage cask, and will not cause sliding or tip-over. The concrete barrier thickness required to prevent penetration is 72.4 cm (28.5 in). The entire wall (concrete and steel liners) of the storage cask is 75 cm (29.5 in) thick. However, an automobile as a missile (1,810 kg (3,990 lb) with a velocity of 212 km/hr (132 mpr)) may slide the storage cask if the coefficient of friction between the concrete pad and the storage cask were less than or equal to 0.26. This is near the low end of the coefficient of friction range. If the coefficient of friction were greater than 0.26, the storage cask will not slide. It is estimated the stresses in the cask attributable to missile impact will be much smaller than the tip-over case discussed in Section 4.1.3.2.

In addition, a second study assumes a larger vehicle with a weight of 3,251 kg (7,160 lb), propelled by a very severe tornado having a wind speed of 134 m/s (300 mpr). This wind speed is slightly higher than any tornado wind speed recorded to date. To assess the potential impact of such a missile striking a storage cask, the kinetic energy of this missile is compared to that of an aircraft crash. Since the kinetic energy of the large vehicle wind-driven impact would be less than 1% of the kinetic energy of a large aircraft impact, it is concluded that the impact of a very large vehicle traveling as a tornado missile at a relatively high velocity will not result in cask failure.

4.1.3.4 Shockwaves on the Storage Cask from Explosions

Tanker trailer. The nearest public highway is at least 914 m (3000 ft) from the ISFSI. The shockwaves caused by a tanker trailer containing explosive materials (e.g., gasoline, liquid, natural gas) at this distance from the storage cask will not jeopardize the integrity of the MPC. Reference 31 was utilized to evaluate this event. The cask is designed for a 69 kPa (10 psi) peak transient external pressure. At 914 m (3,000 ft), the peak pressure attributable to the explosion would be less than 10 percent of the pressure magnitude for which the cask is designed. Therefore, the MPC will remain intact.

Gas pipeline. The nearest gas pipeline (natural gas) is 7.2 km (4.5 miles) from the subject site. The shockwaves caused by the pipeline explosion will not jeopardize the integrity of the MPC. The methods described in Reference 31 and Reference 32, which analyzed a tanker trailer explosion, were utilized to evaluate this event. To compare a pipeline explosion with the tanker trailer explosion, Equation 1 in Reference 31 was used for a distance of 7.2 km (4.5 miles). This resulted in a 6.9 kPa (1 psi) transient

pressure on the storage cask, which is negligible. Based on these assessments, it is concluded that the storage cask will remain intact, and the integrity of the MPC will not be jeopardized by a pipeline explosion.

4.2 Thermal Loads

4.2.1 Heating During Normal Operation, Blocked Vents, and Fires

4.2.1.1 Heatup Model

The thermal analysis employed the use of Fluent (Reference 33), a computational fluid dynamics (CFD) program, to model the relevant physical phenomena resulting from both the fire and blocked vents scenarios of the dry cask. Fluent is a general-purpose CFD program with the ability to model a wide range of practical problems by solving the conservation equations for mass, momentum, energy and chemical species using a control volume based, finite difference method. Complex 2-D, axisymmetric and 3-D geometries can be modeled. Fluent has been validated for a wide range of flow conditions, including laminar and turbulent flow in various geometries, natural and forced convection problems, heat exchange flow, and combustion phenomena. Additionally, the NRC staff reviewed Holtec International's confirmation of Fluent code's capability to reliably predict temperature fields in the dry storage application using an independent full-scale test on a loaded cask. (Reference 34).

CFD analyzes fluid flow, heat and species transport in two or three dimensions. In the present analysis, the computational domain includes the storage cask and the ambient conditions. The domain is divided into control volumes, and the governing conservation equations are solved for each control volume, providing detailed information of all the flow variables. The conservation equations are reduced to a set of algebraic equations by discretization, which are then solved by numerical techniques.

The geometrical configuration and the computational grid generated for the storage cask are shown in Figure 10. The MPC is inside the storage cask. The fuel basket containing fuel assemblies is inside the MPC. A combination of heat source and porous media was used to model the MPC. The chosen grid was refined until a grid independent solution was obtained. Two exploded views are shown in Figure 10 to show the airflow channel around the MPC. Arrows indicate the airflow direction. The sides and top boundaries of the computational domain were extended far away from the dry cask structure to safely apply pressure boundary conditions at the top and the sides. Axisymetry was used in this model. Thus, the vents in the computational model appear narrower than the physical model so that the total airflow cross-sectional area in both models are identical.

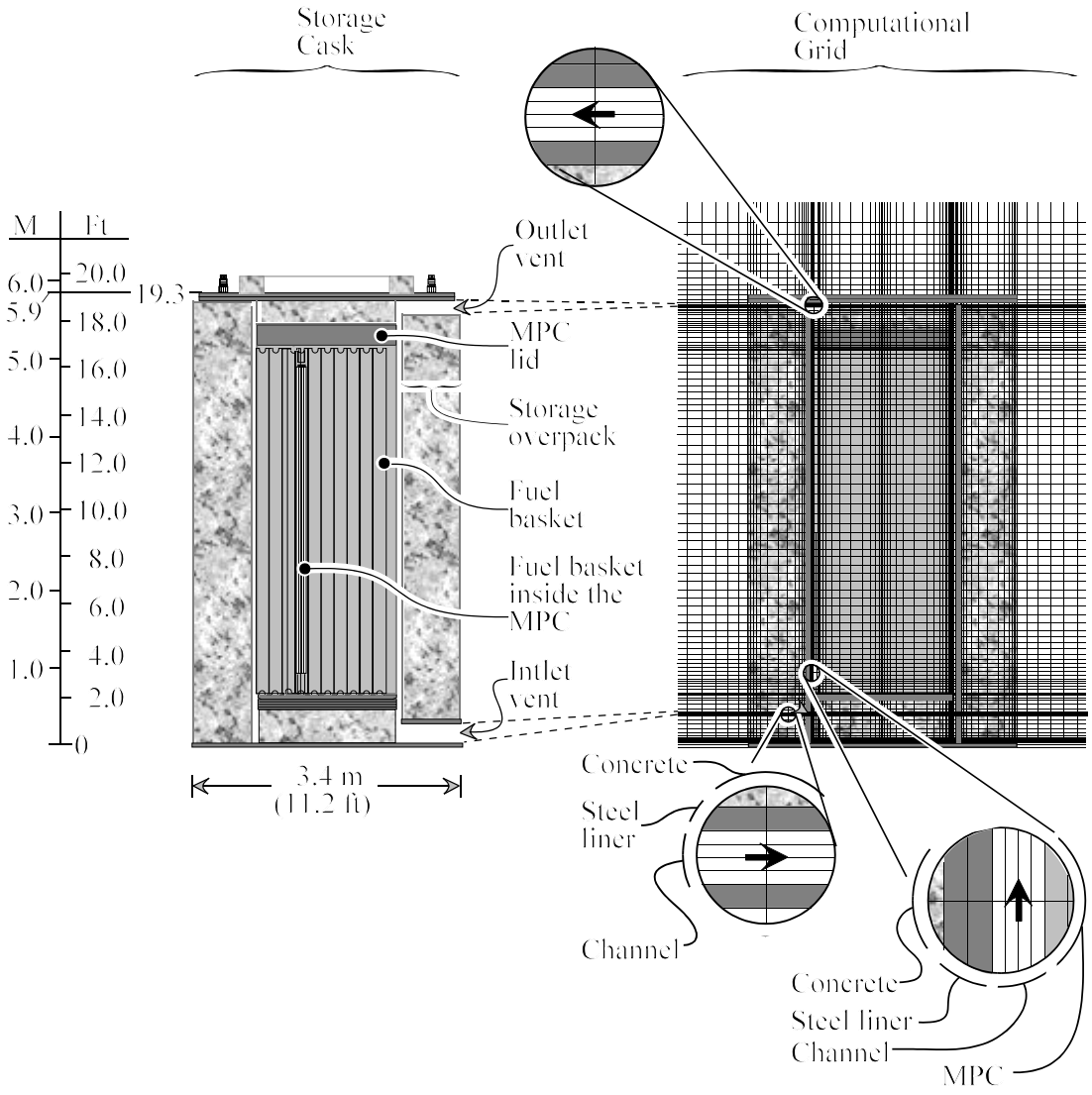

Figure 10. Geometrical Configuration and the Computational Grid Generated for the Storage Cask

Normal storage conditions were obtained first using steady state analysis to be used as initial conditions for the transient analysis. The MPC-68 design holds 68 BWR fuel assemblies. It consists of a fuel basket inside a cylindrical shell. Within the fuel basket, a grid work of stainless steel plates forms an array of square cross-section compartments, each holding a single fuel assembly. The fuel basket is positioned within the shell by basket supports. To allow thermal expansion of the fuel basket, small gaps exist between the fuel basket and the basket supports. Heat is continuously transported from the MPC interior to the periphery of the fuel basket by conduction through the stainless steel plates. Materials present in the MPC include stainless steels (Alloy X), Boral neutron absorber, aluminum Alloy 1100 heat conduction elements, and helium. Materials present in the HI-STORM storage cask include carbon steels and concrete.

Effective values of thermal conductivity, density and heat capacity were taken from Reference 34 and Reference 35. These effective thermal properties were evaluated using ANSYS (a finite element code).

The analysis looked at the combined effect of conduction and radiation inside the MPC. For accurate analysis, all the properties in Fluent were supplied as a function of the temperature and mass fraction. Kinetic theory was used to derive the thermo-physical properties of pure substances like air or helium. The normal storage condition as well as the blocked vent scenario were modeled in a steady mode. The fire scenario was modeled in a transient fashion using a second order time marching scheme for three hours.

In all the cases, the convective terms in the transport equations used a second order forward differencing scheme. Semi Implicit Method for Pressure-Linked Equations (SIMPLE) was used to bridge the momentum to the continuity equation. All the modes of heat transfer (i.e., conduction, radiation, and convection) were taken into account. Porous medium was used to model the axisymmetric inner basket region and the peripheral gap between the basket and the MPC shell. Turbulence is modeled using low Reynolds k-epsilon model. In this model, the conservation equations for turbulence kinetic energy and its dissipation were solved. A full buoyancy effect was added in the turbulence production and its dissipation. Standard wall functions were not used to bridge the sub-laminar layer near the walls to the fully turbulent flow in the core region as in widely used standard k-epsilon model. Instead, full integration to the wall was carried out using fine mesh near the wall. The discrete ordinates method was used to model radiation. Only surface-to-surface radiation was considered. Absorption and scattering in the gas phase was neglected (no participating media was considered). All walls were modeled as thick walls. Conduction was modeled through each wall in all directions. The computational domain was extended away from the cask boundaries. No boundary conditions were assigned at the inlet and outlet vents for the airflow. The external walls of the cask were allowed to exchange heat with the surrounding atmosphere through convection and radiation.

The heat source representing the decay heat from the fuel rods was assumed to not be uniformly distributed. Instead, it was distributed as a function of the axial burn-up peaking factor. The axial burn-up peaking factor for BWR fuel is provided in Reference 34. The total heat decay used was 21.4 kW.

In the fire scenario, the combustion of the jet fuel was considered. An air-fuel ratio of 14.67 was used. Product gases (flue gas) arise from combustion. As a result, an additional conservation equation was solved to track the species generated in the combustion. The solution of the problem involved a total of eight conservation equations to be solved simultaneously.

4.2.1.2 Response of the Storage Cask to Heat Loads

Normal Steady-State Operation

The results of the steady state for normal storage operation were compared to the analysis performed in Reference 34, and shown in Table 11.

Table 11: Comparison of Results for Normal Storage Conditions

Parameter	Reference 34 Analysis	Recalculated CFD Analysis
Maximum cladding temperature (°C)	393	298
Average temperature inside the MPC (°C)	250	179
Maximum MPC shell (°C)	175	180
Normal operating pressure inside the MPC (kPa)	564	564

The maximum fuel temperature values in Reference 34 is more conservative. In Reference 34, to be conservative, atmospheric pressure was used inside the canister. This lower pressure will result in low helium density inside the canister, thus, less mass to cool the inside of the canister. Additionally at higher pressure the hotter helium will be at the top of the canister instead of the middle as seen in Reference 34. This upward temperature profile shift as seen in Figure 11 will increase the temperature of the MPC wall at the top as seen in Table 11.

MPC centerline fuel temperatures as a function of axial direction are shown in Figure 11. A maximum temperature of 298°C (568°F) was reached in the fuel region with the highest burn-up peaking factor.

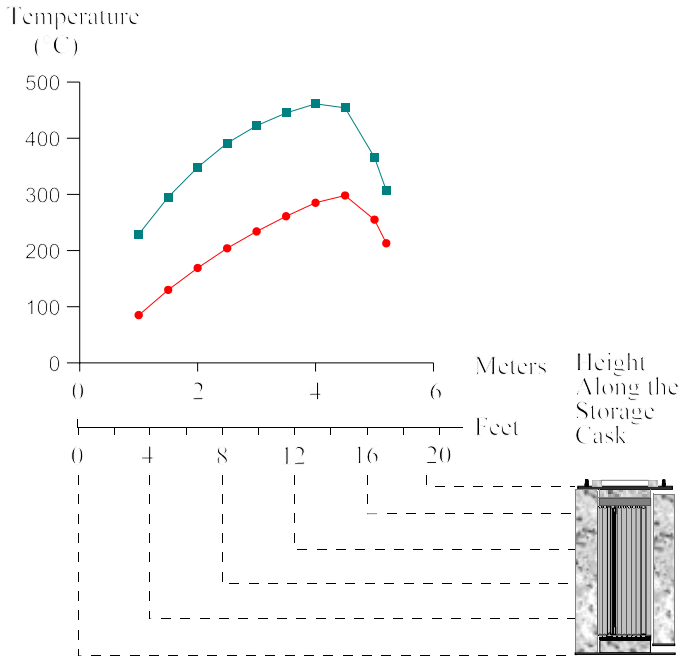

Figure 11. Centerline Fuel Temperature
• Normal Operating Temperature
▪ Temperature with Blocked Vents

Figure 12 illustrates the temperature variation as a function of the axial position at three radial positions across the cask concrete overpack. As expected the inner surface of the concrete will be at higher temperature for the normal storage operation. Figure 12 also reflects the increase of the air temperature as it flows upward in the cooling passage between the MPC and the cask. The maximum temperature of the MPC shell under normal conditions is 180 °C as shown by the time zero temperature in Figure 15.

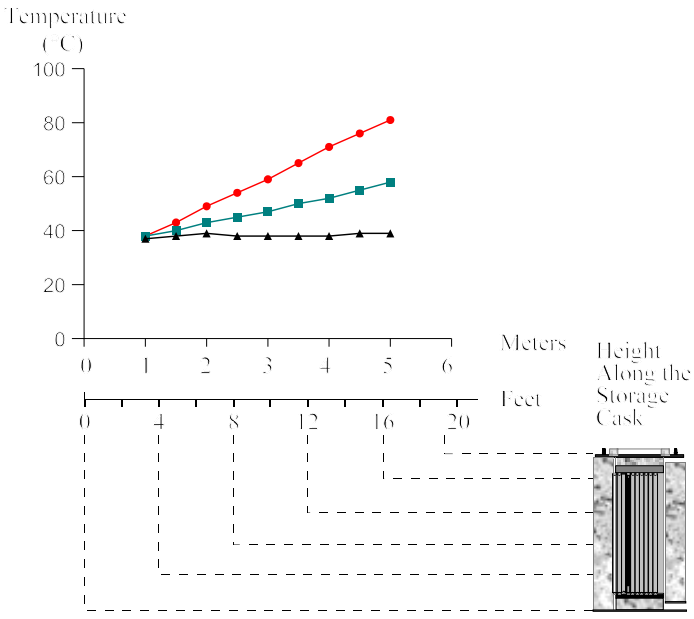

Figure 12. Storage Overpack Concrete Temperature During Normal Operation

- • Inner Boundary Temperature
- ▪ Middle of Concrete
- ▲ Outer Border Temperature

Blocked Vents

A steady state as well as transient analyses were performed assuming all the vents were closed. The transient analysis showed that it will take approximately 25 days to reach steady state values. The analysis was performed using the Fluent CFD program (Reference 33).

In Appendix C, Figure C.21 shows that a maximum temperature of 461°C (862°F) was reached in the fuel region with the highest burn-up peaking factor.

In Appendix B, Figure B.12 shows that the maximum temperature in the MPC shell for the blocked vents scenario was 283 °C (542 °F).

Figure 13 shows the storage cask concrete temperature variation as function of the axial direction. A maximum temperature of 216 °C is reached in the concrete overpack. None of the blocked vent or other thermal scenarios resulted in conditions that could fail the MPC.

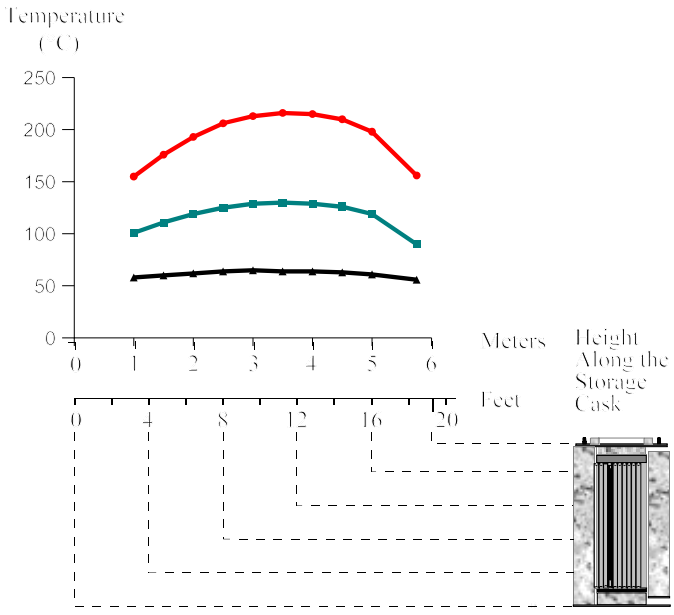

Figure 13. Storage Overpack Concrete Temperature with Bottom Vents Blocked

- Inner Boundary Temperature
- Middle of Concrete
- Outer Border Temperature

Fires

An accident scenario was developed that takes into account a crash of a Gulfstream IV aircraft from a nearby airport, and used, as a key assumption, the volume of fuel this aircraft carries. An 82.5 MW (heat release rate) engulfing external fire was therefore modeled in a transient mode. The intensity of the fire is based on a conservative bounding estimate using the amount of fuel that could combust over a three hour period as a result of the crash of a Gulfstream IV, the largest private/commercial aircraft which takes off and lands at any of the four airfields located around the site, however a credible fire scenario will be less that 30 minutes.

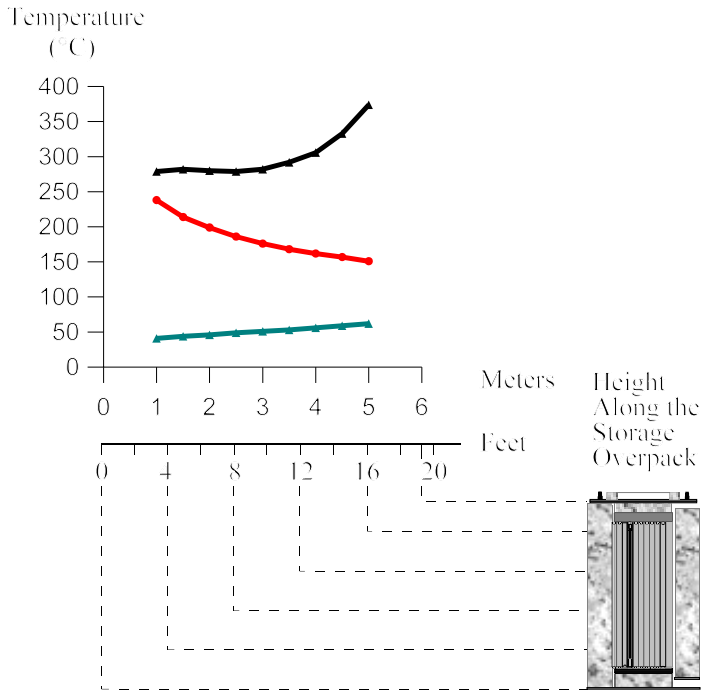

Figure 14. Temperature of Storage Cask after 3-hour Fire with an Energy of 82.5 MW
• Inner Boundary Temperature
▪ Middle of Concrete
▲ Outer Border Temperature

As the fire started, hot gases emanating from the fire surrounded the entire cask. The stream introduced to the cooling passage is now hot and consists of combustion product gases as well as air. The analysis was performed using the Fluent CFD program (Reference 33). A peak temperature of 1200 °C (2433 °F) was reached in the fire region. In the fire region immediately surrounding the cask, temperatures closer to the outer wall of the cask are significantly lower than the maximum temperature reached in the fire zone. As cooler air mixes with hot gasses, it flows upward along the surface of the cask.

Figure 14 shows the temperature variation as function of the axial direction in the cask concrete structure at three radial locations at the last time step of the analysis (180 min). The concrete wall inner border temperature (middle curve) reflects the temperature change of the hot mixture as it flows up the cooling channel. The mixture will lose heat to the MPC as it flows upward. The external border of the cask concrete layer (upper curve-triangles) and the middle of the concrete (lower curve-squares) are more affected by the hot gases bordering the dry cask from the outside. (Reference 36, Reference 37, Reference 38).

Figure 15 depicts the rise in MPC shell temperature during a 3-hour fire scenario. The maximum temperature reached in 180 minutes was 352 °C (666 °F). Note, steady state i.e. equilibrium temperature had not been reached at the three hour point. In Appendix C, Figure C.19 shows that the maximum fuel temperature reached was 298 °C (568 °F).

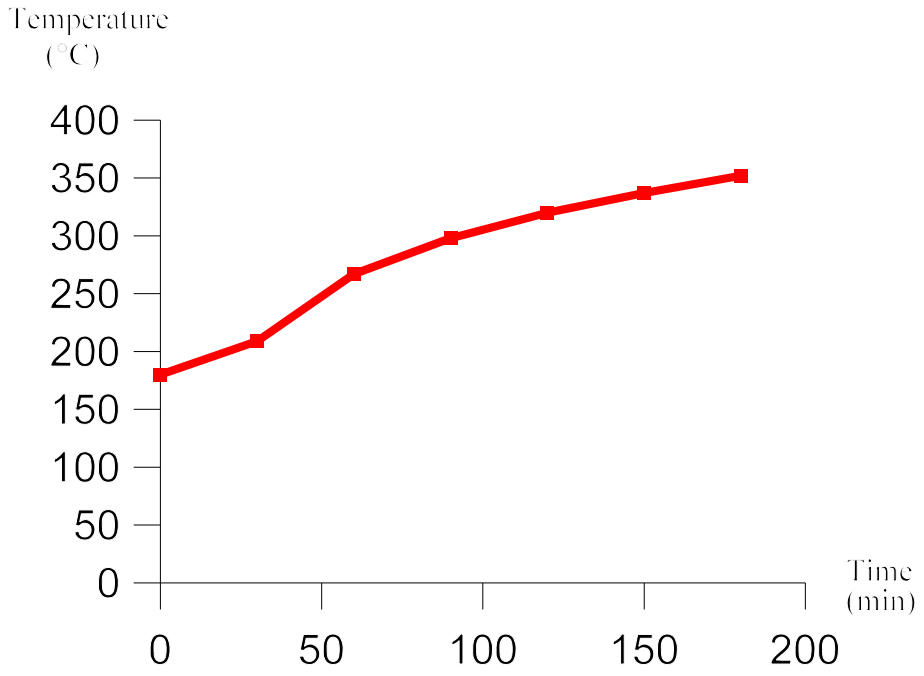

Figure 15. Maximum MPC Shell Temperature in a Fire Scenario

4.2.2 Heating During Lightning Strikes

4.2.2.1 Lightning Dissipation Model

Reference 2 states that lightning would cause no damage to the storage cask. The underlying assumption is that the lightning energy is discharged to ground. Reference 39 (on requirements of the lightning protection code addressed in Reference 40) states that a direct connection to a grounding system is a necessary element of lightning protection for metal towers and tanks, the category best matching the storage cask. However, the storage cask at the subject plant does not have direct grounding. Therefore, a detailed analysis of the potential event scenarios resulting from a lightning strike was conducted to more fully characterize the potential consequences of a lightning strike on the storage cask in both grounded and ungrounded configurations.

For the pilot PRA, the material representing the MPC contents was assumed for calculation purposes to be homogenized by using average properties for electrical and thermal analyses. A model with uniformly distributed, homogenized material will have continuous electrical paths throughout the structure. While the material has average properties to account for the spatial dilution of the material, the possible paths for currents to flow are continuous in all directions. In contrast, the MPC is made up of discrete components with voids and discontinuities between them, making their electrical contact imperfect. Because the homogeneous model allows current to flow uniformly throughout the MPC and contents, the predicted average power deposition would likely be higher than in the physical situation where the current is along much more restricted paths. The homogeneous model gives average predictions and cannot give information about local maxima and minima. A much more detailed and complex model would be required to obtain accurate local values for heat deposition or temperature. However, this also means that

locally, the power deposition can be much higher than the average values calculated with the simple models. Analysis of both grounded and ungrounded models of the storage cask predict that power deposited within the MPC is insufficient to cause temperature increases that could cause internal damage or rupture of the MPC. The models predict a power deposition to cause only a small average temperature increase in the MPC of approximately 2 °C (4 °F).

4.2.2.2 Response of the Storage Cask to Lightning Strikes

Power Deposition in Concrete Radiological Shielding. Substantially more power is deposited in the concrete radiological shielding within the storage cask when the cask is ungrounded compared to when grounded. The ratio of power deposition in grounded and ungrounded casks varies during the excitation pulse from a factor of 2 to a factor of 13 more power deposited in the concrete in an ungrounded cask. As an overall average, about 3 times as much power is deposited in the concrete shielding in an ungrounded cask than in a grounded cask. In either case, the peak and average temperature rises in the concrete were small. In a two-dimensional calculation, with an initial temperature of 66 °C (151 °F) (Reference 2), the average temperature rise was found to be about 0.2 °C (0.4 °F). The peak temperature rise was found to be 5.9 °C (10.6 °F) in the grounded cask and 25.3 °C (45.5 °F) in the ungrounded cask. The two-dimensional results for an ungrounded cask indicate the possibility of a local temperature excursion sufficient for some damage to the concrete (e.g., fracture or cracking), but that is not considered to be sufficient to cause rupture of the steel liner encasing the concrete.

Power Deposition in the Storage Cask Lid. The largest power deposition density occurs at the lightning strike location, which was assumed to be on the storage cask lid in these simulations. Because of the wide variation of spatial resolution between various models, different simulation models predicted widely varying peak temperatures at the lightning strike location. A failure of the storage cask lid does not appear to be a credible outcome in any of the models.

Voltage on the Outer Shell of the Storage Cask. A major difference between grounded and ungrounded storage casks is the voltage profile on the outer shell of the storage cask. With the cask grounded, the cask voltage at the interface with the pad will be close to zero. With the cask ungrounded, the voltage at the concrete interface is several megavolts, causing concern for any personnel, if they were near the cask during a lightning strike. In a real lightning strike, voltages will also be higher in the concrete pad and soil for both grounded and ungrounded casks because the currents cannot be spread and dissipated as quickly as in an idealized case. However, these voltages should cause no structural damage to the storage cask itself. (Reference 41)

4.2.2.3 Conclusions

The lack of a ground connection to the cask allows high electric potentials to develop on the cask near the concrete pad. These electrical potentials may result in arcing to nearby structures. Without a ground connection, voltages on the cask near the concrete pad can reach several megavolts and could pose a significant electrical hazard to workers if they were near the cask. Grounding the cask significantly modifies the voltage distribution on the outer shell of the cask, reducing it to near zero at the concrete pad.

Although lightning currents are predicted to penetrate both the storage cask and MPC for both the grounded and ungrounded configurations, calculations indicate that the MPC will remain intact. Grounding the cask appears to have little effect on power deposition in the interior of the MPC, but results in a 3-fold decrease in the average power deposited in the concrete shielding within the cask. Though the concrete immediately below the simulated lightning strike location on the cask lid is heated by current penetrating through the steel lid, the deposited energy is insufficient to cause structural damage. The temperature rise in all regions of the cask, except for the metal at the strike location itself, is well below the level where damage to the integrity of the storage cask would occur. Localized heating of

the metal lid at the lightning strike location is predicted to be sufficient to melt and vaporize some material. However, this occurs only in a very localized region at the lightning strike location and a failure of the storage cask does not appear to be a credible outcome.

4.2.3 Response of the Fuel Rods to Thermal Loads

The thermal models described in Section 4.2.1.1 do not model the spent fuel assemblies in the MPC; therefore, the cladding temperatures are not explicitly known. However, the temperature of the helium fill gas within the MPC is modeled for these accident scenarios (blocked vents and 3-hour fire).

One of the key assumptions made in this assessment is the following:

- The cladding temperature is equal to the temperature of the helium.

For thermal loads, spent fuel rod failure is determined by comparing the cladding temperature to the temperature limit imposed by Reference 2. The reference lists 394 °C (742 °F) as the Zircaloy temperature limit for BWR spent fuel assemblies that are 5 years old. This temperature limit is based on a methodology developed by Pacific Northwest National Laboratory for calculating permissible peak clad temperatures for generic commercial spent fuel rods. More recent (November 2003, ADAMS Accession No. ML022110372) Interim Staff Guidance Memorandum No. 11, "Cladding Considerations for the Transportation and Storage of Spent Fuel" identifies the temperature limit as 400 °C (752 °F) for normal conditions of storage and short term loading operations. For, off-normal and accident conditions like fire and blocked vent scenarios, the maximum cladding temperature should not exceed 570°C (1058 °F). Fuel damage does not occur at this temperature. However, events that result in temperatures exceeding this limit are, for the purposes of this PRA, conservatively assumed to cause damage to portions of the fuel.

Analysis performed using the Fluent CFD program (Reference 33) shows that once steady-state is achieved, the maximum helium temperature in the MPC under normal conditions is 298°C (568 °F). If vent blockage occurs, this temperature will increase until a new equilibrium condition is reached. Appendix C, Figure C.12 shows that the cladding temperature reaches a steady temperature of 462 °C (862 °F) after vent blockage has occurred. The cladding temperature for the blocked vents scenario did not exceeded the accident temperature limit.

The analysis was performed using the Fluent CFD program (Reference 33). During a 3-hour fire, the Zircaloy temperature only reaches 298 °C (568 °F), which is less than both the short term temperature limit of 570 °C (1058 °F) and the long term temperature limit of 400 °C (752 °F). Even though the long term temperature limit is approached, the fuel will not fail as a result of exceeding the long term temperature limit during this short term event because the long term temperature limit was based on a change in material properties and not failure of the cladding. The time needed for the fuel temperature to equal temperature limits specified in Reference 2 is 3.7 hours.

4.3 MPC Integrity

4.3.1 MPC Integrity Models

The MPC is the confinement boundary for the spent fuel. A drawing of the welds joining the shell and plate components of the MPC is shown in Figure 16. The MPC is made entirely of austenitic stainless steel. The 1.27 cm (0.5 inch) thick cylindrical shell is constructed with one circumferential and four axial seam welds. The two axial welds on each side of the MPC are slightly offset at the circumferential weld. The cylindrical shell is then welded to a 6.35 cm (2.5 inch) thick baseplate. These are full penetration submerged arc welds which undergo dye penetrant (PT) and radiographic examinations. They are not post weld heat treated to remove residual stresses. After the MPC is loaded with spent fuel assemblies, the MPC lid is welded to the shell. This 0.75 inch (1.9 cm) thick weld undergoes dye penetrant (PT) examinations after the root, intermediate (0.95 cm (0.375 inch)), and final weld passes.

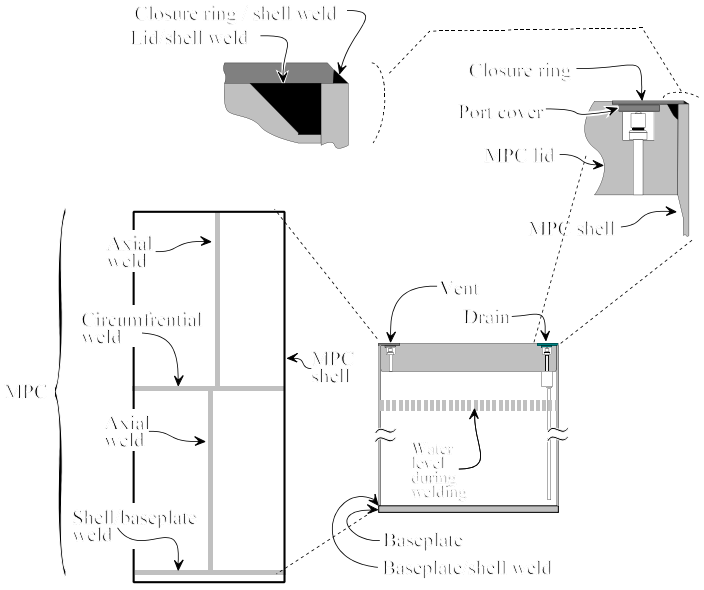

Figure 16. Welds of the MPC

The vent and drain ports used for hydrostatic testing, drying, and inerting are welded closed with cover plates. These welds undergo a final penetrant examination only. The MPC lid-to-shell weld and the vent and drain cover plate welds form the primary seal to the MPC lid. A closure ring is then placed on the MPC lid and welded to the shell and lid to form a redundant seal. The vent and drain cover plate welds and the ring welds are also performed using the Tungsten-inert gas (TIG) process. This design ensures the MPC environment is separated from the outside atmosphere by two independent lid welds. The MPC lid welds were not considered in the MPC failure assessments for the following reasons:

- The TIG process used on the lid produces is expected to produce a much tougher weld than the submerged arc (SA) weld used in the shell of the MPC.
- The redundancy of the lid design requires at least two welds to fail in order for MPC confinement to be compromised.
- The applied stresses at these locations are less than the stresses in the MPC shell for all events analyzed.

The following failure mechanisms were postulated for the MPC under mechanical and thermal loads:

- Weld Fracture,
- Exceeding the Limit Load, and
- Creep Rupture.

All three failure mechanisms were considered for thermal events, while only weld fracture was postulated for mechanical impacts. For the purposes of this PRA, failure mechanisms are assumed to be independent. The probability of MPC failure is given as the sum of the failure probabilities from each failure mechanism.

The failure models used in this PRA do not attempt to predict the hole size in the MPC for a given failure probability. Any failure is assumed to create a hole in the MPC large enough to allow the particles and gases within the MPC to be released. This assumption was made because of the difficulty inherent in trying to predict the equivalent hole size produced from a particular MPC failure mode.

The thermal analyses described in Section 4.2 indicated steady state conditions of the MPC under normal conditions would be attained prior to the various handling and transfer events used to move fuel out to the storage pad. These conditions are an internal pressure of 0.56 MPa (81 psi) with an MPC temperature that varies from 73 °C (163 °F) to 180 °C (356 °F).

Several mechanical impact accident scenarios are considered:

- Drop of the transfer cask onto the refueling floor (Stages 4 - 8, 11-13, 15-17). The transfer cask is dropped on a concrete floor from heights less than 0.91 m (3 feet). All such drops are bounded by the 5 ft drop onto the concrete floor.

- Drop of the transfer cask onto the storage cask (Stage 18). This is a handling accident, in which the transfer cask is being lowered from a height of up to 24.4 m (80 feet) and falls on the storage cask.

- Drop of the MPC while moving the MPC into the storage cask (Stages 20 - 21). The MPC falls from a height of 5.8 m (19 ft) while being lowered from the transfer cask to the storage cask.

- Drop of the transfer cask onto the concrete floor (Stage 18). This is a handling accident, in which the transfer cask is being lowered from a height of up to 30.5 m (100 feet) and, rather than striking the storage cask, falls onto the concrete floor.

- Drop of the storage cask during the transfer phase (Stages 23, 24, 26 - 33). The storage cask is dropped from a height of 0.30 m (1 feet) on concrete, gravel, or asphalt.

It was assumed that the MPC is under normal steady state conditions during the mechanical load impact scenarios listed above. In addition, all of the fuel is assumed to be intact during these events. Fuel cladding failure would cause the internal pressure of the MPC to increase. If a mechanical impact event did cause fuel cladding failure, the resulting increase in pressure would not occur during the accident scenario. The increase in internal pressure due to fuel cladding failure would be a result of the mechanical loading, but because of the extremely short duration of the impact, it would not effect the MPC internal pressure until after the mechanical loading is complete.

There are six stages (stages 11-13, and 15-17) in which the transfer cask could be dropped 0.6 meters (2 ft) onto the refueling floor. Stress levels at this drop height are not sufficient to cause failure of the MPC, and are bounded by the analysis of 5 foot drop onto the concrete floor. Therefore a drop from this height was not pursued in the mechanical impact scenarios.

4.3.1.1 Weld Fracture Model

The failure analysis model for weld fracture was based on test data of Type 308 weld deposited stainless steel specimens, and specimens taken from the stainless steel weldments of Process Water Piping of nuclear production reactors constructed in the 1950's at the Savannah River Site (Reference B.19). The mean and standard deviation of the reduction in cross sectional area of these specimens was calculated from the data and converted to true strain at failure. The true strain at failure data was then adjusted for the effects of strain rate, temperature and state of stress. These results provided a normal distribution of failure data, which was used directly to determine the probability of weld fracture given the maximum strain calculated for each impact event.

4.3.1.2 Limit Load Model

For the case of an MPC with no flaws, a flow stress model was used to predict MPC failure. Failure occurs if the primary membrane stress equals or exceeds the flow stress of the material.

The probability of failure was calculated by performing Monte Carlo simulations at various temperatures. The probability of MPC failure is the number of MPC failures divided by the total number of simulations. At a given temperature, the applied stresses were calculated. The yield and ultimate tensile strengths of the material were sampled so the critical flow stress values could be determined. If the circumferential or axial stresses of the MPC were greater than the membrane flow stress, failure was predicted. Similarly, if the bending and membrane stress of the MPC shell-to-baseplate weld exceeded the bending plus membrane flow stress, failure was also predicted. If either of these limits were exceeded, the MPC was considered failed.

4.3.1.3 Creep Rupture Model

The methodology used to predict creep rupture of the MPC is based on the model developed by Argonne National Laboratory for creep rupture of steam generator tubes (Reference 42). In this model, the structure accumulates a fraction of creep damage after exposure to any specific time/temperature/stress condition. If the sum of these creep damage fractions exceeds 1, failure is predicted.

The probability of creep rupture failure as a function of temperature was determined as follows. The MPC stresses at any time-temperature condition were determined. For this stress, the Larson-Miller parameter required to cause creep rupture was sampled from a distribution. Given this temperature and Larson-Miller parameter, the time required to cause creep rupture failure was determined. The incremental creep damage was calculated by dividing the actual time spent in these conditions by the time needed to cause creep rupture. This procedure was repeated for the next time-temperature-stress condition. Once the summation of creep damage fractions exceeds 1, MPC failure would be predicted at the corresponding temperature.

Over time, the heat load in the storage cask would decrease because of the reduced decay heat. This heat reduction would cause a corresponding reduction in MPC temperature and internal pressure even if the cooling vents were blocked. The following conservative assumption is made.

- The internal heat load of the MPC does not decrease over time.

Monte Carlo simulations were performed to determine the probability of creep rupture failure. A simulated MPC consists of both flawed and unflawed regions. The flawed region consists of the four axial welds, one circumferential weld, and one shell-to-baseplate weld. Since the occurrence of large crack-like flaws in these welds is small, relatively few failures are predicted. Only welds are analyzed using this model, since plates are not expected to contain any crack-like flaws. It is assumed that the only flaws of potential concern are produced during welding. If any of the regions were predicted to fail, the

MPC was considered to fail. The probability of MPC failure is the number of failures divided by the number of simulations.

Under thermal loads the only significant MPC stresses are attributable to internal pressure. Stresses are calculated using the classical shell theory equations for pressurized cylinders. The highest stress associated with internal pressure loads occurs at the shell-to-baseplate connection. Section 3.4.4.3.1.2 of Reference 2 analyzed the MPC stresses due to an internal pressure of 689 kPa (100 psi) at various locations. The results indicated that the membrane plus bending stress at the MPC shell-to-baseplate connection was 303.3 MPa (43,986 psi). The axial membrane stress for this situation is 23.6 MPa (3,419 psi). The difference in these values gives the bending stress acting on the shell-to-baseplate weld as 280.0 MPa (40,567 psi). The total stress at other pressures was assumed to be directly proportional to those at 0.69 MPa (100 psi). Therefore, at a pressure of 0.565 MPa (82 psi), the total stress at this location is only 248.7 MPa (36,068 psi). Subtracting the axial membrane stress of 19.05 MPa (2762 psi) gives a bending stress of 229.6 MPa (33,306 psi).

Appendix B (Figure B.14) shows the temperature variation as a function of axial height for the steady-state conditions of the MPC under normal operating conditions with internal pressure of 0.56 MPa (81 psi). If all four cooling vents of the cask become blocked, the MPC temperature and internal pressure would increase until a new steady-state condition was reached. In this case, the potential of the MPC failing due to creep rupture is introduced. See Appendix B, Sections B.1.7 and B.1.8 for a more detailed discussion of MPC creep rupture response to blocked vents. In summary, none of the blocked vent or other thermal scenarios resulted in conditions that could fail the MPC.

4.3.2 Probability of MPC Failure

Mechanical Loads

Appendix A evaluated the structural response of the MPC for various drop scenarios. The objective was to determine the maximum effective plastic strain on the MPC confinement boundary for each of these scenarios. The analyses showed that the most highly stressed regions of the MPC are near the base of the cylindrical shell and in the weld joining the shell to the 2.5 inch thick baseplate.

To determine if the integrity of the confinement boundary is compromised, the maximum effective plastic strain in the MPC must be compared to an appropriate strain failure criterion. For a valid comparison, the conditions under which the maximum effective plastic strain is calculated, and the conditions under which the failure strain limit is measured, should be consistent. The comparison, therefore, must account for how the strain is measured, as well as the effects of strain rate, temperature and state of stress. Appendix B, Section B.1.4 establishes a valid basis for this comparison, and estimates the probability of exceeding the failure strain limit for a given drop event.

Table 12 provides a summary of MPC failure probabilities for various mechanical impact loads. Those stages where the MPC is sealed are briefly discussed below.

If the transfer cask were dropped during Stages 11 through 17, the probability of MPC failure is $<1 \times 10^{-6}$. During these stages the transfer cask is sealed and carried one to two feet above the refueling floor. In Stage 18, the transfer cask is lowered 24.4 meters (80 feet) to the storage cask. If the transfer cask is dropped 80 feet onto the storage overpack, the probability of MPC failure is very small (0.0002). On-the-other-hand, should the transfer cask drop 100 feet and impact the concrete floor, the probability of failure is approximately 0.02.

During Stages 20 and 21, the MPC can potentially be dropped 5.8 m (19 ft) into the storage overpack. If this were to occur, the probability of MPC failure is 0.28.

During stages 29 through 33 if the storage cask were to be dropped from a height of 0.3 m (1 ft) onto concrete, asphalt, or gravel, the failure probability of the MPC is $<1x10^{-6}$. For both the end drop and the rotation drop, the cask transporter can cause the storage cask to slide, but not tip-over. The stresses generated during sliding events are much lower that for the drop events or tip-over and would not cause the MPC to fail.

The probability of MPC failure in the event of tip-over during storage is calculated to be $<1x10^{-6}$. The dry storage cask system SAR also analyzed a tip-over and concluded that it would not lead to MPC failure. The probability of cask tip-over due to a number of different potential events, such as seismic events, high winds, collision by vehicles, tornado driven missile impacts, and shock waves from tanker or pipeline explosions was evaluated, and for all such events it was concluded that there would be no tip-over and therefore zero probability of damage to the MPC.

Table 12. Summary of MPC Failure Probabilities for Various Mechanical Impact Loads

Event Scenario	Impact Surface (Target)	Drop Height (feet)	MPC Failure Probability[(1)]
Transfer Cask Vertical Drop	Concrete Floor	5	< 0.000001
		40	0.000360
		70	0.002600
		100	0.019600
	Storage Cask	5	0.000002[(2)]
		40	0.000014
		80	0.000203
Drop of MPC from Transfer Cask into Storage Overpack during Transfer Operations	Storage Overpack Pedestal	19	0.282000
Storage Cask Vertical Drops on Various Surfaces	Concrete	1	< 0.000001
	Asphalt	1	< 0.000001
	Gravel	1	< 0.000001
Storage Cask Tip-over	Concrete Pad	NA	< 0.000001

(1) See Note 1 of Table B.3 and Section B.1.4 of Appendix B.
(2) This result is not consistent with other results presented in the Table, i.e., it should be <0.000001. This is due to the fact that the response results for this case were based on the original (unmodified) LS-DYNA analysis, which, due to a number of factors, produced very conservative results at low drop heights.

Thermal Loads

Evaluations of the probability of MPC failure due to fracture, load limit, and creep rupture from thermal loads are detailed in Appendix B, Sections B.1.3, B.1.5 - B.1.7. Failure models were created in Microsoft Excel with an add-on module called @RISK (www.palisade.com). This module allows Monte Carlo simulations to be run in Excel by allowing values in the spreadsheet cells to be sampled from statistical distributions. The spreadsheet cell specified as output identifies each iteration as either an MPC success

or failure. This process is repeated many times in a Monte-Carlo simulation. The probability of failure was calculated by dividing the total number of MPC failures by the total number of iterations performed. If normal steady-state conditions are maintained for the full 20-year license period of the cask, no MPC failures are expected. If the storage cask is exposed to an external fire for 3 hours or all four cooling vents become blocked, the MPC temperature and pressure will increase, but no MPC failures are expected.

Even with the yield and tensile strengths below the minimums, the limit load model was never the limiting failure mechanism in any of the heat-up scenarios. None of the blocked vent or other thermal scenarios resulted in conditions that could fail the MPC.

4.4 Fuel Failure

4.4.1 Fuel Integrity Model

The peak g loads imposed on a fuel rod from the vertical drop scenarios considered in the PRA far exceed the elastic buckling load of the fuel rods in the assemblies. Therefore, to determine the strain demand on the fuel cladding, the inelastic buckling capacity of the fuel rods must be considered. The approach taken in Appendix C was to analyze the fuel rod as an elastic-plastic beam-column with initial curvature under dynamic impact. Failure of the fuel rod is determined by comparing the maximum strain in the cladding to a strain limit based on experimental data.

Since the impact event entails the interaction of potentially hundreds of rods, their spacer grids, tie plates, fuel spacers, basket, cask, and target under dynamic loading, computational efficiency was achieved by modeling a single fuel rod. Thus an explicit finite element analysis model of a single fuel rod with lateral displacement constraints was used to study the inelastic behavior of a fuel rod under dynamic impact loads (See Appendix C for details).

4.4.2 Fuel Rod Cladding Failure

For each drop height, Table 13 lists the maximum principal strain in the cladding, the failure strain limit and whether or not fuel cladding failure occurs based on the limit strain. For the drop of the transfer cask (TC) onto the concrete floor, additional drops of 20 and 55 feet were added to the standard drop heights of 1, 5, 40, 70, and 100 feet in order to highlight transitions in buckling behavior or differences in response due to target stiffness.

Table 13. Probability of Fuel Cladding Failure for Various Drop Scenarios

Event Scenario	Impact Surface (Target)	Drop Height (feet)	Maximum Principal. Strain in Cladding (in/in)	Strain Limit Selected for High Burnup Fuel (in/in)	Probability of Fuel Cladding Failure
Transfer Cask Vertical Drop	Concrete Floor	1	0.0043	0.010	0.0
		5	0.0062	0.010	0.0
		20	0.0072	0.010	0.0
		40	0.011	0.010	1.0
		55	0.025	0.010	1.0
		70	0.037	0.010	1.0
		100	0.052	0.010	1.0
	Storage Overpack	5	(1)	na	0.0
		40	(1)	na	1.0
		80	(1)	na	1.0
MPC Drop into Storage	Storage Overpack	19	0.090	0.010	1.0
Storage Cask Tip-Over	Concrete Pad	na	0.0055	0.010	0.0

(1): This drop was not evaluated for cladding response. Results for the transfer cask drop onto the concrete floor from the same height were used to determine cladding failure.

The results show that the cladding yield strain of 0.0084 in/in is not exceeded until drops of the transfer cask are in the 20 to 40 foot range. The results also show that target stiffness has a significant influence on cladding strain. For example, the 20 foot drop of the TC on to the concrete floor results in a strain less than yield, where as, the 19 foot drop of the MPC into the storage overpack, which is a much harder impact, produces cladding strains that are ten times greater than yield. This is because the buckling modes for these two impacts are completely different, as discussed in Appendix C.

The cladding strain at failure (rupture or breach) of high burnup fuel, with circumferential hydrides, which is fuel with a burnup greater than 45 GWd/MTU, is expected to range from 1.0% to 3.0%. For the purpose of the PRA, the lower value of 1.0% strain is selected as the strain limit at failure.

Appendix D of the PRA shows that the particulate release fraction from a spent fuel rod is a function of three variables: (1) the fraction of the fuel rim layer that fractures, (2) the percentage of particulate entrained by gasses during release, and (3) the number of tears (breaches) per rod. In addition, the fraction of the rim layer fractured and the number of breaches per rod are in turn functions of the g loads experienced by the fuel and the severity of the buckling that takes place during a given drop.

In a detailed PRA each of these variables would be associated with a probability distribution and sampled as part of an overall simulation. However, because of the level of effort inherent in such an approach, Appendix D simplifies the effort by recommending an upper bound value for release fractions to be used in the consequence analysis. This in turn simplified the effort in Appendix C by not requiring an estimate of the number of breaches per rod, but only whether or not the rod breaches at all. Also, since the analysis of fuel rod failure is based on a single pin model, it was assumed that when one rod fails, all rods fail, although this is very unlikely.

A tip-over of the storage cask will cause a peak lateral load of 45g on the fuel assemblies. Based on an evaluation of eight different laterally loaded BWR and PWR fuel assemblies ranging from 7x7 to 17x17 arrays, Reference 43 concludes that, for the particular cladding properties used, the cladding yield strain of 0.0077 in/in is reached for a lateral loading of 63g. Since this is a linear elastic analysis, the strain at 45g would be 0.0055 in/in, which is much less than the cladding failure strain limit of 0.01 in/in.

The failure probability of fuel rods if a single assembly were dropped, as in Stage 1, is estimated by using data on individual assemblies. To estimate a failure probability when no failures have been observed, the 50 percent confidence limit can be used. For a binomial distribution, the 50 percent confidence limit when no failures have been observed is calculated by dividing 0.7 by the number of cases. Thus, the probability of fuel assembly failure is estimated as 6.4×10^{-2} (0.7/11 = 0.064). (See Section 3.3.1.)

5. SECONDARY CONTAINMENT ISOLATION

5.1 Containment Isolation Reliability Model

Given a release of radioactive material inside the secondary containment following a drop of the transfer cask, the three distinct functions that occur are to detect radioactive material, isolate the containment, and operate the SGTS. Each of these functions is accomplished by redundant and independent trains of systems. The release of radioactive material will be detected by one or more of six detector systems that signal the secondary containment to isolate. Each of these detector systems consists of two trains, each train having two detectors. Both detectors in a train must detect radiation to isolate the secondary containment. Only one of the 12 trains is needed to isolate the secondary containment.

The secondary containment is modeled as one large volume as shown in Figure 17. The letters in circles next to the names of the HVAC systems relate these systems to the event tree that is illustrated in Figure 18. The success criteria for the secondary containment model are as follows:

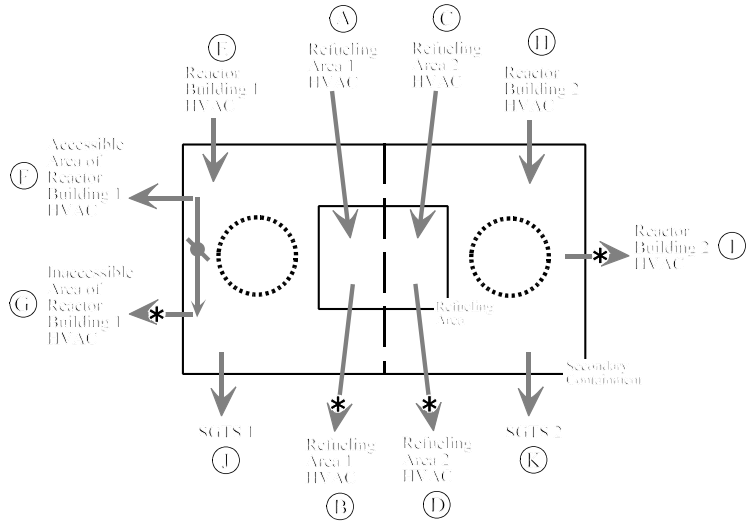

Figure 17. Secondary Containment HVAC Model

- During normal operation, all direct paths to the external environment are closed.
- A negative differential pressure is maintained between the inside of the secondary containment and the environment.
- When an isolation signal occurs, the SGTSs of Unit 1 and Unit 2 take suction from the inside of the secondary containment, filtering the intake and directing the exhaust to the plant stack (elevated release).

The event tree used to determine the probability of failing to isolate the secondary containment is shown in Figure 18. The top events of the event tree are the failure of valves along the ventilation paths to close and the failure of fans to stop moving air through the secondary containment. Each top event is a valve or fan of the ventilation system, except for the last two top events, which are the SGTSs. The valves and fans are paired in their respective system for brevity and clarity. The systems have letters (A) though (K) corresponding to the same systems illustrated in Figure 17. The top events are quantified with fault trees that model the fans, valves, and radiation sensors to initiate the isolation of the secondary containment if radioactive material were released from a transfer cask. Inputs to the fault trees are determined from published sources of reliability data, such as Reference 44 and Reference 45.

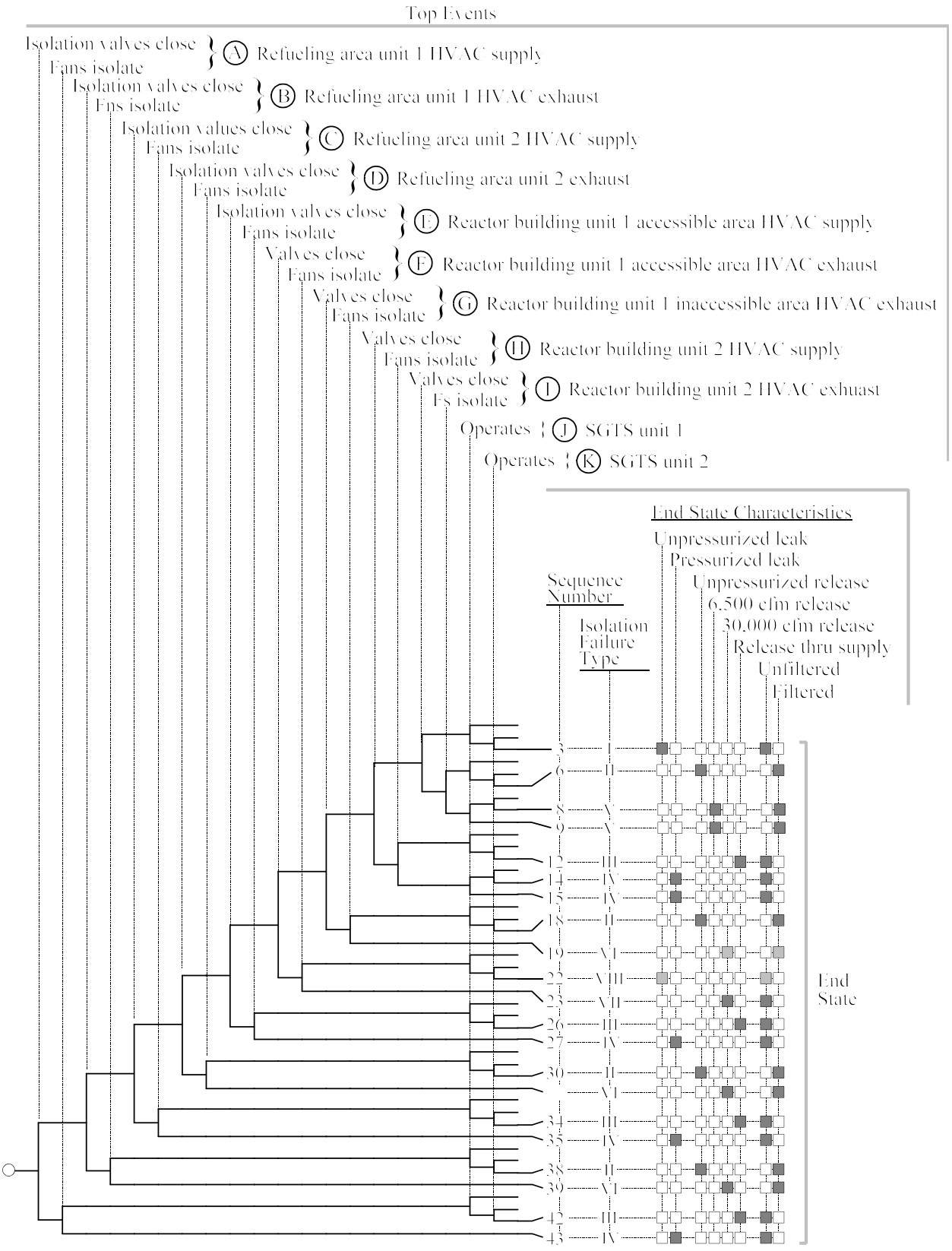

Figure 18. Secondary Containment Isolation Event Tree

The event tree delineates the ways in which the secondary containment isolation can fail by modeling the failure of valves to close, fans to isolate, and the SGTSs to operate. It does not model the progression of events that would occur if the secondary containment receives an isolation signal. If the secondary containment fails to isolate, thereby opening a release path for radioactive material, other release paths are not modeled. The analysis conservatively treats all the material that is released from the transfer cask as being released to the environment.

The 20 top events delineate 43 sequences in the event tree analysis. Of these sequences, 22 result in successful isolation of the secondary containment. The secondary containment successfully isolates when one or both SGTS(s) functions, even if there is an open path between the secondary containment and the outside atmosphere. SGTSs filter the release through an elevated plant stack. The other 21 sequences result in a failure to isolate the secondary containment. Eight types of secondary containment isolation failures are delineated in Figure 18. The isolation failure types (IFTs) are defined in Table 14.

The assumptions made in the development and evaluation of the event tree model are the following:

- Doors, hatches, and personnel locks are secured according to procedures before the cask operation begins.

- The possibility of an open door or other access opening during the cask operation is negligible. The justifications for this assumption are as follows. First, the HVAC system automatically adjusts to provide a negative differential pressure across the secondary containment boundary. Second, if a door or other access opening were inadvertently left open, the HVAC would not be able to draw a vacuum. An open door in the secondary containment would alarm in the control room. Workers would be directed to close the open door. The handling phase of the operation would cease until the negative pressure in the secondary containment could be reestablished.

- Because the SGTS filters are passive components, they have a negligible probability of failing to reduce the radioactive material content of the gas passing through them.

- If the HVAC systems isolate and both SGTSs fail to operate, the elevated temperature inside the secondary containment, with respect to the outside air, provides a driving pressure for a release of radioactive material from the failed MPC. However, as compared to other releases from reactor accidents, the flow rate is small.

5.2 Probability of Secondary Containment Isolation Failure

The results of probability calculations for sequences in Figure 18 are shown in Table 14. To calculate the probability of the secondary containment failing to isolate, only the sequence probabilities are summed as shown in Table 15. The small total probability of 1.5×10^{-4} is attributable to the large amount of redundancy in the secondary containment isolation systems.

Table 14. Secondary Containment Isolation Failure Types

Isolation Failure Type (IFT)	Probability†	Sequences	Description
I	1.4×10^{-4}	3	Unpressurized leak. All systems have isolated (automated design response of the isolation system or over-current trip of HVAC fan due to closure of the isolation valves) and both SGTS fail. Leak occurs through cracks, around doors, etc.
II	3.1×10^{-8}	6, 18, 30, 38	Unpressurized filtered release through exhaust. Release through HVAC exhaust system due to exhaust isolation valves failing to close. Supply and exhaust fans isolate. Exhaust filtered release through reactor building vent plenum.
III	2.7×10^{-8}	12, 26, 34, 42	Unpressurized unfiltered release. Release through HVAC supply system due to supply isolation valves failing to close. Supply and exhaust fans isolate. Unfiltered release through supply louvers.
IV	8.0×10^{-6}	14, 15, 27, 35, 43	Pressurized-leak. All HVAC exhaust systems isolate but the secondary containment is pressurized by failure of HVAC supply system to isolate with fan continuing to run. Leak occurs through cracks, and around doors.
V	1.3×10^{-8}	8, 9	Filtered release at 6,000 cfm. Reactor building Unit 2 exhaust system fails to isolate with fan running and either SGTS fails. Exhaust filtered release through reactor building vent plenum.
VI	6.9×10^{-6}	19, 31, 39	Filtered release at 30,000 cfm. Refueling area Unit 1, refueling area Unit 2 or reactor building Unit 1 inaccessible area HVAC exhausts fail to isolate, associated fan continues to run at 30,000 cfm. Exhaust filtered release through reactor building vent plenum.
VII	2.3×10^{-6}	23	Unfiltered release at 30,000 cfm. Reactor building accessible area HVAC exhaust fails to isolate. Fan continues to run at 30,000 cfm. Unfiltered release occurs through reactor building vent plenum.
VIII	7.6×10^{-9}	22	Unpressurized unfiltered release. Reactor building accessible area HVAC exhaust fails to isolate. Fan isolates. Unfiltered release through reactor building vent plenum.

† Note: Values in this table are shown as they are computed in the SAPHIRE software.

Table 15. Sequences Where the Secondary Containment Fails to Isolate

Sequence Number	Probability	Sequence Number	Probability
3	1.4×10^{-4}	23	2.3×10^{-6}
6	$7.6\text{x}10^{-9}$	26	$2.7\text{x}10^{-8}$
8	$2.8\text{x}10^{-9}$	27	8.0×10^{-6}
9	$1.0\text{x}10^{-8}$	30	$7.6\text{x}10^{-9}$
12	$4.9\text{x}10^{-12}$	31	2.3×10^{-6}
14	$1.5\text{x}10^{-12}$	34	4.9x10-^{12}
15	$6.2\text{x}10^{-12}$	35	$1.6\text{x}10^{-9}$
18	$7.6\text{x}10^{-9}$	38	$7.6\text{x}10^{-9}$
19	2.3×10^{-6}	39	2.3×10^{-6}
22	$7.6\text{x}10^{-9}$	42	$4.9\text{x}10^{-12}$
		43	$1.6\text{x}10^{-9}$
		Total	1.5×10^{-4}

6. CONSEQUENCES

6.1 Source Term

This consequence assessment addresses the severe accident scenario related to the inadvertent drop (100 feet drop) of the HI-STORM 100 Cask system while in the stage 18 of the transfer process. This consequence assessment was performed to support development of a probabilistic risk assessment (PRA) for dry cask storage for the specific BWR reactor facility analyzed in the report. In order to examine radiological consequences, release fractions for this accident were developed. Release fractions were estimated as the product of a rod-to-canister release fraction and a canister-to-environment release fraction. Input was obtained from Sandia National Laboratories (SNL) for the development of source term. Detailed re-analysis on source term analysis is documented in Appendix D.

This assessment was performed using the MELCOR Accident Consequence Code System (MACCS2) (Reference 8 and Appendix E, Reference E.2) for a boiling water reactor (BWR) facility. Specific data needed to model a HI-STORM Dry Cask 100 feet drop accident scenario for the MACCS2 consequence calculation were collected and used. The important parameters/variables required to model the BWR site are: the radionuclide inventory, the source term (i.e. release fraction, release start time, and release duration), the initial plume dimensions (related to the system geometry), the plume heat content, the population density/distribution, and the subject site weather. Other input parameters and models necessary for a MACCS2 calculation were taken from the NUREG-1150 study MACCS2 input file prepared for the Surry nuclear power plant. The input file is documented in Appendix C of the MACCS2 code manual and is referred there as Sample Problem-A (SP-A)[1]. This SP-A MACCS2 input file was used due to the availability and pedigree of this input file. Additionally, the SP-A input parameters are suitable to model the subject site dry cask storage consequence calculation. A summary of the results obtained by MACCS2 is presented in Table 18. A discussion of the parameters used for the subject site variables, shown in Table 18, can be found in Appendix E, from Sections E.3 to E.11.

The consequence measures chosen for this study were the mean values given by MACCS2 for individual risk of early fatality within 1.6 km (1 mi) and the individual risk of cancer fatality within 16 km (10 mi) of the site boundary.[2] The 1.6 km (1 mi) value is the distance from the exclusion area boundary (EAB), assumed to be 0.5 km (0.3 mi), out to a distance of 2.1 km (1.3 mi). These distances and consequence measures were chosen to allow comparison to the NRC's quantitative health objectives for reactor accident risk. Since cask accident consequences in terms of individual risk of early fatality and cancer fatality are small, the mean consequence values calculated for individual lifetime dose commitment (the mean values of the variable known in MACCS2 as “peak dose found on spatial grid”) may also be of interest. Therefore, this section includes the estimated mean individual lifetime dose between 1.2 and 1.6 km (0.75 and 1.0 mi) as measured from the release point. Also, close-in consequences are generally more representative of the source term, while consequences further away tend to be controlled by assumptions on long-term relocation.

An impact on the cask will fail a fraction of the fuel rods (F_{rods}) and make their contents available for release. A portion of this available material will be released from the rod to the cask environment (F_{RC}). Part of the inventory that has been released to the cask will be transported through the breach in the cask to the environment (F_{CE}). The fractional release from the cask (F_{rel}) can be approximated by the equation:

---

1 / Note: Evacuation was not considered in the MACCS2 consequences calculations for this study.

2 / Note: All consequence measures given in Appendix E are mean values as calculated by the MACCS2 code unless stated otherwise. The mean values in MACCS2 are defined as the average (expected) consequences over all weather conditions (Reference E.2).

$$F_{rel} = F_{rods} \times F_{RC} \times F_{CE} \quad (1)$$

The fuel rods can have radionuclides on the cladding surface in the form of solid Chalk River Unidentified Deposits (CRUD), inside the fuel rod as gases and volatile fission products, and within UO_2 fuel grains as both solids and gases. Due to the different physical forms of the radionuclides, Eq 1 is analyzed separately for each group of similar radionuclides.

This release fraction model (Appendix D) accounts for the different properties of the rim region formed in high burnup fuel and the reduction in ductility of the cladding due to higher burnup and hydrogen absorption. The methodology, as presented, is only applicable to impact type events and not those that result in an elevated temperature due to a long duration fire.

The fraction of the rods fractured (F_{rods}), calculated in Appendix C, is dependent on the energy imparted to the rods, which in most cases is a function of drop height. The release from the rods to the cask makes use of the properties of high burnup fuel and analyzes the particulate release from the rim and body regions of the fuel separately. Fracture of the fuel into fines is based on a modification of the equations in the DOE Handbook (See Appendix D) that relates the fraction of fuel that fragments into a respirable size to the impact energy that the fuel experiences. F_{RC} will be dependent on the number of fracture sites in a rod, the entrainment of the fines in the gas stream during the depressurization of the rod, and the extent to which the rim region actually fractures. Uncertainty in these parameters is analyzed. The release of radionuclides from the cask to the environment is based on the fraction of gas that is ejected when the cask depressurizes to atmospheric pressure. An ideal gas law relationship is assumed. An analysis of the propensity for settling and plating out of particulate, by a number of mechanisms, so they are not in the gas stream during depressurization is also conducted. Details can be found in Appendix D.

6.1.1 Source Term Estimates

In addressing source term estimates, the discussion necessarily includes consideration of release fraction, release start time and release duration.

6.1.1.1 Release Fraction

The release fractions calculated in Appendix D are based on the number of fuel fractures calculated in Appendix C.

6.1.1.2 Release Start Time

In the MACCS2 calculation for the cask drop event, it was conservatively assumed that as soon as the accident occurs, the release to the environment occurs immediately.

6.1.1.3 Release Duration

The probability of failure of the MPC, in the event of an 100 ft drop, is discussed elsewhere in this report. While the likelihood of failure of the MPC in this type of event is in reality quite low, in order to examine radiological consequences, release fractions for this accident were developed. Release fractions were estimated as the product of a rod-to-canister release fraction and a canister-to-environment release fraction. The release fractions presented in Table 16 for the 100 ft dropped transfer cask are the fraction of inventory that can be released by depressurization from the cask at the time of the accident. Details are provided in Appendix D.

Table 16. Release Fraction Values for an 100 Ft Drop of the Transfer Cask

Radionuclide	Release Fraction	Release Fraction with Filtration
Nobel Gases	0.12	0.12
Particles	7×10^{-6} to 1.2×10^{-3}	7×10^{-7} to 1.2×10^{-4}
CRUD	1.5×10^{-3}	1.5×10^{-4}

6.2 Consequences

6.2.1 Consequence Model

The major inputs for the calculation, including a brief description, are shown in Table 17. Details are given in Appendix E.

Offsite consequences from radioactive material released from a transfer cask or storage cask during a severe accident are modeled with the MACCS2 code (Reference 47). A plume of radioactive gases and aerosols are released from a point and dispersed in the atmosphere, exposing the surrounding population. The characteristics of the release, such as the amount of material, the type of material, and the heat content, are determined from other studies (see Appendix E). The consequence measure that is used in risk estimates is an expected value of the consequences from the dose calculations given a release of radioactive material (i.e., source term). The calculated consequence measures are early fatalities and latent cancer fatalities as seen in Table 18. Sheltering and evacuation were not considered in the MACCS2 consequence analysis.

Table 17. Major Inputs for Consequence Calculations

Input	Description
Radionuclides Inventory:	Specifies the radionuclides that are to be modeled.
Source Term:	Specifies the characteristics of the radioactive plume such as the number of releases (i.e., plume segments), the heat content, the time of the release, and the duration of the release.
Meteorological Data:	Hourly information of one year of meteorological data at the subject site. Each hourly data set includes: the stability of the atmosphere, the wind speed, the wind direction, and the precipitation.
Population Data:	Population distribution surrounding the release point developed from census data for the subject site location.
Emergency Response:	Emergency response actions modeled in the region surrounding the release point. Emergency response actions modeled was relocation. Relocation defines the actions taken at the appropriate time to move individuals residing in zones where dose criteria are expected to exceed critical values, and the duration they will be kept in a relocated status.

Table 18. MACCS2 Consequence Calculation Results

Release Fraction			Release Height meters (feet)	Individual Risk of Prompt Fatality within 16 km (10 miles)	Individual Risk of Cancer Fatality within 16 km (10miles)	Individual Peak Dose (1.2-1.6 km Sv (rem)
Noble Gases	Particles	CRUD				
.12	1.2×10^{-3}	1.5×10^{-3}	50 (164)	0	3.6×10^{-4}	1.85 (185)
.12	1.2×10^{-3}	1.5×10^{-3}	120 (393)	0	2.1×10^{-4}	0.14 (14)
.12	1.2×10^{-4}	1.5×10^{-4}	50[1] (164)	0	5.2×10^{-5}	0.22 (22)
.12	7×10^{-6}	1.5×10^{-3}	50 (164)	0	4.3×10^{-6}	0.026 (2.6)
.12	7×10^{-6}	1.5×10^{-3}	120 (393)	0	2.6×10^{-6}	0.0036 (0.36)
.12	7×10^{-7}	1.5×10^{-4}	50[1] (164)	0	4.3×10^{-7}	0.0028 (0.28)

[1] Results corresponding to a release fraction with filters operable.

6.2.2 Consequence Measures

The dose conversion factors (DCF) used in this study are the same as those used in the NUREG-1150 study (DOSDATA.INP). The DCF's were provided by K. Eckerman from Oak Ridge National Laboratory (ORNL) for the NUREG-1150 study (Reference E.4). These DCF's include definitions for 19 organs and has DCF for 60 radionuclides important in reactor accidents. DOSDATA.INP DCF file is appropriate to generate long term health effects calculations. The dose conversion factor file used is not suitable to generate acute health effect calculations (e.g. early fatalities) for the Dry Storage Cask PRA study. The MACCS2 calculation with DOSDATA.INP DCF will generate overestimated values for acute health effects. Even with this limitation for the DCF file with acute health effects, the MACCS2 calculations predicted zero early fatalities.

It should be noted the estimated consequences (individual probability of a latent cancer fatality) from a release of the inventory of the MPC, for example, for high fuel burnup and a release height of 50 meters, include the essentially negligible contribution from noble gases ($\sim10^{-10}$), and the contribution from radionuclides other than noble gases is 3.6×10^{-4}. These estimated values are based on the output of the MACCS2 code calculations.

7. RISK ASSESSMENT

7.1 Risk Models

Reference 1 defines risk for use at NRC as the risk triplet. The elements of risk are the scenarios, the frequencies of the scenarios, and the consequences of the scenarios. Reference 1 also states that a measure of risk is the consequences multiplied by the frequency of the consequences. The measure of risk is given by Equation 6 for one initiating event:

$$R = f\sum_{n=1}^{m} P_n K_n \qquad (6)$$

where: R = aggregate risk
f = frequency of the initiating event (1/time)
P_n = conditional probability of the n^{th} accident scenario given the initiating event
K_n = consequence of the nth accident scenario

The aggregate risk is the risk measure used in this study.

To determine the risk of all plausible accident scenarios in the stages of the dry cask storage operation, Equation 6 can be rewritten as Equation 7.

$$R = \sum_{j}\sum_{m} f_{j,m}\sum_{n} P_{j,m,n} K_{j,m,n} \qquad (7)$$

where: R = aggregate risk
$f_{j,m}$ = frequency of the m^{th} initiating event while in the j^{th} stage
$P_{j,m,n}$ = conditional probability of the n^{th} accident scenario given the m^{th} initiating event while in the j^{th} stage
$K_{j,m,n}$ = consequence of the n^{th} accident scenario from the m^{th} initiating event while in the j^{th} stage

The aggregate risk of storing spent fuel in a dry cask is the risk incurred during the service life of a cask. As shown in Table 1, the service life is divided into three phases.

- handling within the refueling building
- transfer to the storage pad
- storage on the storage pad

An important consideration is that the risk of handling and transfer is demand-related while the risk of storage is time-related. Thus, the risks of the three phases must be expressed in a manner that permits them to be added to obtain the total risk. For each phase, the units of risk are consequences per year, expressed as either prompt or individual probability of a latent cancer fatality.

Consider a cask in the first year of its service life at the subject plant. During this year, the cask passes through the handling and transfer phases and begins the storage phase. In this study, the handling phase is treated as a demand-related activity because of its short duration. Because the handling phase lasts no longer than a few days, time-related external initiating events that could disturb the lifts of the transfer cask or otherwise challenge the integrity of the transfer cask are unlikely to occur. For example, an earthquake is unlikely to occur during the short period of lifting. The transfer cask is not subject to other external events, such as high winds or floods, because all the handling is done inside the containment. For these

reasons, the time-related risk during the handling phase is negligible relative to the demand-related risk. In the handling phase, the only demand-related initiating event is a drop while the cask is lifted, moved, or lowered by the crane.

The only initiating event that can occur in the handling phase is a drop of the transfer cask or a drop of the MPC (Stages 20 and 21). The risk associated with drops in the handling phase is given by Equation 7. Therefore, there is no need to sum over the initiating events. Equation 7 is rewritten as Equation 8, where the first summation is over all stages during the handling phase.

$$R^H = \sum_j f_j^H \sum_n P_{j,n}^H K_{j,n}^H \qquad (8)$$

where: R^H = risk of the handling phase
f_j^H = frequency of dropping the transfer cask or MPC during the j^{th} stage in the handling phase
$P_{j,n}^H$ = probability of a release of radioactive material to the environment during the nth sequence given that the cask is dropped in the j^{th} stage of the handling phase
$K_{j,n}^H$ = consequence of a release of radioactive material during the n^{th} sequence the transfer cask is dropped during the j^{th} stage of the handling phase

The frequency of each lift is expressed as 1 per year during the first year of service life. The handling risk is expressed as the individual probability of a prompt or latent cancer fatality per year, but it applies only to the first year of service life.

The risk of the transfer phase is determined analogously to the risk of the handling phase. Although the transfer phase occurs outside of the secondary containment where time-related events such as high winds and floods can occur, the transfer phase activities are performed only under favorable weather conditions. An earthquake is very unlikely to occur during the brief transfer period. A fire from the diesel fuel in the overpack transporter will not lead to a radionuclide release. For these reasons, the time-related risk during transfer is negligible relative to the demand-related risk. In the transfer phase, the only demand-related initiating events are drops.

The risk in the transfer phase is given by Equation 9. The first summation is over the stages during the transfer phase. The second summation is over all of the demand-related initiating events that can occur during the transfer phase.

$$R^T = \sum_j \sum_m f_{j,m}^T \sum_n P_{j,m,n}^T K_{j,m,n}^T \qquad (9)$$

where: R^T = risk of the transfer phase
$f_{j,m}^T$ = frequency of the mth initiating event during the j^{th} stage of the transfer phase
$P_{j,m,n}^T$ = probability of a release of radioactive material during the n^{th} sequence given the m^{th} initiating event in the j^{th} stage of the transfer phase.
$K_{j,m,n}^T$ = consequence given a release of radioactive material during the nth sequence given the m^{th} initiating event in the j^{th} stage of the transfer phase

During the storage phase, the overpack cask is subject to time-related initiating events (e.g., earthquakes, high winds) that can challenge the integrity of the overpack and the MPC. Because the storage phase has only one stage, the risk in the storage phase is given by Equation 9 without the first summation. This equation is rewritten as Equation 10, where the first summation is over all initiating events that can occur in the storage phase.

$$R^S = \sum_m f_m^S \sum_n P_{m,n}^S K_{m,n}^S \qquad (10)$$

where: R^S = risk of the storage phase
f_m^S = frequency of the m^{th} initiating event while in the storage phase
$P_{m,n}^S$ = probability of a release of radioactive material during the nth sequence given the m^{th} initiating event while in the storage phase
$K_{m,n}^H$ = consequence of a release of radioactive material during the n^{th} sequence given the m^{th} initiating event while in the storage phase

The storage risk is expressed as the individual probability to the public of a prompt or latent cancer fatality per year.

The aggregate risk during the first year of operation is the sum of the risks of the three operational phases. During the first year of operation, the MPC passes through the handling and transfer phases and moves into the storage phase. The handling and transfer phases last a small fraction of a year, so that the MPC is in storage for almost a full year. Accordingly, the aggregate risk of the transfer cask and overpack cask for the first year of its service life is given by Equation 11.

$$R(1) = R^H + R^T + R^S \qquad (11)$$

After the first year of operation, the overpack cask is no longer handled or transferred. Only the storage risk is incurred for each year of the remaining 19 years of the MPC's service life.

The total risk of the cask during 20 years of its service life is equal to the first year risk plus 19 times the storage risk. The contribution of handling and transfer to risk is much larger than the risk incurred during storage.

7.2 Risk Results

For this pilot PRA, the risk calculations are summarized in Table 19. Each row of the table represents an initiating event in a stage. The initiating events in Table 19 are those listed in Tables 4, 5, and 6 that have the potential to affect the subject plant or breach the MPC. Each initiating event has only one accident scenario – the failure of the MPC and fuel rods. Aggregate risk is the sum of the risks of the accident scenarios. Table 19 shows the risk for the first year of service and the annual risk for subsequent years. The risk during the first year consists of the risk from the handling and transfer phases and part of the storage phase. The risk of subsequent years consists only of the annual risk of storage on the independent spent fuel storage installation (ISFSI).

The risk measure in Table 19 is the annual individual risk of a latent cancer fatality. Because all offsite releases result in doses to individuals that are below the threshold for prompt fatalities, no prompt fatalities are expected.

The components of risk (frequencies of initiating events, probabilities of subsequent events following the initiating events, and the consequences of the scenarios) are shown in the columns of Table 19. These components are consistent with the definition of risk in Reference 1 where the frequency of the scenario is the product of the initiating event frequency and the event probabilities. The accident scenarios consist of MPC failures and, in the handling phase, releases from the secondary containment. The numbers in the last column of Table 19 are the products of the entries in the previous columns and are the risks of the scenarios.

The notes for each scenario in Table 19 state the sections in this study that discuss the corresponding initiating event frequency, the probability of MPC failure, the probability of a radioactive release from the

containment (where applicable), and the consequences as measured by the individual probability of a latent cancer fatality given the occurrence of the scenario. The notes also identify which radionuclides are released from the containment noble gases only (NG), radionuclide inventory other than noble gases (OT), or all radionuclides in the inventory of the MPC (All). The distinction is necessary because the noble gases are not filtered by the containment isolation system while the remainder of the radionuclide inventory is filtered.

For example, consider the initiating event of a drop of the transfer cask in Stage 3 while it is being lifted out of the cask pit. The drop frequency is 5.6×10^{-5}/yr because the transfer cask is lifted once in Stage 3 and the drop probability is 5.6×10^{-5}/yr (Section 3.3.2). Because the drop height is as much as 13.0 m (42.5 ft) all of the fuel rods are assumed to breach the cladding (Section 4.4.2) and the probability of MPC failure is 1 because the lid has not yet been welded to the MPC shell (Sections 4.1.2.1 and 4.1.2.4); thus, the probability of a release from the fuel rods and the MPC is 1. The release consists of both noble gases and the radionuclide inventory in the MPC other than noble gases (OT). Because the noble gases are not filtered by the containment isolation system, the probability of a radionuclide release is 1. The consequences of a release of noble gases is 1×10^{-9} probability of a latent cancer fatality (Section 6.3.2). For the noble gas release, the product of the four risk components is 5.6×10^{-14}. The inventory of other radionuclides will be released only if the containment isolation system fails, which has a probability of 1.5×10^{-5} (Section 5.1). The subject plant has high burnup fuel. From Table 18, the individual probability of a latent cancer fatality if the filters are off with high burnup fuel is 4.1×10^{-6}. For the release of other radionuclides, the product of the four risk components is 3.4×10^{-15}. The total risk for this scenario is 5.9×10^{-14} annual individual probability of a latent cancer fatality.

Table 19. Summary Table of Dry Cask Storage Risk Calculations

Stage: Initiating Event	Initiating Event Frequency	Probability of release from fuel rod and MPC	Radionuclides released	Probability of Release from Containment	Consequences	Risk
1: Fuel assembly dropped	2.2×10^{-3}	6.4×10^{-2}	NG	1	1.5×10^{-12}	1.9×10^{-16}
2	Not Applicable					0
3: Transfer cask dropped	5.6×10^{-5}	1		1	1.0×10^{-10}	5.6×10^{-15}
4: Transfer cask dropped	5.6×10^{-5}	0				0
5: Transfer cask dropped	5.6×10^{-5}	0				0
6: Transfer cask dropped	5.6×10^{-5}	0				0
7: Transfer cask dropped	5.6×10^{-5}	0				0
8: Transfer cask dropped	5.6×10^{-5}	0				0
9 -10	Not Applicable					0
11-17: Transfer cask dropped	5.6×10^{-5}	0	All			0
18: Lowering transfer cask thru equipment hatch 100 ft drop	5.6×10^{-5}	0.020	NG	1	1.0×10^{-10}	1.1×10^{-16}
			OT	1.5×10^{-4}	3.6×10^{-4}	6.0×10^{-14}
19	Not Applicable					0
20: Transfer cask drop - 19 ft drop	5.6×10^{-5}	0.28	NG	1	1.0×10^{-10}	1.6×10^{-15}
			OT	1.5×10^{-4}	3.6×10^{-4}	8.5×10^{-13}
21: Transfer cask drop - 19 ft drop	5.6×10^{-5}	0.28	NG	1	1.6×10^{-10}	1.6×10^{-15}
			OT	1.5×10^{-4}	1.5×10^{-4}	8.5×10^{-13}
22 - 24	Not Applicable					0
25	Not Applicable					0
26-33: Storage cask dropped	-	0		X		0
34 tipped by seismic event	7.0×10^{-7}	0		X		0
34 struck by aircraft	3.7×10^{-9}	0.14		X	3.6×10^{-4}	1.9×10^{-13}
34 struck by meteorite	3.5×10^{-14}	1	All	X	3.6×10^{-4}	1.3×10^{-17}
34 heated by aircraft fuel	3.7×10^{-9}	0		X	N / A	0
TOTAL 1ST YR RISK						2.0×10^{-12}

Subsequent Years of Storage

34 tipped by seismic event	7.0×10^{-7}	0		X		0
34 struck by aircraft	3.7×10^{-9}	0.14	All	X	3.6×10^{-4}	1.9×10^{-13}
34 struck by meteorite	3.5×10^{-14}	1	All	X	3.6×10^{-4}	1.3×10^{-17}
34 heated by aircraft fuel	3.7×10^{-9}	0		X	N/A	0

Notes: "NG" = noble gases; "OT" = radionuclides other than noble gases
"All" = noble gases and all other types of radionuclides released
"X" = probability of release from containment in the storage phase is not applicable

Notes For Table 19

1. Stage 1: Loading fuel assemblies into the MPC. The probability of dropping a fuel assembly, 2.2×10^{-3}, is the product of the probability of dropping a single assembly, 3.2×10^{-5} (Section 3.3.1), and the number of spent fuel assemblies loaded into a cask, 68. The drop probability is discussed in Section 3.3.1. The probability of the fuel failing given that it is dropped is 6.4×10^{-2} (Section 4.4.2).

   The noble gases that are released pass through the water of the spent fuel pool and the secondary containment filters. The probability of release from the containment is 1. Other radionuclides are retained by the water. This is discussed in Section 3.1. Because this release is from a cask holding 68 assemblies, the consequence for one assembly is 1/68 of this release, or 1.5×10^{-12}. The risk of Stage 1 is the product of the fuel assembly drop frequency, the probability of the fuel failing, the probability of a release of nobles gases from the containment, and the consequences of the noble gas release, or 1.9×10^{-16}.

2. Stage 2: Placing the MPC lid on the MPC and engaging the lift yoke on the transfer cask. The transfer cask is on the floor of the cask pit where it cannot fall any farther. There are no initiating events that can occur in this stage. Therefore, the risk of Stage 2 is zero.

3. Stage 3: Lifting the transfer cask out of the cask pit. The probability of dropping the transfer cask is 5.6×10^{-5} (Section 3.3.2). All of the fuel rods fail (Section 4.4.2). The MPC is unsealed, thereby rendering it ineffective in confining radionuclides. Section 4.1.2.1 discusses cracking and possibly more severe damage or failure of the spent fuel cask pit floor that may occur if the cask is dropped from the maximum height of 42.5 feet above the floor of the cask pit. Because the subject plant has a`single-failure-proof crane and professional rigging personnel are contracted to move the cask, the consequences of a drop of the transfer cask on the structural integrity of the cask pit do not have to be evaluated. It is assumed that the consequences to the integrity of the MPC and fuel from such a drop are the same as for a free drop in air of 40 feet. For a 40 foot drop onto concrete, Table 13 shows that 100% of the fuel cladding is breached. Since the MPC is not sealed during this stage, the probability of a release from the MPC is conservatively assumed to be 1.0. This assumption is conservative because it is expected that the preponderance of the radioactive inventory will remain in the cask under a drop. The water is too cold and the time is too short to have breaching other than the inventory in the pellet-cladding gap. The water may wash the particulate that would have settled to the cask interior. The noble gases that are released pass through the water of the spent fuel pool. Other radionuclides are retained by the water. Because the noble gases are not removed by the filters, the probability of noble gasses release from containment is 1. The consequences of a release of noble gases is $1.0\text{x}10^{-10}$ (Section 6.2.2). The total risk for this scenario is $5.6\text{x}10^{-15}$ annual individual probability of a latent cancer fatality.

4. Stage 4: Moving the transfer cask over a railing of the spent fuel pool. The probability of dropping the transfer cask is 5.6×10^{-5} (Section 3.3.2). The MPC is unsealed and remains in the upright position when dropped (Section 4.1.2.2). No fuel rods are expected to fail if the cask drops 3 feet during this stage. The risk of Stage 4 is zero.

5. Stage 5: Moving the transfer cask to the preparation area (1st segment). The difference between Stage 4 and Stage 5 is that the transfer cask is lowered from about 0.9 m (3 ft) above the refueling floor to about 0.3 m (1 ft). The possibility of dropping the transfer cask stems from the lowering. The other constituents of risk are as discussed in the note for Stage 4.

6. Stage 6: Moving the transfer cask to the preparation area (2nd segment). The possibility of dropping the transfer cask stems from the changed direction of travel along the load path of the refueling floor. The other constituents of risk are as discussed in the note for Stage 4.

7. Stage 7: Moving the transfer cask to the preparation area (3rd segment). The possibility of dropping the transfer cask stems from the changed direction of travel along the load path of the refueling floor. The other constituents of risk are as discussed in the note for Stage 4.

8. Stage 8: Lowering the transfer cask onto the preparation area. The difference between Stage 8 and Stage 5 is that the transfer cask is lowered from about 0.3 m (1 ft) above the refueling floor to the refueling floor. The possibility of dropping the transfer cask stems from the lowering. The other constituents of risk are as discussed in the note for Stage 4.

9. Stage 9: Preparing (drain, dry, inert, seal) the MPC for storage. Stage 10: Installing the short stays and attaching the lift yoke. The transfer cask is on the refueling floor and cannot fall. There are no other initiating events in Stages 9 and 10. The risk of Stages 9 and 10 is zero.

10. (Stages 11-17) Stage 11: Lifting the transfer cask. Stage 12: Moving the transfer cask to exchange the bottom lids of the transfer overpack (1st segment). Stage 13: Moving the transfer cask to exchange the bottom lids of the transfer overpack (2nd segment). Stage 14: Replacing the pool lid with the transfer lid. Stage 15: Moving the transfer cask near the equipment hatch. Stage 16: Holding the transfer cask. Stage 17: Moving the transfer cask to the equipment hatch. The frequency of dropping the transfer cask in any one of the stages is 5.6×10^{-5} (Section 3.3.2). No fuel rods are expected to fail. These stages are represented by one row in Table 19 because the risk of each stage is zero.

11. Stage 18: Lowering the transfer cask to the storage overpack through the equipment hatch. The probability of dropping the transfer cask is 5.6×10^{-5} (Section 3.3.2). The probability of MPC failure is 0.0002 for the 80 foot drop onto the storage overpack and 0.02 (0.0196) for the 100 foot drop onto the concrete floor. The more conservative 100 foot drop results are used. (Section 4.1.2.3 and 4). The entire inventory of radionuclides is considered to be released. Noble gases are not removed by the filters and their probability of release from the containment is 1. The consequences of a release of noble gases is 1.0×10^{-10} (Section 6.2.2). The total risk for this scenario is 1.1×10^{-165} annual individual probability of a latent cancer fatality . The inventory of other radionuclides will be released only if the containment isolation system fails, which has a probability of 1.5×10^{-4}. The probability of latent cancer fatality if the filters are off is 3.6×10^{-4}. For the release of other nuclides, the product of the risk component is 6.0×10^{-14}.

12. Stage 19: Preparing (remove short stays, disengage lift yoke, attach long stays) to lower the MPC. The transfer cask is on the storage overpack where it cannot drop. The doors of the transfer lid of the transfer cask are closed, hence, the MPC itself cannot drop. There are no initiating events in this stage. The risk of Stage 19 is zero.

13. Stage 20: Lifting the MPC and opening the doors of the transfer lid.
Stage 21: Lowering the MPC through the transfer cask into the storage overpack.
The frequency of dropping the MPC in any one of the stages is 5.6×10^{-5} (Section 3.3.2). This frequency is the same as that in the preceding stages because the crane used to lift the transfer cask and the MPC itself is the same and the rigging is similar. For this drop, 100% of the fuel is assumed to fail (Section 4.4.2). The probability of the MPC failing is 0.28 (Sections 4.1.2.6 and 4.3.2).

14. Stage 22: Moving the storage cask into the airlock on Helman rollers. Stage 23: Moving the storage cask out of the airlock on Helman rollers. Stage 24: Moving the storage cask away from the secondary containment on Helman rollers. The storage cask is on rollers and cannot be dropped because it is not lifted. The base of the storage cask on the platform of the rollers is sufficiently wide so that it cannot tip. There are no other initiating events that occur in these stages. These stages are represented by one row in Table 19 because the risk of each stage is zero.

15. Stage 25: Preparing (install lid, vent shield cross-plates, vent screens) the storage cask for storage. The storage cask is stationary while it is being prepared and cannot be dropped. The base of the storage cask is sufficiently wide that it cannot tip. There are no other initiating events that can occur. Hence, the risk is zero.

16. Stage 26: Lifting the storage cask above the Helman rollers with the overpack transporter. Stage 27: Moving the storage cask above a cushion on the preparation area. Stage 28: Holding the storage cask above the cushion while attaching a Kevlar belt. Stage 29: Moving the storage cask above the concrete surface of the preparation area. Stage 30: Moving the storage cask above the asphalt road. Stage 31: Moving the storage cask above the gravel surface around the storage pads. Stage 32: Moving the storage cask above the concrete storage pad. Stage 33: Lowering the storage cask onto the storage pad. The MPC failure probability and the fuel failure probability are both zero if the storage cask is dropped from an elevation of 0.3 m (1 ft) onto concrete, asphalt, or gravel (Section 4.1.3.1). Because the risk is zero, the initiating event frequencies and the consequences are not determined. These stages are represented by one row in Table 19 because the risk of each stage is zero.

17-24. Stage 34: Storing the storage cask on the storage pad for 20 years. To calculate the risk, this stage is divided into substages depending on the initiating event. The risk is also calculated separately for the first year of service and for the subsequent 19 years on the storage pad. However, because the duration of the handling and transfer phases is much less than one year, the frequencies of all initiating events in the first year of service are essentially the same as the corresponding frequencies for subsequent years on the storage pad.

17. Storage cask tipped by a seismic event during the first year of service. The initiating event frequency is 7×10^{-7} (Section 3.3.3). If the storage cask tips over no fuel rods are expected to fail (Sections 4.1.3.2 and 4.4.2). Even if the rods don't fial, a tip-over will dislodge CRUD from the rod surface. This crud is available for release. The risk is zero because the MPC does not fail.

18. Storage cask struck by an aircraft during the first year of service. The frequency of the strikes that could impact the storage cask is 3.7×10^{-9} (Section 3.3.7). Based on the results in Section A.4.9.3, the probability of breaching the MPC, if struck by an aircraft during landing or takeoff is extremely small and is assumed to be zero. However, many commercial aircraft overflying the site would be larger than a Gulfstream IV and could impact the cask at high velocity. Since the makeup and characteristics of commercial aircraft overflying the site are not known and have not been evaluated, it is conservatively assumed that all commercial aircraft overflying the site are larger than a Gulfstream IV and that the probability of MPC breach due to the impact of an overflying commercial aircraft is, for the purpose of the PRA, 1.0. Therefore, the probability of MPC failure and release, if struck by an aircraft, is, for the purpose of the PRA, equal to the frequency of overflight crashes ($5.1\text{x}10^{-10}$, see Section 3.3.7) divided by the total frequency of aircraft crashes ($3.71\text{x}10^{-9}$, see Section 3.3.7), which is 0.14. Because the ISFSI is outside the containment, the radionuclides are released to the environment. Because all of the fuel rods are assumed to fail, the consequences are 3.6×10^{-4} (Section 6.3.1, Table 18). The risk is the product of the aircraft strike frequency, the MPC failure probability and the consequences, or 1.9×10^{-13}.

19. Storage cask struck by a meteorite during the first year of service. The frequency of meteorites that could breach the storage cask is 3.5×10^{-14} (Section 3.3.5). The probability of a release from the MPC is conservatively set to 1, for the purposes of this PRA. Because the ISFSI is outside the secondary containment, the radionuclides are released to the environment. Because all of the fuel rods are assumed to fail, the consequences are 3.6×10^{-4} (Section 6.3.1, Table 18). The risk is the product of the meteorite strike frequency, the MPC failure probability and the consequences, or 1.3×10^{-17}.

20. Storage cask heated by burning fuel when an aircraft crashes during the first year of service. It is assumed that a fire will result whenever an aircraft hits the storage cask. The frequency of this is the sum of the frequencies of takeoff or landing crashes plus overflight crashes. From Section 3.3.7, the frequency of the storage cask being struck by an aircraft and heated by burning jet fuel is 3.7×10^{-9}. From Appendix B, Section B.1.8, any fire caused by a takeoff, landing or overflight crash will not fail the cask. Hence the probability of a release and the risk are both zero.

21-24. These notes are the same as notes 17 through 20, respectively for each year of the subsequent 19 years of storage.

8. OTHER ASPECTS OF DRY CASK STORAGE RISK

Conditions that could potentially affect the response of the MPC to loads are shown in Table 19.

Other possible conditions are described in the paragraphs of this section and summarized in Table 20. None of these conditions is expected to affect the integrity of the MPC.

Table 20. Conditions Potentially Affecting MPC Response to Initiating Events

Conditions Affecting the MPC Storage	Section
Excessive hot fuel assemblies mistakenly loaded	8.1
Criticality	8.2
Corrosion from coastal atmosphere	8.3
Corrosion from long term industrial releases	8.3
Pressurization from corroding fuel	8.4
Pressurization from failed fuel	8.4
Hydrogen gas accumulation when the MPC lid and shell are welded	8.5

8.1 Mis-loading of Spent Fuel into the MPC

For the purposes of the PRA, sensitivity analyses were performed to determine MPC failure probabilities for a gross mis-loading of wrong fuel assemblies into the MPC. The scenario of a gross series of errors, resulting in every fuel assembly loaded into the MPC being incorrect/insufficiently cooled is not considered credible, but useful for the purposes of exploring the impact of such an event. In these scenarios the heat load in the MPC was increased from 21 kW to 33 kW, 66 kW, and 126 kW. These heat loads correspond to fuel that has cooled in the spent fuel pool for 5 years, 2.5 years, 1 year, and 0.5 years, respectively. Even if every single fuel assembly loaded into the MPC were incorrect, no MPC failures are predicted for heat loads of 21 kW, 33 kW, and 66 kW. But if the heat load were 126 kW, the MPC could be expected to fail from creep rupture. The probability of failure in such an unlikely case would be 0.02 after 20 years of storage. No fuel failures are expected for heat loads of 21 kW and 33 kW. In these extremely unlikely scenarios, fuel failure could be expected to occur when the heat load is 66 kW and 126 kW. The fuel temperature would reach 543 °C (1010 °F) and 809 °C (1488 °F), respectively when the cask reaches thermal equilibrium. The long term temperature limit for dry fuel storage is 400 °C (752 °F). [It is highly unlikely that rods at 543 °C would fail. Also, 400 °C is not a rod failure criterion. It was chosen to limit the hydride reorientation problem. It also limits creep.] Based on the extremely low likelihood of a gross mis-loading scenario, made all the more unlikely by the significant procedural requirements, fuel assembly verifications and instrumentation used in the process, it is concluded MPC integrity will not be affected by any occurrences of fuel mis-loading.

8.2 Potential for Criticality

A criticality study was performed on the transfer cask in Stage 3 where the MPC is loaded with spent nuclear fuel while it is in the cask pit. This study was intended to provide insights as to degree of sub-criticality expected during limiting (not conservative) MPC loading operations. The reader is encouraged to keep in mind that these assumptions, while possible, are highly unlikely because we are effectively assuming that reactor operators will be discharging fuel well before its operational lifetime. Further depletion in the core will reduce the eigenvalues shown in this section and, therefore, the results of this study can be considered limiting, This study is not a rigorous nuclear criticality analysis of MPC operation.

Since the results demonstrated roughly a 20% sub-critical margin, a more detailed analyses was deemed unnecessary. The analysis is only of events and conditions that are within the scope of the PRA as discussed in Section 1.2. The possibility of criticality in other stages, such as Stage 34 where the storage cask is in the ISFSI, was also studied. Given the assumptions of this analysis, the results are applicable to only BWR fuel in the subject cask. A General Electric designed BWR fuel assembly was studied because it is highly enriched and contains large amounts of burnable poisons that will tend to maximize the reactivity increase effect. The BWR assembly was the most reactive assembly found in available fuel design references. Burnable poisons were modeled as four concentric annuli, and the assembly was burned pin-by-pin in 1000 megawatt-days per metric ton (MWd/t) steps. The enrichment was used as designed; the fuel depletion was modeled using the as designed assembly, not by assuming an initial homogeneous enrichment.

The SCALE suite of codes (Reference 48) was used to perform this analysis. The fuel was depleted with the TRITON module and criticality analysis were performed with KENO-VI using the 238 group ENDF/B-V library.

The fuel in the canister was modeled to the same level of detail as in the burnup calculation. The model was essentially two-dimensional. A 15.2 cm (6 inch) "slice" of the fuel using its most reactive axial zone and applied reflective top and bottom boundary conditions was modeled. One quarter of the MPC basket was modeled with two lines of symmetry. The basket can be modeled as being surrounded by an effectively infinite annulus of water because an infinite reflector should yield the most reactive configuration.

To allow for fuel compression/expansion studies, it was confirmed that an isolated cell of the basket model yields effectively equivalent answers as the entire model. By this we mean that an isolated cell gave approximately the same eigenvalue as the complete MPC model. The fuel compression/expansion study assumed a reduction (or increase) of the pin pitch to ensure that there is not a compression (or expansion) accident condition that could lead to a significant increase in reactivity which would cause the eigenvalue to approach a 5% sub-critical margin. The MPC poisons were assumed to stay in the cask. This model is sufficient for trending studies given the expectation that the results will be highly sub-critical.

Four concerns of criticality are the following:

- excessive heat generation can overpressurize the MPC,
- excessive gamma radiation may be insufficiently shielded,
- excessive neutron radiation may be insufficiently shielded, and
- radio-nuclides could be released if the fuel cladding were to fail.

Several calculations were performed to evaluate MPC performance. The first observation is that the compression/expansion study demonstrates that there are no credible compression/expansion scenarios which lead to an increase in the eigenvalue to anywhere near the 5% sub-critical margin. Similar analyses are shown in Reference 49. The second observation is that there are no low density, optimal moderation configurations which means that pool draining events will not lead to a reduction in the sub-critical margin. Figure 19 and the work in Reference 50 confirm this by showing the predicted eigenvalue at the upper bound 95th percentile confidence interval with reduced water density. As is evident from the figure, even when changes in water density are considered, the fuel in the MPC is highly sub-critical. In summary, the criticality analyses performed for this study, while limited in scope, show similar trends as other studies by confirming that the configuration is under-moderated and highly sub-critical.

When the MPC is dry, criticality is not physically possible under any conditions in the absence of other neutron sources. This is true because the original fuel enrichment was limited to 5 weight percent which is a limit based in part on the requirement that unmoderated criticality is not possible, even for BWR fuel at its most reactive point in life. This position is based on experimental data and calculations in Reference 51.

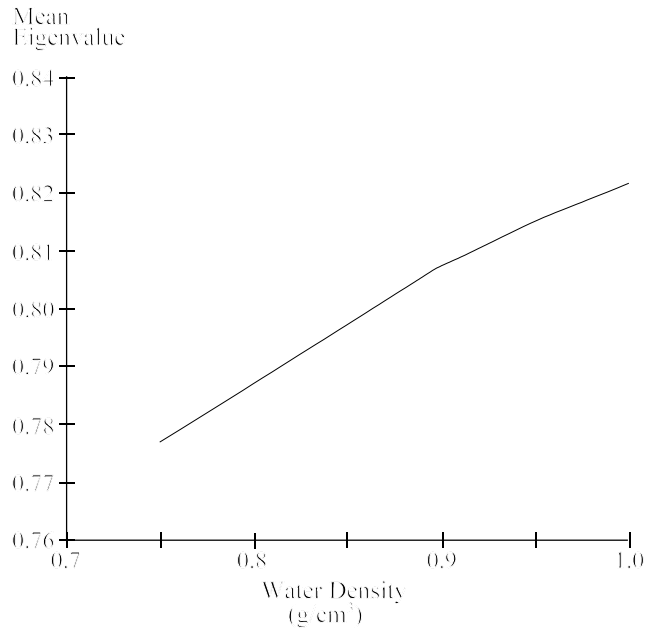

Figure 19. Upper 95th Percentile Confidence Interval Eigenvalue for MPC-68 in Pure Water at 27°C (81°F)

The boral plating in the MPC-68 basket is an effective means of criticality control; criticality is not allowed whether moderated or unmoderated. No credible scenario which would eliminate the boral and leave the geometry of the fuel intact has been identified. Even if the boral plates were to separate from the basket structure, they would have limited room to move and, once the basket is sealed, there is no credible means by which they could fall out of the basket. If the contents of the MPC-68 were to somehow relocate, the boral would relocate with the debris. In all likelihood, this postulated configuration would be highly subcritical because of the boral and because a bed of debris is not an optimal geometry. At the enrichments used in BWR fuel, a square pitch lattice is the optimal geometry for criticality. In the absence of moderation, experiments and calculations have demonstrated that criticality is not possible at the enrichments currently used in LWR fuel.

8.3 Corrosion

The MPC, which acts as the confinement boundary for the HI-STORM dry cask storage system, is constructed entirely from austenitic stainless steel Types 304, 316, 304L, or 316L. All of these stainless steel grades are corrosion resistant in high-humidity and industrial environments. Therefore, coastal and industrial atmospheres should have no effect on the confinement ability of the MPC (Reference 52).

The MPC is drained, dried, and filled with helium. Helium is an inert gas; it does not react with the fuel cladding or the internal structures of the MPC.

8.4 Pressurization

BWR fuel rods are normally pressurized with helium to 0.69 MPa (100 psi) (Reference 14). The fuel failure analysis of Appendix C uses a conservative assumption of 15.5 MPa (2250 psi) for internal fuel rod pressure. If the fuel rods were to breach, such as by creep rupture, the pressure in the rods would pressurize the MPC. An incremental increase in pressure from all of the fuel rods in the MPC rupturing is addressed in the Appendix B assessment of the response of the MPC to mechanical and thermal loads, Section B.1.8, 'Results.' Fuel failure would cause the internal pressure of the MPC to increase. If a mechanical impact event did cause fuel failure, the resulting increase in pressure would not occur during the drop accident scenarios. The increase in internal pressure due to fuel failure would be a result of the mechanical loading, but because of the extremely short duration of the impact, it would not affect the MPC conditions until after the mechanical loading is complete.

The failure analysis of the vent blockage scenario assumed bulk internal pressure takes into account the increased pressure from fuel failure. These results are shown in Appendix B, Table B4. The failure analyses show that even after 20 years of vent blockage and 20% fuel failure, the added pressure from failed fuel does not result in any expected MPC failures.

Calculations discussed in more detail in Appendix C determined that for the vent blockage scenario, all fuel rods located within a 0.38 m (1.25 ft) radius of the cask center will have a maximum clad temperature exceeding the long term temperature limits. Using a ratio of areas affected, the fraction of fuel expected to exceed long term temperature limits is 0.20.

8.5 Hydrogen Generation in the MPC

In Stage 9, the transfer cask is in the preparation area where the MPC lid is welded to the MPC shell. The water in the MPC is lowered to about 0.3 m (1 ft) below the lid. While welding the lid to the shell, the root pass, several intermediate passes, and the final pass are tested with dye penetrant. The water level is then raised to the lid elevation, and the MPC is pressurized to hydrostatically test the weld. Should no leakage occur, the MPC is drained, dried, and filled with helium. The cover plates and closure ring are then installed and welded.

When the MPC contains water, reactions can occur that generate hydrogen gas. When the water level is below the MPC lid prior to hydrostatic testing, hydrogen gas can accumulate in the space between the lid and the surface of the water while the lid is welded to the shell. To prevent accumulation, the subject plant vents the space by pumping argon into the MPC through the drain line. The argon percolates through the water to the top of the MPC and exits through the port, purging hydrogen from the space.

Another reason for purging the space between the water surface and the lid is to eliminate any possible adverse effect that hydrogen could have on the lid-to-shell weld. Hydrogen in weld metal can cause cracks if the concentration is high enough and the material being welded is carbon steel or alloy steel. The type of stainless steel presently used for spent fuel canisters is highly resistant to hydrogen induced cracking. Despite this resistance to hydrogen induced cracking, this step to preclude hydrogen from the weld area is always implemented to further assure high quality welds.

The lid/shell and the closure ring/shell welds are not evaluated in the PRA because the lid/shell weld is more robust than the other welds of the MPC. Less ductile welds, such as the baseplate weld, are evaluated in the PRA. For the following reasons the lid/shell weld is not evaluated.

- Because of the welding process, the lid/shell weld and the closure ring/shell weld is expected to be tougher than other welds of the cask.

- The MPC lid has redundant welding, consisting of the lid/shell weld and the closure ring/shell weld.

- Stress in the lid/ shell weld are low for all drop events.

The baseplate weld is modeled in the failure models of the MPC.

9. CONCLUSIONS

Starting with a comprehensive list of initiating events (Tables 3, 4, and 5), the annual risk to the public from the onsite handling, transfer, and storage of a single transfer cask and storage cask at a specific BWR site is estimated. First, the frequencies of all initiating events which could affect the subject cask at the subject site are estimated. Second, the responses of the MPC and fuel to the mechanical and thermal loads induced by the initiating events are determined. Third, the consequences of a release of radioactive material to the environment is calculated in terms of the individual probability of a latent cancer fatality. (No prompt fatalities are predicted.) Finally, these results are combined to estimate the risk to the public in terms of the annual probability of a latent cancer fatality.

Because no uncertainty analysis was performed, the identification of the dominant contributors was based on the point estimates developed by this study. The dominant contributors might possibly change if uncertainty were considered.

The risk estimates are extremely low. Many of the scenarios have zero risk because either their initiating events cannot occur at the subject plant or no radioactive release will result. As Table 19 shows, the risks of the scenarios with nonzero risk are extremely low because they are the products of two or three very small numbers.

For example, the initiating event of the drop sequences has a frequency of 5.6×10^{-5} per year and with a probability of 0.02 failure of the MPC. If only noble gases are released, the consequence probability is 1.0×10^{-10}, if other radioactive materials are released, the consequence probability is 3.6×10^{-4}, and the probability of the secondary containment failing to isolate is 1.5×10^{-4}. Thus, the risk of the noble gas release is:

$$(5.6\times10^{-5})(0.02)(1.0\times10^{-10}) = 1.1\times10^{-16}$$

and with a probability of 0.02 failure of the MPC, the risk of the release of other radionuclides is:

$$(5.6\times10^{-5})(0.02)(1.5\times10^{-4})(3.6\times10^{-4}) = 6.0\times10^{-14}$$

Results for handling phase stages 4 through 33 where in Table 19 the "Probability of Release from Fuel Rods and MPC" is shown as zero, have an actual probability of release of radioactive material of less than $1x10^{-6}$. This produces extremely low risk and is shown in the risk columns of Table 19 as zero.

There are two other stages (Stages 1 and 3) in the handling phase that have negligible risk. These stages involve release of noble gases if the containment fails to isolate. The releases occur because the lid of the MPC is not welded shut until Stage 9. The risk of a noble gas release in stage 1 is 3.2×10^{-20} and in stage 3 is 8.4×10^{-19}.

The estimated aggregate risk is an individual probability of a latent cancer fatality of 2.0×10^{-12} during the period encompassing the initial cask loading and first year of service, and 1.9×10^{-13} per year during subsequent years of storage. The only significant contributions to the risk during the handling phase are from drops of the transfer cask. There is zero risk associated with the transfer phase. During the transfer phase (movement of the storage cask out to the storage pad), drops of the transfer cask are not high enough to induce sufficient stresses on the transfer cask to fail the MPC. During the storage phase, the dominant contribution to the risk is from aircraft striking the storage cask, although the risk is still extremely small.

10. REFERENCES

1. Memorandum from William D. Travers, Executive Director for Operations, from Annette L. Vietti-Cook, Secretary, "Staff Requirements - SECY-98-144 - White Paper on Risk-Informed and Performance-Based Regulation," March 1, 1999.

2. HOLTEC International, "HI-STORM Topical Safety Analysis Report," HI-951312, Revision 8, June 25, 1999.

3. U.S. Nuclear Regulatory Commission, "Severe Accident Risks: An Assessment for Five U.S. Nuclear Power Plants," NUREG-1150, December 1990.

4. NRC, "Safety goals for the Operation of Nuclear Power Plants" (Corrections and Republication of Policy Statement), Federal Register, Volume 51, No. 162, pp 30028 - 30033, August 21, 1986.

5. Chapman, O.J.V., and Simonen, F.A. "RR-PRODIGAL Model for Estimating the Probabilities of Defects in Reactor Pressure Vessel Welds," NUREG/CR-5505, Nuclear Regulatory Commission, Washington DC, 1998.

6. R Kenneally, J Price, and D. Koelsch, "Dry Cask Storage Characterization Project, Final report," EPRI, Palo Alto, CA, U.S. Nuclear Regulatory Commission, Washington, D.C., U.S. Dept. of Energy - OCRWM, North Las Vegas, NV, and U.S. Dept. of Energy -Idaho Operations, Idaho Falls, ID, Doc EPRI Doc No. 1002882, Sept 2002.

7. U.S. Nuclear Regulatory Commission, "PRA Procedures Guide," NUREG-2300, January 1983.

8. "Code Manual for MACCS2," NUREG/CR-6613, Vol. 1, May 1998.

9. Hall, Eric J., Radiobiology for the Radiologist, 4th edition, J.B. Lippencott Co, Phil PA 1994.

10. Generic Letter 89-22, "Resolution of Generic Safety Issue No. 103, 'Design for Probable Maximum Precipitation'," October 19, 1989.

11. National Oceanic and Atmospheric Administration, National Weather Service Hydrometeorological Report (HMR) No. 51, Probable Maximum Precipitation Estimates, United States Est of the 105th Meridian, June 1978.

12. U.S. Nuclear Regulatory Commission, "A Survey of Crane Operating Experience at U.S. Nuclear Power Plants from 1968 through 2002," NUREG-1774, July 2003.

13. U.S. Department of Energy, "Integrated Data Base Report - 1994: U.S. Spent Nuclear Fuel and Radioactive Waste Inventories, Projections, and Characteristics," DOE/RW-006, Rev. 11, September 1995.

14. U.S. Nuclear Regulatory Commission, "A New Comparative Analysis of LWR Fuel Designs," NUREG-1754, December 2001.

15. U.S. Nuclear Regulatory Commission, "Information Digest," NUREG-1350, Vol. 11, 1999.

16. U. S. Nuclear Regulatory Commission, "Control of Heavy Loads at Nuclear Power Plants: Resolution of Generic Technical Activity A-36," NUREG-0612, July 1980.

17. U.S. Nuclear Regulatory Commission, "Revised Livermore Seismic Hazard Estimated for Sixty-Nine Nuclear Power Plant Sites East of the Rocky Mountains," NUREG-1488, April 1994.

18. U.S. Nuclear Regulatory Commission, "Tornado Climatology of the Contiguous United States," NUREG/CR-4461 (PNL-5697), 1986.

19. Fujita, T. Theodore, U.S. Tornadoes, Part One, 70-Year Statistics, Satellite and Mesometeorology Research Project (SMRP) Department of the Geophysical Sciences, The University of Chicago, SMRP Research Paper Number 218, Library of Congress Catalog Card Number 86-51637, National Technical Information Service PB 87-127742, Copyright 1987.

20. D.A. Kring, Meteorites and Their Properties, Lunar and Planetary Laboratory, University of Arizona, Tucson, 32 pp. Second Edition published in 1998.

21. French, Bevan M., Traces of Catastrophe, A Handbook of Shock-Metamorphic Effects in Terrestrial Meteorite Impact Structures, Lunar & Planetary Institute, 1998.

22. Cassidy, William A., Estimated Frequency of a Meteorite Striking An Aircraft, University of Pittsburgh, Department of Geology and Planetary Science, December 17, 1997.

23. HI-STORM 100 LAR 1014-1, Revision 1, Supplement 1, October 2000.

24. Watson, A.I., Holle, R. L., An Eight-Year Lightning Climatology of the Southeast United States Prepared for the 1996 Summer Olympics, Bulletin of the American Meteorological Society, Vol.77, No. 5, May 1996.

25. "Expected Frequency of Direct Lightning Flashes to a Structure," IEA Standard 97 and "Protection of Structures Against Lightning - Part 1: General Principles - Section 10: Guide A: Selection of Protection levels for Lightning Protection Systems," IEC 61024-1-1, Ed. 1.0 b:1993.

26. U.S. Nuclear Regulatory Commission, "Standard Review Plan for the Review of Safety Analysis Reports for Nuclear Power Plants," NUREG-0800, Rev. 2, Section 3.5.1.6, "Aircraft Hazards," July 1981.

27. "Guidance and Data for Impact Frequency Calculation," Appendix B to DOE Standard 3014-96.

28. Lawrence Livermore Software Technology, LS-DYNA Computer Code, Version 960, March 2001.

29. U.S. Nuclear Regulatory Commission, "Standard Review Plan for the Review of Safety Analysis Reports for Nuclear Power Plants," NUREG-0800, Rev. 2, Section 3.5.1.4, "Missiles Generated by Natural Phenomena," July 1981.

30. ACME Boiler and Pressure Vessel Code, Section III, (1989), American Society of Mechanical Engineers.

31. U.S. Nuclear Regulatory Commission, "Evaluation of Explosions Postulated to Occur on Transportation Routes Near Nuclear Power Plants," Regulatory Guide 1.91 (Draft Report), Revision 1, February 1978.

32. Mechanics Research, Inc., for the Tennessee Valley Authority, "Nuclear Power Plant Risks from a Natural Gas Pipeline." 1974.

33. Fluent (Computational Fluid Dynamics Software), Release 6, Fluent Incorporated, Lebanon, NH, 2000.

34. HI-STORM 100 Thermal Calculations, November 2000.

35. American Concrete Institute, ACI 349-01, "Code Requirement for Nuclear Safety Related Concrete Structures," Farmington Hills, MI, 2001.

36. Society of Fire Protection Engineers (SFPE), The SFPE Handbook of Fire Protection Engineering, Second Edition, Bethesda, Maryland, Chapter 3-11, Section 3, pp. 3-202, and 3-199, 1995.

37. Kramer, M.A., et. al., "Measurements of Heat Transfer to a Massive Cylindrical Object Engulfed in a Regulatory Pool Fire," Proceedings of NHTC'01: 35th National Heat Transfer Conference, Anaheim, California, June 10-12, 2001.

38. Drysdale, D., An Introduction to Fire Dynamics, John Wiley and Sons, 1996.

39. NFPA-780, "Standard for the Installation of Lightning Protection Systems," Quincy, MA: National Fire Protection Association, 1995.

40. NUREG-1536, Standard Review Plan for Dry Cask Storage Systems, Chapter 2 "Guidance: Principal Design Criteria," February 1, 1996.

41. J.R. Brauer and B.S. Brown, EMAS User's Manual Version 4, Ansoft Corporation, July 1997.

42. U. S. Nuclear Regulatory Commission, "Failure Behavior of Internally Pressurized Flawed and Unflawed Steam Generator Tubing at High Temperatures – Experiments and Comparison with Model Predictions," NUREG/CR-6575, ANL-97/17, March 1998.

43. Chun, R., Witte, M., Schwartz, M., "Dynamic Impact effects on Spent fuel Assemblies," LLNL, UCID-21246, 1987

44. General Electric Corporation, "ABWR Standard Safety Analysis Report - Chapter 19D, Probabilistic Evaluations," Amendment 31, July 1993.

45. Combustion Engineering, Inc., "CESSAR Design Certification, System 80+ Standard Design FSAR, Appendix 19.5A – Data Calculations for Generic Component Data," Amendment M (March 15, 1993) and Amendment W (June 17, 1994).

46. T. L. Sanders, et. Al., "A Method For Determining the Spent-Fuel Contribution to Transport Cask Containment Requirements," Sandia National Laboratories, SAND90-2406, October 1992.

47. J. N. Jow, et. Al., "MELCOR Accident Consequence Code System (MACCS), Model Description," NUREG/CR-4691, Sandia National Laboratories, SAND-1562. Vol. 2. February 1990.

48. "SCALE: A Modular Code System for Performing Standardized Computer Analyses for Licensing Evaluation", Vols. I-III, NUREG/CR-0200, Rev. 6 (ORNL/NUREG/CSD-2/R6), May 2000.

49. NUREG-1738, "Technical Study of Spent Fuel Pool Accident Risk at Decommissioning Nuclear Power Plants," February 28, 2001.

50. "Reexamination of Spent Fuel Shipment Risk Estimates," NUREG/CR-6672, March 2000.

51. H.C. Paxton and N. L. Pruvost, "Critical Dimensions of Systems Containing U235, Pu239, and U233," 1986 Revision, Los Alamos National Laboratory Report LA-10860-MS, July 1967.

52. American Society for Metals, “Corrosion Resistant Materials,” Metals Handbook Desk Edition, 1985.